PEOPLE'S DEMOCRATIC REPUBLIC OF ALGERIA

Ministry of Higher Education and Scientific Research

Ecole Nationale Polytechnique

Mechanical Engineering Department

Laboratory of Mechanical Engineering and Development

CRD/ SONATRACH

In partial fulfillment of the requirement for
Engineer's Degree

Analysis and modeling of buckling in drillstrings

Seif Eddine BELOUAHED

Kheireddine BOUGHACHICHE

Under the supervision of

PR. Saïd RECHAK

Mr. Abdelouahab BOUGHELOUM

Publicly presented and defended on 06/24/2018

Composition of the Jury:

President	Pr. Belkacem KEBLI	ENP
Supervisors	Pr. Said RECHAK	ENP
	Mr. Abdelouahab BOUGHELOUM	SONATRACH-DF
Examiners	Pr. Arezki SMAILI	ENP
	Dr. Yacine BELKACEMI	ENP

ENP 2018

PEOPLE'S DEMOCRATIC REPUBLIC OF ALGERIA

Ministry of Higher Education and Scientific Research

Ecole Nationale Polytechnique

Mechanical Engineering Department

Laboratory of Mechanical Engineering and Development

CRD/ SONATRACH

In partial fulfillment of the requirement for
Engineer's Degree

Analysis and modeling of buckling in drillstrings

Seif Eddine BELOUAHED

Kheireddine BOUGHACHICHE

Under the supervision of

PR. Saïd RECHAK

Mr. Abdelouahab BOUGHELOUM

Publicly presented and defended on 06/24/2018

Composition of the Jury:

President	Pr. Belkacem KEBLI	ENP
Supervisors	Pr. Said RECHAK	ENP
	Mr. Abdelouahab BOUGHELOUM	SONATRACH-DF
Examiners	Pr. Arezki SMAILI	ENP
	Dr. Yacine BELKACEMI	ENP

ENP 2018

Dedicated

TO MY MOTHER

TO MY FATHER, SISTER AND MY FAMILY

I AM PROUD OF MY PARENTS WHO HAVE GROWN TWO CHILDREN WITH MANY SACRIFICES. THEY HAVE BEEN THE MAIN FORCE AND GUIDE DURING MY EDUCATION AND ROOTED THE MANY PRINCIPLES TO ME SUCH AS HONESTY, DETERMINATION AND PASSION FOR SUCCESS.

TO MY DEAR AUNT 'MAY SHE REST IN PEACE AND MAY GOD REST HER SOUL'.

TO MY FRIENDS 'HAMZA, RAMI, ZINOU, MOH, CLASSMATE, RAOUF, ZAKARIA, BACHIR, IMAD AND NORO'

TO MY COLLEAGE KIKO

S. Belouahed

I dedicate this work to my family who supported me throughout the years, provided me with all I ever needed, encouraging me to take on new challenges and helping me through them.

to all of the mechanical engineering class of 2015-2018, all of the class for all the great discussions we have had, struggles we have gone through and laughs we shared, would not have made this far without every one of you.

Special thanks to Adel ABBAS and Yahia LAKACHE for always for always assisting us with the written courses, could not have passed the classes without them also all the past generations who shared the holy grail of mechanical engineering “la valise”.

My friend who worked this project with me, Seif Eddine BELOUAHED, thank you for your patience and all the efforts exerted during this work.

K. Boughachiche

Acknowledgment

First, our thanks go Prof. S. RECHAK for accepting to guide us in taking on this new challenge, and the trust he put in our ability to overcome it, his attentiveness, availability at all times, patience and invaluable advice all throughout this project.

Our supervisor Mr. A. BOUGHELOUM for being a driving force in this study, his efforts in teaching us about drilling industry and guiding us into this new field in which we had to learn everything

Dr. LOÏC BRILLAUD from DrillScan inc. for providing us with the WellScan software and responses throughout the project

We would like to thank Prof. STEFAN Z. MISKA (Professor at University of Tulsa, Oklahoma, USA), Prof. G ROBELLO SAMUEL (University of Southern California. and Prof B. KEBLI (ENP) for their valuable comments and feedback during our work.

We also would like to thank the members of the examiner committee. Pr. Arezki SMAILI and Dr. Yacine BELKACEMI for spending their valuable time to carefully assess our work.

We are grateful to employees of SONATRACH in Hassi Messaoud from whom we gained considerable technical experience in drilling.

ملخص

الهدف الرئيسي لهذا المشروع ، بالتعاون بين قسم الهندسة الميكانيكية وشركة النفط والغاز الجزائرية سوناطراك ، هو تحليل مشكلة الانبعاج في عمليات الحفر المعقدة داخل الآبار ، وهي ظاهرة فشل ميكانيكي تسبب زيادة في عزم الدوران و اجهاد الاحتكاك التي يمكنها تعريض عمليات الحفر للفشل. أولاً ، نجري دراسة مقارنة للنماذج المختلفة لاجهاد الضغط الأقصى الذي يسبب الانبعاج لتوفير نظرة على التدابير الوقائية التي يتعين اتخاذها. ثم نستخدم نموذج لوبانسكي لتحديد الشكل النهائي لعمود الحفر داخل الآبار العمودية. بالنسبة إلى الآبار المائلة ، يتم إنشاء معادلات التوازن لتحديد لحظة عزم الالتواء أو الانحناء على طول عمود الحفر ويتم تشغيل عمليات المحاكاة الأخيرة باستخدام برنامج WellScan للتحقق من تأثير عوامل الحفر على هذه الظاهرة باستعمالة دراسة حالة فرضية و حالة واقعية ناتجة عن حقل الحفر في حاسي مسعود.

الكلمات الدالة: الانبعاج، الحفر، عمود الحفر، عزم الدوران ، اجهاد الاحتكاك، اجهاد الضغط الأقصى.

Résumé

L'objectif principal de ce projet, en collaboration entre le département de génie mécanique et la société SONATRACH, est d'analyser le problème de flambage des garnitures dans les puits de forage. Tout d'abord, nous avons effectué une étude comparative des différents modèles qui estime les efforts critiques provoquant le flambement, ceci dans le but de permetre au foreure de prendre des mesures préventives. Ensuite, nous avons utilisé le modèle de Lubinski pour identifier la deformation de la garniture après le flambage dans les puits verticaux. Dans le cas d'un puit incliné, les équations d'équilibre ont été établie pour déterminer le moment de flexion le long du train de forage. En dernier des simulations ont été effectuée à l'aide du logiciel WellScan pour étudier l'impact des paramètres de forage sur le phénomène à travers des études de cas hypothetique et réel fourni par un champ de forage à Hassi Messaoud.

Mots clés : Flambage, forage, garnitures de forage, couple, charges de frottement, efforts critiques.

Abstract

The primary objective of this project, in a collaboration between the mechanical engineering and development laboratory "LGMD-ENP" and the development and research center "SONATRACH", is to analyze the buckling problem for drill strings constrained within wellbores, a mechanical failure phenomenon that causes increase in torque and drag loads that can jeopardize drilling operations. First, we make a comparative study of the different models for the critical loads causing buckling to provide insight into the preventive measures need to be taken. Then we use the Lubinski model to identify the post-buckling shape of the drill string within vertical wells. For inclined wellbores, the equilibrium equations are established to determine the bending moment along the drill string and last simulations are run using WellScan software to investigate the effect of drilling parameters on the phenomenon via hypothetical and real case studies provided by a drilling field in Hassi Messaoud.

key words: Buckling, drilling, drill strings, torque, drag, critical loads.

Table of Contents

Table of Tables

Table of Figures

Nomenclature

a, b, c coefficients for drillstrings deformed shape equations (Lubinski)

A_s Surface area for drillstring(ft^2)

$\vec{b}(s)$ binormal

DL dog leg (°)

DLS dog leg severity (°/100ft)

E Young Modulus (psi)

f side force coefficient

f_c contact force per unit length (lbf/ft)

f_{cb} binormal component for the contact force per unit length (lbf/ft)

f_{cn} normal component for the contact force per unit length (lbf/ft)

F_2 horizontal component of the axial force (lbf)

F_{ch} Critical helical axial load (lbf)

F_{cr} Critical Axial Load (lbf)

F_{cs} Critical sinusoidal axial load (lbf)

F Axial Load(lbf)

F side force (lbf)

$F(x), G(x), P(x), Q(x), R(x), S(x), T(x), U(x), V(x)$ power series for the solution of deformed shape by Lubinski

g Specific gravity (ft/s^2)

G_Θ, ϕ gradients for inclination and azimuth ($rad.ft^{-1}$)

I Moment of inertia (ft^4)

ID Inner diameter (ft)

i bending moment coefficient

k_b buoyancy factor

M Bending Moment $(ft.lbf)$

M_T Torque applied on the drillstring$(lbf.ft)$

MD Measured depth (ft)

m dimensionless factor per unit of length (ft)

$\vec{n}(s)$ normal to the tangent

OD Outer diameter (ft)

OD_{hole} Diameter of the wellbore (ft)

p Helix pitch

R radius of curvature (ft)

r_c radial clearance (ft)

TF Ton force, load measurement unit 1 TF=9806.65 N

TVD True Vertical Depth (ft)

$\vec{t}(s)$ tangent vector

U total potential energy $(ft.lbf)$

U_b Potential energy due to bending $(ft.lbf)$

U_c Potential energy due to compression $(ft.lbf)$

U_f Potential energy of the compressive force $(ft.lbf)$

u lateral displacement along the x axis(ft)

v lateral displacement along the y axis(ft)

W_2, WOB Weight on the Bit (lbf)

w_{air} weight in air per unit length (lbf/ft)

w_b weight in mud per unit length (lbf/ft)

$\vec{x}(s)$ wellbore trajectory

x, s position along the beam (ft)

x_1 upper end of the drillstring (dimensionless)

x_2 lower end of the drillstring (bit) (dimensionless)

x_3 contact point (dimensionless)

y lateral displacement (ft)

α Deflection angle of the helix (°)

θ Inclination of the wellbore(rad)

$\kappa(s)$ wellbore curvature per unit length (ft^{-1})

ν Poisson's coefficient

ρ density (sg)

$\tau(s)$ wellbore torsion per unit length (ft^{-1})

ϕ azimuth angle (rad)

Introduction

"*Modern civilization is the product of an energy binge…But humankind's unappeasable appetite for energy makes the solutions ephemeral and the challenge permanent*" - Alfred W Crosby

Energy is the only universal currency: all-natural processes and all human actions are, in the most fundamental physical sense, transformations of energy. Civilization's advances can be seen as a quest for higher energy use required to produce diverse goods. And as humankind looks towards new and more sustainable energies to quench that thirst, it is fossil fuels that cover that need in the present and forthcoming days.

Long gone are the days where fossil fuel deposits are easily accessed. Today to access these energy stores, a notable work of engineering is required, deep wells must be drilled, often in rough terrain, with complicated trajectories to account for geology. This work must withstand enormous pressure produced by adjacent rocks, prevent any damage to the surrounding environment and hold advanced technologies that will allow production in a safe and no detrimental way.

Parameters must be set with precision to optimize such a complicated operation, drafting a detailed plan, an optimal plan is the responsibility of engineers, and for that, they must be provided with the right tools, for the stakes are high, and all mistakes come at a great cost, this holds especially true in Algeria, where income from fossil fuels represents a large portion of our exports, optimizing drilling operations for lower cost is a key goal for the stabilization of the economy.

The national oil & gas company SONATRACH projects to create its own software tools for well drilling. In common discussions between the research center and development and the mechanical engineering and development laboratory, two projects have been identified. Among those two the present one entitled "Analysis and modeling of buckling in drillstrings" at the ENP Algiers.

In this project, we are to study the buckling of drill strings within wellbores, a problem closely related to torque and drag computation for drilling. Identifying the buckling phenomenon and providing the mathematical models to better understand

its causes and consequences in vertical and inclined wellbores with the goal of assisting the industry with the data to avoid the problematic or handle it better when it arises.

As an opening chapter, we will introduce the drilling operation, the technical terms used and identify the different components of a drill string and parameters associated to it, these are the key figures in our study.

In the second chapter, a modest literature review on buckling is presented. This literature starts from Euler's buckling model to more advanced phenomenon's, buckling in the drilling industry and the different critical loads approximations for different types of wells.

In the third chapter, we will study the Arthur Lubinski's buckling in vertical wells, understanding the model and using the results to discuss the phenomenon. In the following chapter another approach for curved wellbores will be undertaken, one that allows us to determine the bending moment and tension within a drill string, identifying additional loads applied on the drill string and their models.

To round up this work, using WellScan software, we will present the impact of some parameters on drilling parameters, and the value of using computational tools to plan out a well and to conclude the manuscript of the project we draw some conclusions and provide recommendations.

Chapter 1 Overview of Drilling the Oil & Gas Industry

This chapter is devoted to give some insights on the drilling operation, the systems used and the common terminology employed by drilling engineers and workers. At the end of the chapter, a well posed problematic is presented to facilitate to the readers the understanding of the present subject. Although we understand that this chapter is quiet long, however, we find it necessary to properly cover all the base knowledge required to comprehend the drilling operations in the oil & gas and how they related to our problem.

1.1 Rotary Drilling

Rotary drilling is a complex mechanical technique in which a drill bit is attached to the Bottom hole assembly where rotational motion is applied to cut the rock in a forward direction. Rotary drilling is new as compared to cable tool drilling. The first rotary drilling rig was developed in France in the 1860's. At the time, it was believed that most hydrocarbons were under hard-rock formations that could be easily produced by the cable-tool rigs. The first rotary drilling rigs were introduced in 1890 to cut soft formations where cable-tool drilling was extremely inefficient due to caving. However, the rotary drilling system that circulates fluid to remove the rock cuttings was first successfully used in Corsicana, Texas in the early 1900 to get water. The first major success for rotary drilling was at Spindletop, Texas in 1901 where oil was discovered at a depth of 1020 ft and produced about 100,000 bbl/day (barrel/day). With time, the improvement of design of rotary drilling system made it easy to bore a hole up to a depth of 30,000 ft. The conventional rotary drilling rigs for an onshore and an offshore are shown in Figure 1-1.

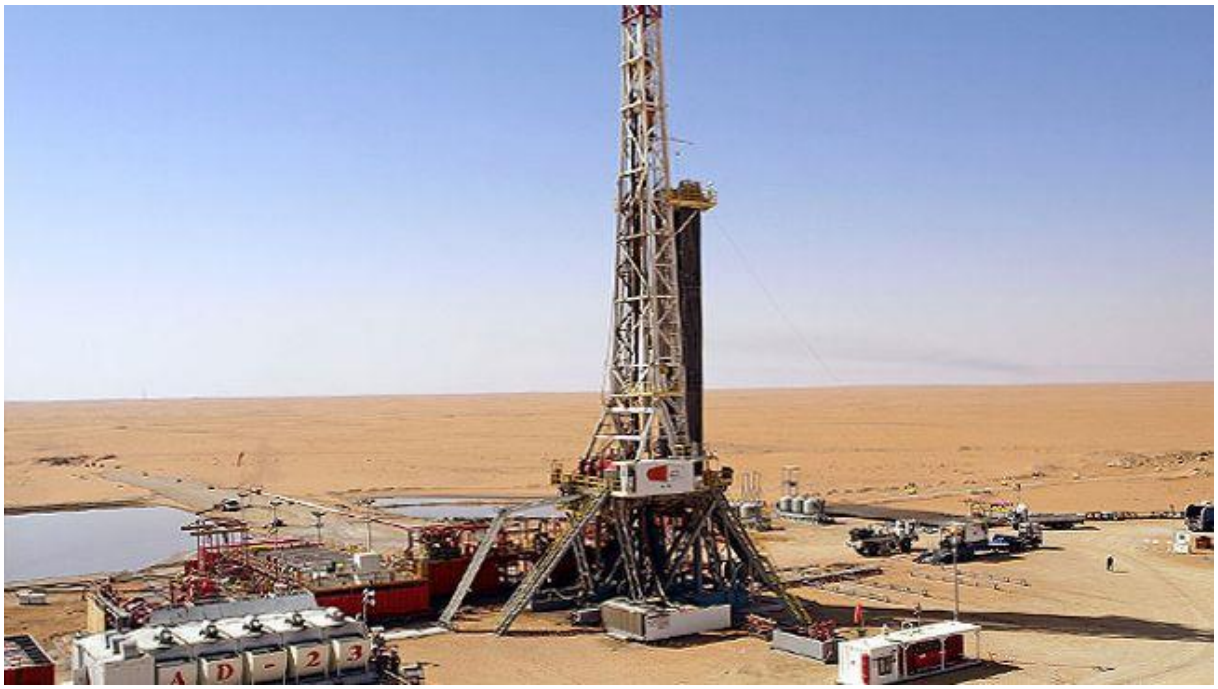

Figure 1-1 A picture of an onshore rotary rig

In the rotary drilling method, a large, heavy drill bit is attached to the tip of the bottom hole assembly where a downward force is applied. The bit is rotated by a drill string composed of high quality drill pipe and drill collar. New sections of drill pipe assembly are added at the top of the hole as drilling progresses. The taller the rig structure, the longer the drill pipe sections that can be strung together. When it is time to replace the drill bit, the whole drill string must be pulled out of the hole. Each pipe is unscrewed and stacked on the rig floor. The cuttings are lifted from the bore hole by injecting drilling fluids (drilling mud) through drill pipe and bit nozzles. The drilling fluid is collected at the surface and passes through different tanks and separators to treat the mud properly. Once the mud is ready, the cycle repeats again.

1.1 Drilling Rigs

Currently, rotary drilling is the standard oil well drilling method for the drilling industry, with almost all operations being performed by rotary-drilling rigs. Rigs will vary widely in size, drilling capability, level of automation, and environment in which they can operate. Nevertheless, the basic rotary-drilling process is the same for all types of rigs. The well is drilled using a bit that, under a downward force and

rotation, breaks the rock into small pieces. The force is provided by the weight of pipes placed above the drilling bit, while rotation generally is provided at surface by equipment that rotates the drill string, which in turn transmits rotation to the bit. As the bit drives into the ground, deepening the well, new pipes are added to the drill string. The small pieces of rock (cuttings), resulting from the bit action, are transported to surface by a fluid (drilling fluid or mud) that is constantly pumped into the hollow drill string all the way to the bottom of the hole, where it passes through small orifices placed at the bit, and returns to surface carrying the cuttings through the annular space formed between the well and the drill string. [1]

Once reaching the surface, the cuttings are separated from the fluid, which is treated for reuse. Generally, rotary rigs are classified as either land rigs or marine rigs. we can show rig classification under those categories.

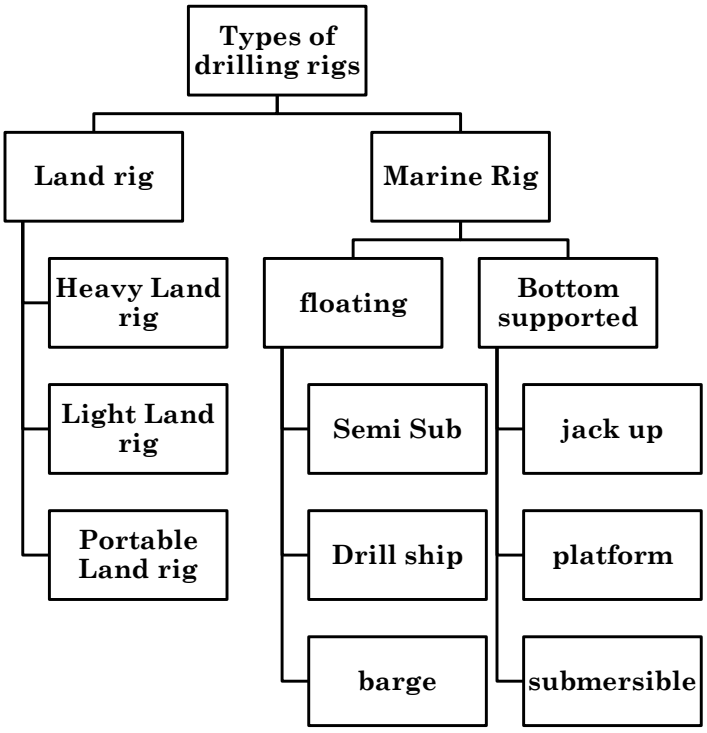

Figure 1-2 Chart for types of drilling rigs

1.1.1 Land rigs

Land Rig (onshore): A Land Rig is a drilling rig which is specially designed to drill holes on onshore locations. The rig can be a large industrial structure with all the drilling equipment and tools, or a small rig which can be transferred from one

location to another. In order to transport them, they are broken down and later assembled at the new site. The classification of onshore drilling rigs is presented in the table below[2]:

Table 1-1 Classification of drilling rig

onshore drilling rigs fall into four groups	Another criterion for classification is the power installed on the rig, which for oil well drilling is in the range of at least 10 HP every 100 feet in depth
Light rigs, down to 2,000 m	Light rigs, up to 650 HP
Medium rigs, to 4,000 m	medium rigs, up to 1,300 HP
Heavy rigs, to 6,000 m	heavy rigs, up to 2,000 HP
Ultra-heavy rigs for greater depths	ultra-heavy rigs, 3,000 HP and more.

1.2 Main Rig systems components:

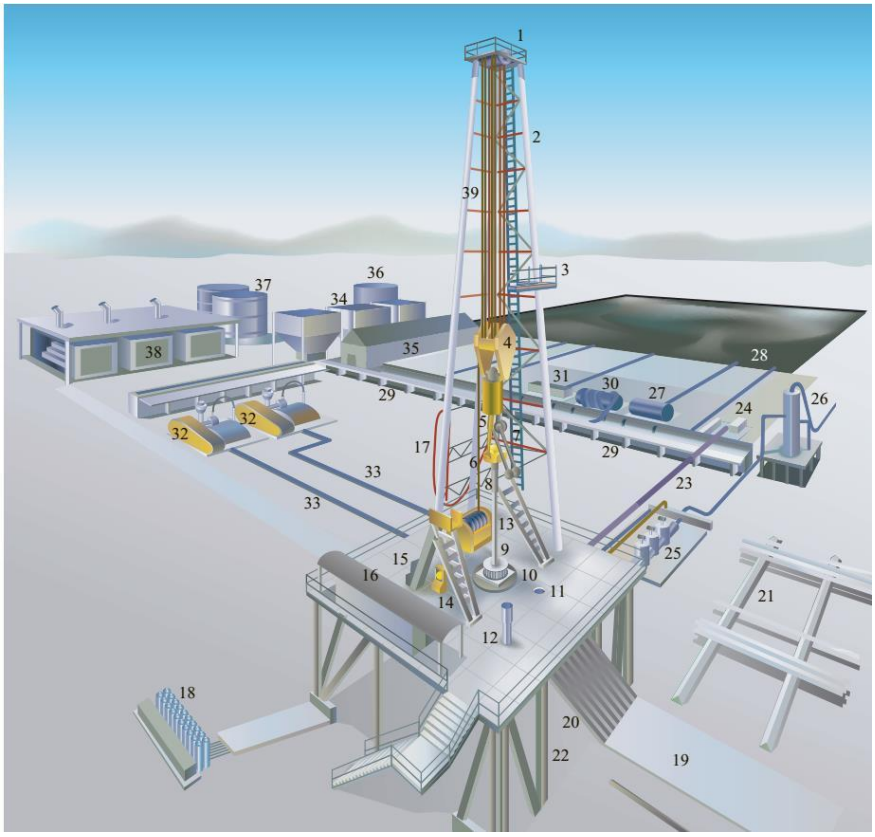

Figure 1-3 A modern rotary drilling rig and its components.

1crown block	2 mast	3 monkey board	4 travelling block	5 hook	6 swivel
7 elevators	8 kelly	9 kelly bushing	10 master bushing	11 mousehole	12 rathole
13 drawworks	14 weight indicator	15 driller's console	16 doghouse	17 rotary hose	18 accumulator unit
19 catwalks	20 pipe ramp	21 pipe rack	22 substructures	23 mud return line	24 shale shaker
25 choke manifold	26 mud gas separator	27 degasser	28 reserve pits	30 desander	31 desilter
32 mud pumps	33 mud discharge lines	34 bulk mud components storage	35 mud houses	36 water tank	37 fuel storage
38engine and generators	39 drilling line				

1.2.1 Rotary System

A rotary system is designed to give the continuous rotation from the surface to the drill string assembly to achieve bit rotation. This system includes all of the equipment used to attain bit rotation. There is a rotating machine (rotary table) on the rig floor, through which drill pipe is run. The drilling bit is screwed on (or made up) to the end of the drill pipe and lowered into the hole. As the hole gets deeper more sections of drill pipe are added to the drill string on surface. When the rotary table is engaged it rotates the pipe and the bit, which cuts away the rock at the bottom of the hole. A schematic diagram of different components of rotary system is shown in the Figure 1-3. The main components of rotary system include swivel, kelly, rotary table rotary drive, drill pipe and drill collars. There are some other related components such as kelly bushing, kelly hose and bit etc. [3]

A set of slips is used to suspend pipe in the rotary table when making or breaking a connection. Slips are usually designed to have three hinged segments, which have a tapered finish outside. The inside has an uneven surface which grips the pipe. Two large wrenches (tongs) are used to break a connection. A stand of pipe is raised up into the derrick until the lowermost tool joint appears. The roughnecks drop in the slip to wedge and support the rest of the string. The breakout tongs are latched above the connection, the makeup tongs below the connection. Both tongs are usually connected by a chain to their respective catheads (the makeup cathead is usually on the driller's side of the draw works). With the makeup tong held in position, the driller operates the breakout tong and breaks the connection. [4]

To make a connection the makeup tong is put above, and the breakout tong below the connection. This time the breakout tong is fixed, and the driller pulls on the makeup cathead until the connection is tight. Although the tongs are used to break or tighten up a connection to the required torque, other means are available to screw up the two joints prior to torquing up [1]:

- For making up the kelly the lower tool joint is fixed by a tong while Kelly is rotated by a kelly spinner, using compressed air.
- A tong may be clamped around the top tool joint while the table is rotated clockwise to unscrew the connection.
- A drill pipe spinner (power tong) may be used to make up or back off a connection (powered by compressed air).

- For making up some subs or special tools (i.e. MWD subs) a chain tong is often used.

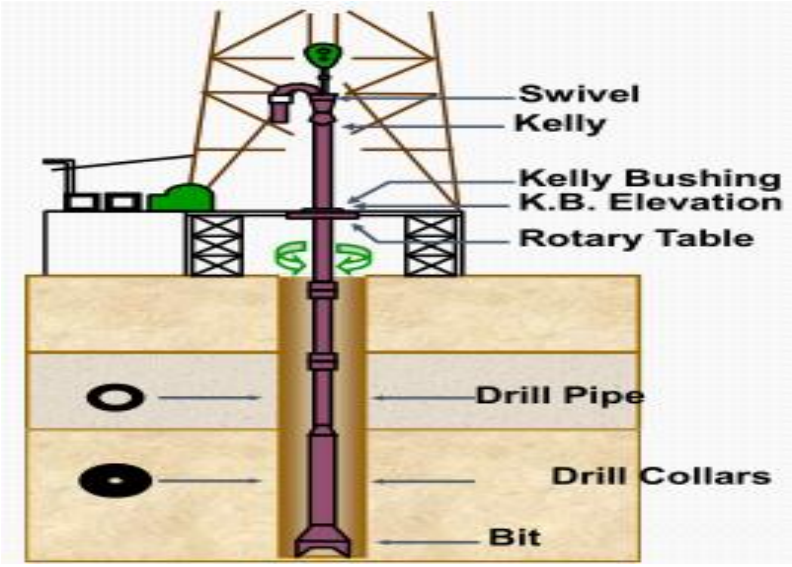

Figure 1-4 Different components of rotary system

Rotary table

The rotary table makes the drill string rotate and supports its weight during operations orduring the connection of a new drill pipe, when it cannot be borne by the hook. [5]

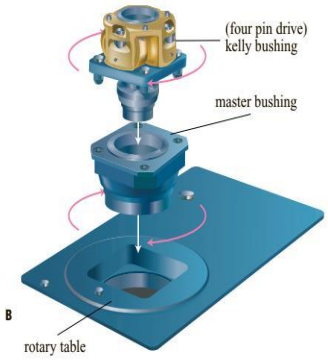

Figure 1-5 Rotary table

1.2.2 Downhole Drilling Tubulars

The drill string assembly consists primarily of the kelly, drill pipe, bottom hole assembly (BHA), and drill bit. The drilling fluid and rotational power are

transmitted from the surface to the bit through the drill string. Figure 1-5 shows the usual arrangement of drill string components and bit. The drill pipe section contains conventional drill pipe, and heavy weight pipe. The drill pipe is attached with a square or hexagonal pipe called kelly at the upper end of the drill string. The BHA may contain the following items such as: drill collars, stabilizers, jars, reamers, shock subs and bit sub. In addition, the drill string may include shock absorbers, junk baskets, drilling jars, reamers, and other equipment. There are some special tools in the BHA or drill pipe, which may include monitor-while-drilling (MWD) tools, and drill stem-testing tools. Finally, there exists drill bit at the lower end of the drill string. Heavy walled large-diameter drill collars furnish bit load. [2]

The drill bit is attached to the drill collars by means of a bit sub. For an effective rock cutting, the lower part of the drill collar is stacked onto the drill bit to provide the WOB. The drill cuttings generated by the rock bit are removed from the bottom of the hole by the drilling fluid, which is circulated inside the drill string and through the drill bit into the annular space between the drill string and the bottom hole wall. Stabilizers are placed above the bit to control the direction in which the drill bit penetrates the formation. Downhole motors with bent subs and rotary-steerable tools are also used for controlling the direction in which the bit drills.

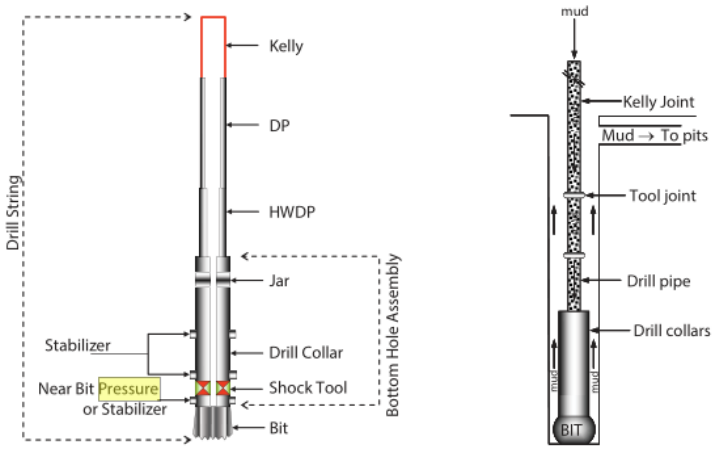

Figure 1-6 Components of the drill string.

Drill Pipe

Drill pipe is the major component of the drill string, which forms the upper part of the drill string. It has a seamless pipe with threaded joints at either end known as tool joints. Each section of pipe is called a joint with a box (female) and pin (male) located on the ends. At the one end of the pipe there is the box, which has the female thread. Drill pipe is threaded together or assembled in sections and put into the hole as the bit turns. The other end is the male thread known as the pin. These tool joints provide a shoulder that suspends the drill pipe in the slips or elevators.

They are standardized according to API standards and classified on the basis of their length (usually about 9.14 m), their outside diameter, their linear weight and their steel grade.

Figure 1-7 Drill pipe arrangement.

Heavy Weight Drill Pipe

The use of a heavy weight drill pipe (HWDP) in the drilling industry has become a widely accepted practice. It has a greater wall thickness than ordinary drill pipe. The pipe is available in conventional drill pipe outer diameters. However, its increased wall thickness gives a body weight of 2–3 times greater than regular drill pipe (Figure 1-6). HWDP provides three major benefits to the user, it reduces drilling cost by virtually eliminating drill pipe failures in the transition zone, it significantly increases performance and depth capabilities of small rigs in shallow drilling areas through the case of handling and the replacement of some of the drill collars, and it provides substantial savings in directional drilling costs by replacing

the largest part of the drill-collar string, reducing down hole drilling torque and decreasing tendencies to change direction. The major functions of HWDP are to reduce failures at transition zone, to reduce downhole torque and drag in directional drilling, and to reduce differential sticking. [1]

Most HWDP have an integral center upset acting as a centralizer and wear pad. It helps prevent excessive tube wear when run in compression. This pipe has less wall contact than drill collars and therefore reduces the chances of differential pipe sticking. HWDP is often used at the base of the drill pipe where stress concentration is greatest. The stress concentration is due to, the difference in cross section and therefore stiffness between the drill pipe and drill collars, and the rotation and cutting action of the bit can frequently result in a vertical bouncing effect.

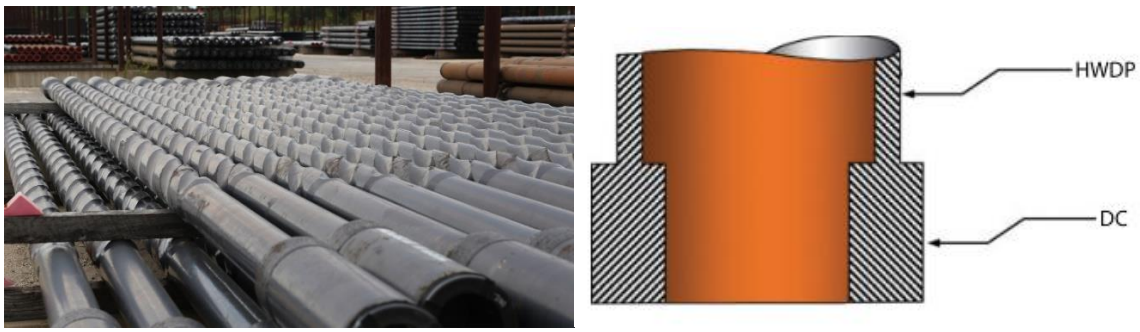

Figure 1-8 Heavy weight drill pipe

Bottom hole Assembly

The bottom hole assembly (BHA) is the component of the drill string located directly above the drill bit and below the drill pipe. The primary component of the BHA is the drill collar. Therefore, it has a significant effect on drill bit performance. The other components of BHA are stabilizers, jars, reamers, crossovers, shocks, hole-openers, and various subs such as bit subs, shock subs. In addition to these main components, the BHA typically consists of a down hole motor, rotary steerable system (RSS), and measurement and logging while drilling tools (MWD and LWD respectively. However, some classify the drill bit as a part of the BHA. It hangs below the drill pipe and provides weight to the drill bit to induce the teeth to penetrate the formation. The functions of BHA are, to protect the drill pipe in the drill string from excessive bending and torsional loads, to control direction and

inclination in directional holes, to drill more vertical and straighter holes, to reduce severities of doglegs, key seats, and ledges, to assure that casing can be run into a hole, to reduce rough drilling (rig and drill string vibrations), and as a tool in fishing, testing, and work over operations.

Drill Collars

Drill collars (DC) are heavy, stiff steel tubulars, which have a much larger outer diameter and generally smaller inner diameter than a drill pipe. They are used at the bottom of a BHA to provide weight on bit and rigidity. The primary function of the drill collar is to provide sufficient weight on bit. The weight of the collar also ensures that the drill pipe is kept in tension to prevent buckling.

Drill collars add weight to the bit and make the bit cutters bite into the rock. Normally multiple drill collars are used to add weight. The purposes of drill collars are to put extra weight on bit, so they are usually larger in diameter than drill pipe and have thicker walls, to keep the drill string in tension, thereby reducing bending stresses and failures due to fatigue, to provide stiffness in the BHA for directional control, to stabilize the bit. The weakest point in the drill collar is the joint, therefore the correct make up torque must be applied to prevent failure.

We have two types of drill collars: Square Drill Collars and Spiral Drill Collars

- Square Drill Collars:

Square drill collars provide the ability to maximize the available weight on the bit when drilling in challenging formations. The square design has a larger cross-sectional area than round drill collars, which increases its stiffness and rigidity to prevent deviation while drilling. The square shape also provides four-point stabilization to prevent buckling. Square geometry makes for a stable and stiff BHA ideal for drilling in hard formations requiring all available weight on the bit. The square drill collar achieves four objectives, it provides continuous centralization over their length, it maximizes bending resistance (stiffness), it maximizes torsional damping, and it minimizes axial vibrations. These collars are usually 1/16 less than bit size and are run to provide maximum stabilization of the BHA. [1]

- Spiral Drill Collars

Spiral drill collars decrease the risk of differential pressure sticking of the BHA the spiral drill collars usually have slip and elevator recesses. Stress-relief groove pins and bore back boxes are optional. In directional drilling, spiral drill collars are preferable. The spiral grooves machined in the collar reduce the wall contact area by 40% for a reduction in weight of only 4%, thus reducing the chances of differential sticking. This is likely to happen when the formation is highly porous, a large overbalance of mud pressure is being used and the well is highly deviated. The problem can be overcome by reducing the contact area of the collar against the wellbore. [1]

Figure 1-9 Spiral Drill Collars

Figure 1-10 Drill Collars

Stabilizers

A stabilizer consists of a length of pipe with blades on the external surface and located above the bit. These blades may be either straight or spiral and there are numerous designs of stabilizers (Figure 1-10). The blades can either be fixed on to the body of the pipe or mounted on a rubber sleeve (sleeve stabilizer), which allows the drill string to rotate within it. According to the blades, stabilizers can be categorized. The function of the stabilizer depends on the type of hole being drilled. However, the functions of stabilizers are, to control hole deviation, to reduce buckling and bending stresses on the drill collars, to prevent wall thickening, to improve performance of the bit, to allow higher WOB since the string remains concentric even in compression, to centralize drill collars in hole and increase

stiffness, increase ability of drill collars to drill smooth straight hole, and to wipe wall of hole to ensure full gage. [5]

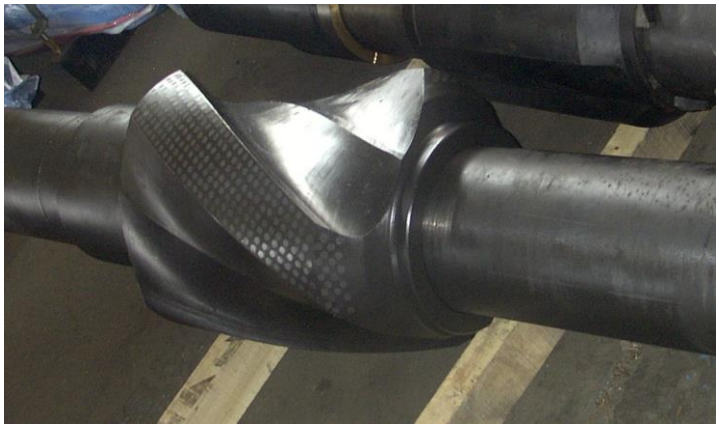

Figure 1-11 Heavy Drilling Stabilizers

Drilling Bit

Technically, the drill bit is not a component of the BHA. However, it does generate and send axial and torsional loads to the BHA. It is located at the bottom end of the drill string and makes contact with the subsurface layers, and drills through them. A drilling bit is defined as the cutting or boring tool, which is made up on the end of the drill string. Its basic function is to cut rock at the bottom of the hole. The bit consists of a cutting element (cutters) and a fluid circulation element (nozzles). The drill bit is rotated mechanically to crush and penetrate new formations. The broken and loosened rocks are known as cuttings, which are removed from the wellbore by circulating drilling fluid down the drill pipe and through nozzles in the drill bit. The bit drills through the rock by scraping, chipping, gouging or grinding the rock at the bottom of the hole. Drilling fluid applies hydraulic power to improve penetration rates. The penetration rate of a bit is a function of several parameters including WOB, RPM, mud properties and hydraulic efficiency. There are several bit sizes ranges from 3¾ inches to 26 inches in diameters. The most commonly used sizes are 17½, 12¼, and 6 ¼ inches.[1] [1]

[1] 1 inches= 0,0254m

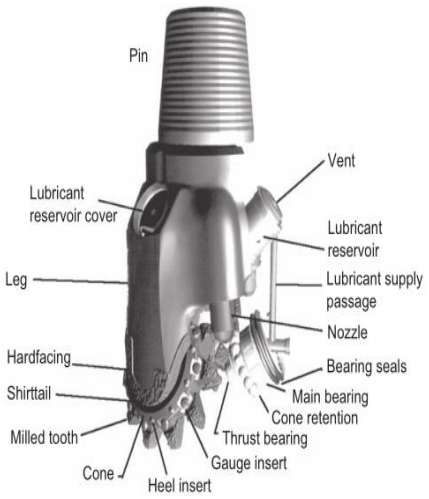

Figure 1-12 Roller Cone Bit

1.2.3 Casing

Casing the borehole is one of the most important parts of drilling operations. However, casing is normally set to serve a specific purpose and is neither arbitrary nor compulsory for any hole condition. The casing transforms the well into a stable, permanent structure able to contain the tools for producing fluids from underground reservoirs. It supports the walls of the borehole and prevents the migration of fluids from layers at high pressure to ones at low pressure. Moreover, the casing enables circulation losses to be eliminated, protects the hole against damage caused by impacts and friction of the drill string, and acts as an anchorage for the safety equipment such as BOPs. Failure of casing or tubing results in expensive reworking and may lead to loss of the well, or loss of life. Casing serves the following important functions in the well. [6]

- It helps to keep the hole open and provides support for weak, vulnerable or fractured formations.it prevents the collapse of the borehole during drilling, and the hole from caving[2] in or washing out[3].

[2]Pieces of rock that came from the wellbore but that were not removed directly by the action of the drill bit.

- It prevents cross channeling between two or more subsurface fluid-bearing layers.
- Prevent contamination of freshwater well zones.
- Prevent unstable upper formations from caving-in and sticking the drill string or forming large caverns.
- It minimizes the formation of damage by drilling mud (i.e. water-sensitive shale, hydrocarbon-bearing zones).
- It provides a passage for hydrocarbon fluids and most production operations are carried out through special tubing, which is run inside the casing

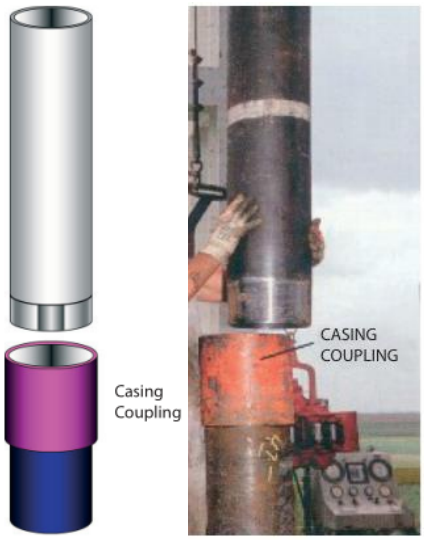

Figure 1-13 Installing conductor casing

1.3 Drilling parameters

There are parameters that significantly affect drilling operations. These parameters are normally used for drilling optimization. Therefore, it is important to know about those parameters. In general, drilling parameters may be broadly classified under two types, rig and bit related parameters, and formation parameters. The rig and bit related parameters can be controlled but the formation parameters have to be dealt with. The formation parameters recorded for drilling optimization are critically important to be representative of data they are meant to reflect. Many drilling

[3]An enlarged region of a wellbore. A washout in an open hole section is larger than the original hole size or size of the drill bit. Washout enlargement can be caused by excessive bit jet velocity, mechanical damage by BHA components,

parameters affect the performance of the drilling operation. If they are not adjusted properly, they will make the operation less economical. Rig and bit type parameters are broadly categorized as weight on bit or hook load, rotational speed (RPM), torque, and hydraulic parameters (i.e. Bit hydraulics) – flow rates, density of drilling fluid etc.

However, WOB, RPM, flow rate, bit hydraulics, and more importantly the type of bit are the most important drilling parameters affecting drilling operations because they are affecting rate of penetration (drilling speed) and the economics of drilling. The parameters that come under the formation type are local stresses, mineralogy, formation fluids, rock compaction and abrasively of formation. Beyond the above stated parameters, determining the rate of penetration is among the most sought-after parameters in drilling industry. This is due to the fact that it allows for optimization of drilling parameters to decrease drilling costs and enhance drilling process safety. Among the above factors, some of the parameters are discussed below.

1.3.1 Weight on Bit

Represents the amount of weight applied onto the bit. It is the abbreviation for "Weight on Bit". This load is then transferred to the formation which in turn is the energy created together with string speed that advances drill string. It is measured through the drilling line, usually by means of having attached a strain gauge, which measures the magnitude of the tension in the line itself and gives the weight reading based on the calibration. This sensor measures a unique value, which is the over- all weight (Hook-load) of the string including the weight of the block and Top Drive System (TDS).

1.3.2 RPM

This parameter stands for "revolutions per minute". It represents the rotational speed of the drill string. With the invention of TDS, the reading is directly linked to the electronics of the unit itself. It is considered that the measurements for this parameter are accurate as long as the acquisition system set-up has been thoroughly made up.

1.3.3 Torque

This parameter is the torque of the drill string while it is rotating. It is measured by means of TDS systems. Previously the readings for this parameter were relative. This parameter is going to be significantly important for inclined and highly deviated wellbores, which is also related with the wellbore cleaning issues.

1.3.4 ROP (Rate of Penetration)

This parameter is the most important parameter, since all of the calculations in this study are based on estimations of ROP. It is measured through the relative change of the position of the block in time. Accurate calibrations are very important in order to have a representative ROP parameter.

1.3.5 Drag

The force required to move the drill string due to the drill string being in contact with the wall of the borehole.

1.3.6 mud weight

The mass per unit volume of a drilling fluid, synonymous with mud density. Weight is reported in lb/gal (also known as ppg), kg/m3 or g/cm3 (also called specific gravity or SG), lb/ft3 or in hydrostatic gradient, lb/in2/ft (psi/ft). Mud weight controls hydrostatic pressure in a wellbore[4] and prevents unwanted flow into the well. The weight of the mud also prevents collapse of casing and the open hole. Excessive mud weight can cause lost circulation by propagating, and then filling, fractures in the rock. Mud weight (density) test procedures using a mud balance have been standardized and published by the API[5].

1.4 Directional Drilling

In the early times of oil well drilling most wells were drilled vertically (a conventional method), straight down into the reservoir. Although these wells were

[4] The hole made by the drilling bit, which can be open, cased, or both, also called borehole, hole, or wells.

[5] The American Petroleum Institute

considered to be vertical, they rarely were. Some deviation in a wellbore will always occur, due to formation effects and bending of the drill string. The first recorded instance of a well-being deliberately drilled along a deviated course was in California in 1930. This well was drilled to exploit a reservoir which was beyond the shoreline underneath the Pacific Ocean. It had been the practice to build jetties out into the ocean and build the drilling rig on the jetty. However, this became prohibitively expensive and the technique of drilling deviated wells was developed. Since then many new techniques and special tools have been introduced to control the path of the wellbore.

An operating company usually hires a directional drilling service company to: provide expertise in planning the well; supply special tools; and to provide on-site assistance when operating the tools. The operator may also hire a surveying company to measure the inclination and direction of the well as drilling proceeds.

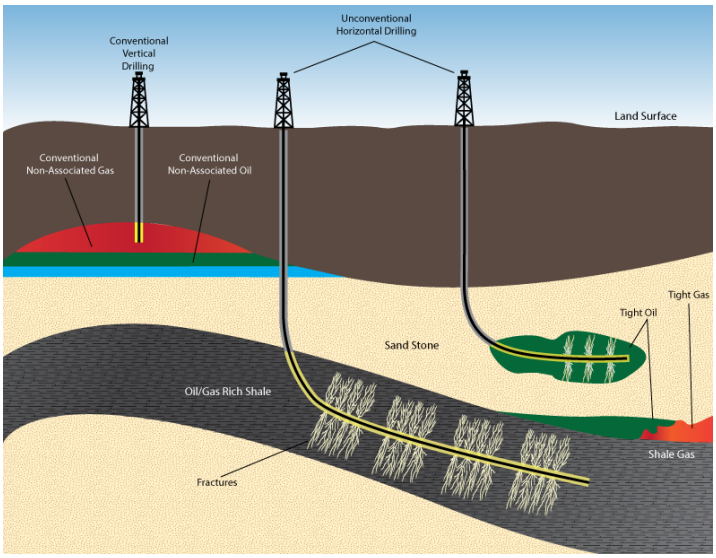

Figure 1-14 vertical and horizontal drilling wells

1.5 Applications of Directional Drilling

There are many reasons for drilling a non-vertical (or deviated) well. Some typical applications of directionally controlled drilling are:

- Multi-well Platform Drilling

Multi-well Platform drilling is widely employed in the North Sea. The development of these fields is only economically feasible if it is possible to drill a large number of

wells (up to 40 or 60) from one location (platform). The deviated wells are designed to intercept a reservoir over a wide aerial extent. Many oilfields (both onshore and offshore) would not be economically feasible if not for this technique.

- Fault Drilling

If a well is drilled across a fault the casing can be damaged by fault slippage[6]. The potential for damaging the casing can be minimized by drilling parallel to a fault and then changing the direction of the well to cross the fault into the target.

- Inaccessible Locations

Vertical access to a producing zone is often obstructed by some obstacle at surface (e.g. river estuary, mountain range, city). In this case the well may be directionally drilled into the target from a rig site some distance away from the point vertically above the required point of entry into the reservoir.

- Sidetracking and Straightening

It is in fact quite difficult to control the angle of inclination of any well (vertical or deviated) and it may be necessary to 'correct' the course of the well for many reasons. For example, it may be necessary in the event of the drill pipe becoming stuck in the hole to simply drill around the stuck pipe (or fish) or plug back the well to drill to an alternative target.

- Salt Dome Drilling

Salt domes (called Diapirs) often form hydrocarbon traps in what are overlying reservoir rocks. In this form of trap, the reservoir is located directly beneath the flank of the salt dome. To avoid potential drilling problems in the salt (e.g. severe washouts, moving salt, high pressure blocks of dolomite) a directional well can be used to drill alongside the Diapir (not vertically down through it) and then at an angle below the salt to reach the reservoir. [1]

[6]The gas movement through liquid phase of the reservoir front. This phenomenon also helps the liquid to move forward to the low-pressure zones (i.e., toward the earth's surface).

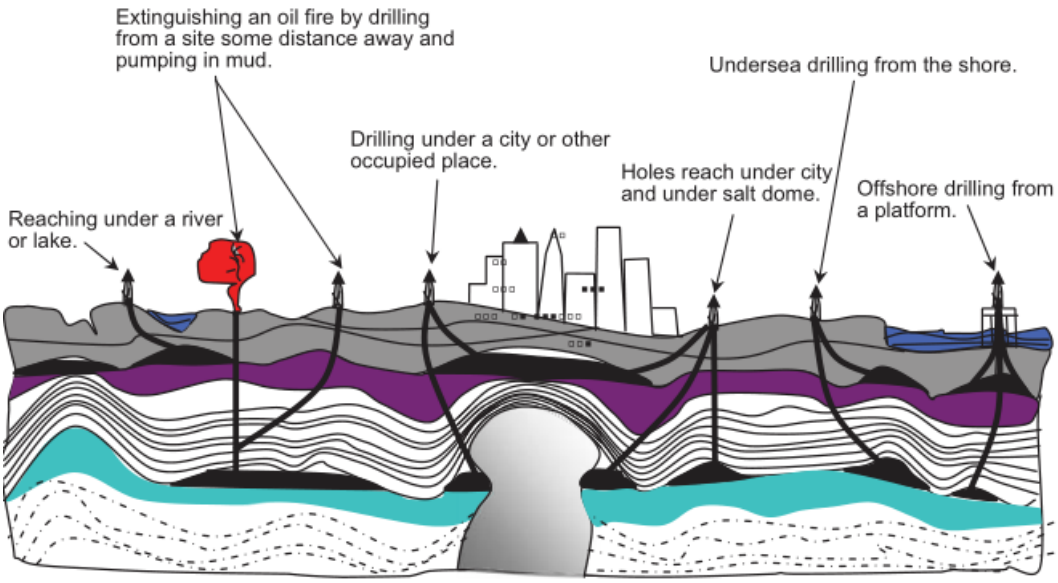

Figure 1-15 Applications of directional drilling

1.6 Basic Terminologies

Although, there are different configurations of a directional well, all directional wells have some or all of the following basic features or terminologies in common

- Kick off point (KOP): is the location at a given depth below the surface where the wellbore is deviated from vertical in a given direction (selected by designer).
- Well inclination: Well inclination is the angle by which the wellbore deviates from the vertical Sometimes referred to as "drift angle".
- End of buildup (EOB): the location where the wellbore has finished increasing.
- Hold angle: Hold angle occurs where the inclination of the borehole is held constant.
- Tangent or slant section: It occurs after a build where the inclination of the borehole is held constant for a certain distance.
- Start of drop: The location where the borehole starts dropping inclination.
- End of drop: Location where the wellbore finishes dropping inclination.
- Target Displacement: Lateral distance from the surface location to the target.
- Drop of rate (DOR): Rate at which the inclination decreases. It is usually expressed in degrees per 100t or degrees per 30m of the coarse length.
- Build up rate (BUR): Change of inclination of a wellbore where the angle is increased. the rate is usually expressed in degrees per 100ft or angular increase per 30m of the MD.

- Dog-leg severity (DLS): A normalized estimate (e.g., degrees/100 feet) of the overall curvature of an actual well path between two consecutive directional survey stations, according to the minimum curvature survey calculation method. With respect to a planned well path, dog-leg severity may at times be synonymous with build gradient and/or turn gradient. DLS - planned well bore dog-leg severity e.g. build gradient at measured depth. DLS is represented as degrees/100 feet or degrees/30 meters.
- TVD: Depth at any point or a station along a wellbore is the vertical distance from the well surface reference point to the station of interest.
- Measured depth (MD): the distance from the well surface reference point to the station of interest along the actual well path.
- Drop off section: that part of the well's trajectory where the drift angle is decreasing (i.e. returning to vertical).
- Easting: one of the coordinates used to plot a deviated well's position on the horizontal plane (along the x axis).
- Northing: one of the co-ordinates used in plotting the position of the wellbore in the horizontal plane along the y axis.
- Survey: to measure the inclination and direction of the wellbore at a particular depth.
- Azimuth (hole direction): the angle in the horizontal plane measured from a fixed reference direction (such as true or geographic north, grid north, or magnetic north) usually measured clockwise. Example of azimuth reading of a point in a directional well is 135 degrees (measuring from a reference north to the location of the point) or S45E measuring from south to east in quadrant reading. A quadrant bearing of a well is the angle in the horizontal plane measured from either a north or south reference direction towards the east or west, defining the direction of the wellbore. By industry convention, 0-degree azimuth coincides with north, 90-degree azimuth with east, 180-degree azimuth with south, and 270-degree azimuth with west. Measuring the inclination of a wellbore (its deviation from the vertical) is comparatively simple, requiring only a pendulum. Measuring the azimuth (direction with respect to the geographic grid in which the wellbore is running from the vertical), however, was more difficult. there are three azimuth reference systems: true (Geographic) north, grid north and magnetic north.

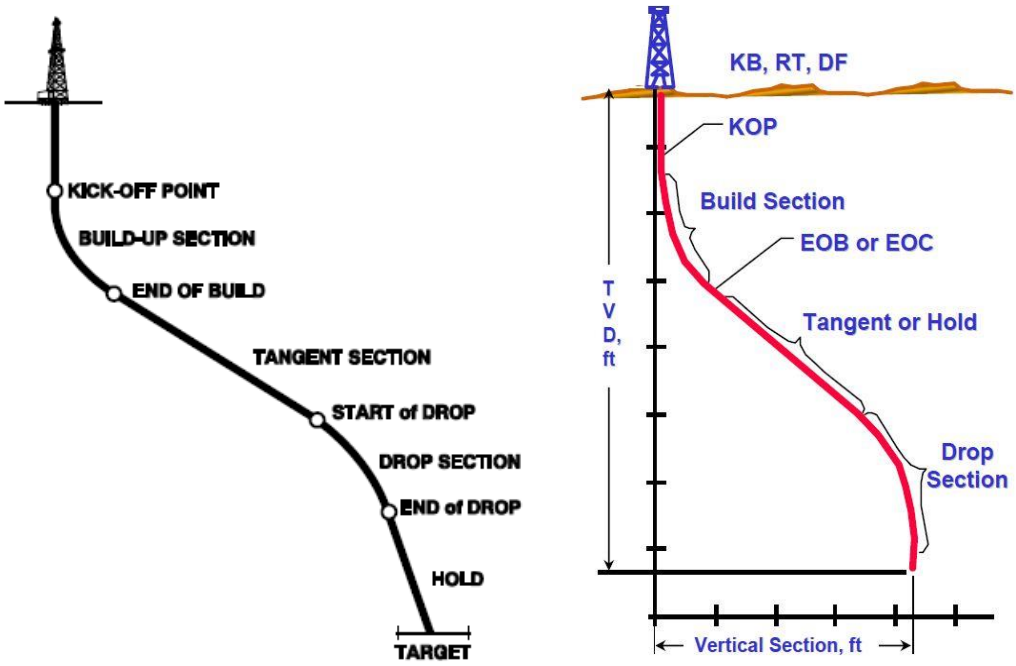

Figure 1-16 Horizontal well trajectory with one buildup trajectory

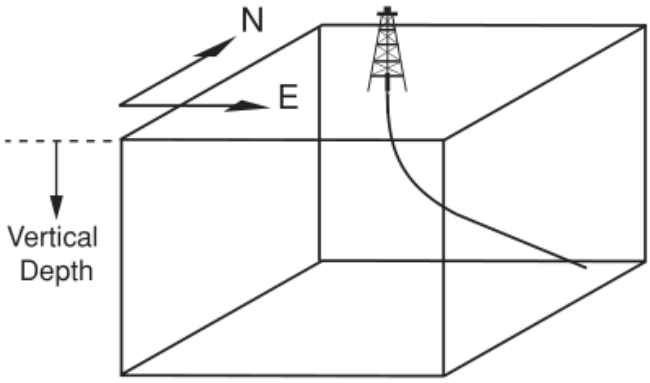

Figure 1-17 Well Planning Reference Systems

1.6.1 Tools and Techniques for Kicking Off the Well

here are three methods of accurately kicking off the well—jetting, whipstock, and downhole motors. The motor techniques are most commonly used because they are fast and accurate. However, the whipstock is still used. Jetting is rarely used, but it's still a valid and inexpensive technique.

Whipstock

This is an old method of deviating the well (which is still used) is the whipstock. This is a wedge with a concave face that is placed in the well. The face of the whipstock is pointed in the direction the well must go. Once the whipstock is set on the bottom, the drill bit starts to rotate and drill away rock on the side of the wellbore. As the bit starts to drill and moves lower down the face of the whipstock, the wedge-shaped profile of the whipstock forces the bit further into the formation.

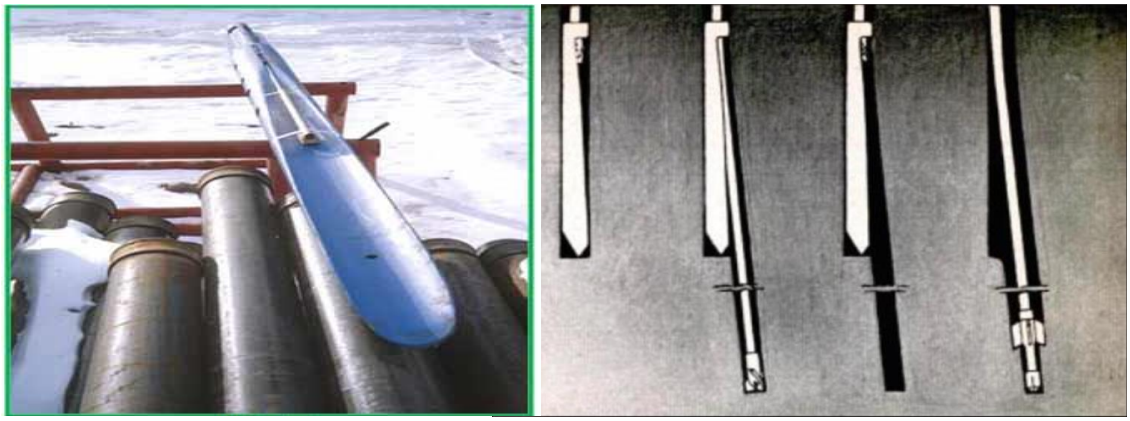

Figure 1-18 Whipstock Used to Deviate a Well

Jetting

Another old method, "low tech" technique that can still be worth using in suitable circumstances. A drill bit using rotating cones to cut the rock usually has three cones. Between the cones are nozzles that direct the flow of high-pressure mud past the cones and to the bottom of the hole.

Downhole motor and bent sub

A downhole motor looks somewhat like a drill collar on the outside. Inside the motor is a mechanism that converts hydraulic horsepower (from drilling mud being pumped through the motor) to rotary power. The drill bit is made up on the bottom of the motor. With the drill string stationary and the mud pumps on, the bit turns and will drill.

1.7 Drilling problematics

As seen, the drilling operation is a complicated task, one that requires the work of many engineers, from different fields, and that level of complexity is bound to generate problems, these are hindering to the operation, as they cause financial losses, time losses and in extreme cases, represent dangers to the human life, and although precautions are taken, accidents do happen.

Some of the major problems that can occur in a drilling operation are lost circulation which is defined as follows:

he significant and continuing loss of whole mud or cement slurry to a formation, is one of the most common and troublesome downhole problems. It has been a hindrance to drilling completion and workover operations ever since rotary rigs first came into use, and it continues to have a profound negative impact on well economics.

Although drilling ahead and primary cementing pose particular risks, lost circulation can occur during any well procedure that involves pumping fluid down the hole. Indications of lost circulation may range from a gradual drop in pit level to a partial or complete loss of returns. In extreme cases, the fluid level in the annulus may drop rapidly, sometimes by hundreds of feet.

Another common issue is kick; a kick is a well control problem in which the pressure found within the drilled rock is higher than the mud hydrostatic pressure acting on the borehole or rock face. When this occurs, the greater formation pressure has a tendency to force formation fluids into the wellbore. This forced fluid flow is called a kick. If the flow is successfully controlled, the kick is considered to have been killed. An uncontrolled kick that increases in severity may result in what is known as a "blowout." This phenomenon is very dangerous and is the major cause for explosions seen in oil rigs, such as the deep-water horizon event that occurred in 2010 in the Gulf of Mexico.

For our work, we will be focusing on the study of another phenomenon, one that affects drilling operations efficiency, inflating costs and significantly delaying time tables in the drilling operations, it is the buckling phenomenon, it increases torque and drag loads on the drill strings, causing failure due to fatigue, shearing,

sticking, and in some extreme cases lock-up, where the drilling operation is completely stopped and extreme measures are needed to rehabilitate the drilling rig. We will be defining this phenomenon, it's parameters and conditions in the following chapters, as well as presenting some models from literature that are used to represent it.

Chapter 2 Buckling in the Oil & Gas Industry

2.Overview of Buckling

Buckling is a mechanical failure mode that occurs when a structure is subjected to compressive stress, it is characterized by a sudden sideways deflection of a structure, causing it to lose its linearity.

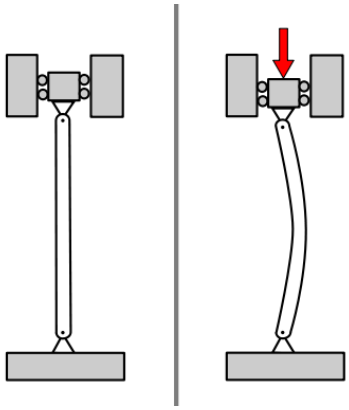

Figure 2-1 A column under a concentric axial load

Unlike other forms of mechanical failures, buckling a structure won't break, it will continue to support the load and further loads in a laterally-deformed state.

Several other definitions have been given to the phenomenon of mechanical buckling. Field engineers consider mechanical buckling as the imminent or instantaneous collapse of a structure due to external and/or internal loads which would not be sufficiently intense to cause mechanical yield of the material in the structure. It is considered a total instability of the structure. Theoretical engineers contemplate mechanical buckling as a confluence of stable and unstable equilibrium states of a system, which includes the structure and its loads, and under which conditions the total potential energy of the system becomes or stays stationary. Mathematicians, on the other hand, ponder buckling as possible states that a system may assume which will show abrupt changes in its behavior. These states may be mathematically characterized by bifurcations, eigenvalues or singularities.

Mechanical buckling can occur in columns, beams, plates, shells, arches, rings, and more complex engineering elements and structures. Axial and lateral force, moment, torque, and pressure are the most common driving loads.

The phenomenon of mechanical buckling has been studied for centuries and constitutes a well-developed but still incomplete branch of the mechanics of

materials. One area of incompleteness is the mechanical buckling of drill strings within bore-holes. [7, 8]

2.1 Euler's buckling

The earliest study of mechanical buckling was performed by Euler, seeking critical loads and the deformed shape of a beam under axial compression loads.

The critical load as defined above for a structure can be obtained by studying the behavior of an ideal column supposed to be perfectly rectilinear initially and compressed by a force applied along its axis. Consider then the case of a beam of vertical thin constant section embedded in a base (support or ground) and loaded along its axis, at the top (Figure 2-2)

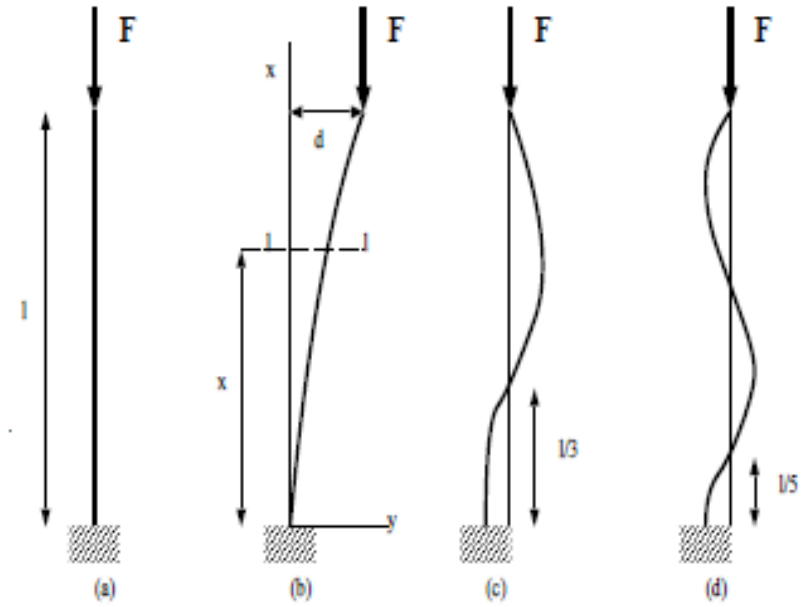

Figure 2-2 The first 3 modes of buckling of a straight beam of constant section embedded at one end and free at the other

In this form the problem of buckling was studied for the first time by Euler in 1744 [9]. We assume the perfectly elastic beam and we also admit that we do not exceed the proportional limit. As long as F remains below the critical value, the Beam is simply subjected to axial compression but remains straight: this rectilinear form of balance is stable. By gradually increasing F, we arrive at a state where the rectilinear form becomes unstable. The critical force (or Euler force) is then defined as being the axial force sufficient for the beam to retain a slightly bent shape (Figure 2-2b)

This force can be calculated using the differential equation of the elastic line and assuming that the beam is slightly bent. By taking the hypothesis of small deformations and adopting the axes indicated on the (Figure 2-2b) we can write the relation which links the bending moment M for any section of the drill pipe to its curvature

$$\mathrm{M} = -\mathrm{F}(\mathrm{d} - \mathrm{y}) = -\mathrm{EIy}'' \tag{2.1}$$

with E the modulus of elasticity of the constituent material of the beam (or Young's modulus) and I, it's moment of inertia. For a tube of outside diameter OD and of inner diameter ID, it is calculated:

$$\mathrm{I} = \frac{\pi}{64}(\mathrm{OD}^4 - \mathrm{ID}^4) \tag{2.2}$$

By posing

$$\omega^2 = \frac{F}{EI} \tag{2.3}$$

The differential equation of the elastic curve then becomes:

$$y'' + \omega^2 y = \omega^2 d \tag{2.4}$$

The general solution of this equation is:

$$y = A\cos(\omega x) + B\sin(\omega x) + d \tag{2.5}$$

where A and B are integration constants which must satisfy the conditions at the fixed ends

$$y = y' = 0 \; for \; x = 0 \tag{2.6}$$

These conditions will be satisfied if:

$$A = -d \; and \; B = 0 \tag{2.7}$$

Therefore

$$y = d(1 - \cos(\omega x)) \tag{2.8}$$

On the other hand, the condition at the upper end requires:

$$y = d \; for \; x = l \tag{2.9}$$

condition that will be satisfied if

$$dcos(wl) = 0 \tag{2.10}$$

which requires either $d = 0$, case in which there is no arrow (Figure 2-2a), or $\cos(\omega l) = 0$, i.e.:

$$\omega l = (2n - 1)\frac{\pi}{2} \tag{2.11}$$

where n is any integer. This equation determines the values of ω for which there is buckling, each value of ω corresponding to a buckling mode. The smallest value of $\omega \times l$ satisfying the previous condition corresponds to n = 1. In this case, we obtain:

$$\omega l = l\sqrt{\frac{F}{EI}} = \frac{\pi}{2} \tag{2.12}$$

From which we draw the famous Euler formula which gives the lowest axial load that can maintain the beam in a slightly curved form

$$F_{cr} = \frac{\pi^2}{l^2 \times k} EI \tag{2.13}$$

with k = 4 for the beam shown in (Figure 2-2b)

The angle ω x varies here from 0 to $\frac{\pi}{2}$ and the shape of the elastic curve is the one presented in the (Figure 2-2b).

By successively varying n = 2, 3, the corresponding values of the other critical forces are obtained:

$$F_{cr} = \frac{9\pi^2}{l^2 \times 4} EI \tag{2.14}$$

$$F_{cr} = \frac{25\pi^2}{l^2 \times 4} EI \tag{2.15}$$

The angle ωx varies in these two cases from 0 to $\frac{3\pi}{2}$ and 0 to $\frac{5\pi}{2}$ and the corresponding elastic curves are those shown respectively in Figure 2-2c and Figure 2-2d. To arrive at the shape of the Figure 2-2c a load nine times higher than the critical load and for that of the Figure 2-2d a charge twenty-five times higher is necessary.

It is thus possible to calculate the critical loads for all the other modes based on the solution of the previously treated case and on the coefficient k which characterizes the distance separating two points of inflection of the beam. For example, in the case of a beam whose two ends are hinged, it is obvious for reasons of symmetry that each half of the beam is in the same conditions as the entire beam of Figure 2-2.

We will thus obtain a critical force in which the coefficient k =1 (first mode).

Similarly, for a beam embedded at both ends, k will be ½ (second mode).

2.2 An overview of buckling of drill strings within boreholes

To drive a drill bit through geological formations and open a bore-hole, axial force on the drill bit and drill bit rotation are required at the bottom of a drill string where the drill bit is located. The drill bit is rotated by turning the drill string at the surface, or by special motors located at the bottom of the drill string. Usually

these motors are positive displacement motors (PDM)[7], powered by the hydraulic energy of the flowing drilling fluid. [8]

The axial force comes from the weight of thick walled tubes called drill collars, which are normally positioned in the lower portion of the drill string. The axial force is applied on the drill bit by slacking off part of the weight of the drill string. A lower portion of the drill string will be in compression while an upper portion will be subjected to axial tension. Increases in weight on the drill bit will eventually buckle the lower portion of the drill string. Drill collars are normally placed in the compressed section to prevent the fatigue of drill pipes. The drill collars will not fatigue because of their wall thickness and resulting stiffness.

When a drill string buckles inside the bore-hole, its geometrical configuration changes. The drill string interacts with the wall of the bore-hole in such a way that both the contact length and the contact force increase during buckling. This interaction results in a friction force, known as drag, which can absorb part or all the weight reserved for the drill bit. If the available force at the bit falls below a threshold value, the drill bit cannot advance and drilling must be terminated. Moreover, to rotate the bit operating under drill string buckling conditions requires higher torque. These fatigues the drill string reducing its life. To keep the drill bit advancing economically, excessive drill string buckling must be prevented.

[7]A downhole motor used in the oil field to drive the drill bit or other downhole tools during directional drilling or performance drilling applications. As drilling fluid is pumped through the positive displacement motor, it converts the hydraulic power of the fluid into mechanical power to cause the bit to rotate.

Figure 2-3 The picture of drill pipe buckling

To prevent excessive drill string buckling it is necessary to identify and control the mechanical parameters which affect the phenomenon. A number of competent researchers have dedicated their careers to the investigation, modeling, understanding, and explanation of drill string buckling. Their works were pertinent to three types of straight bore-hole configurations: vertical, inclined, and horizontal. Their models for vertical, inclined, and horizontal straight bore-holes have been presented, discussed, and employed in congresses, technical magazines, and companies. Also, large amounts of money have been invested in research centers and centers for advanced studies to accurately describe and model this phenomenon.

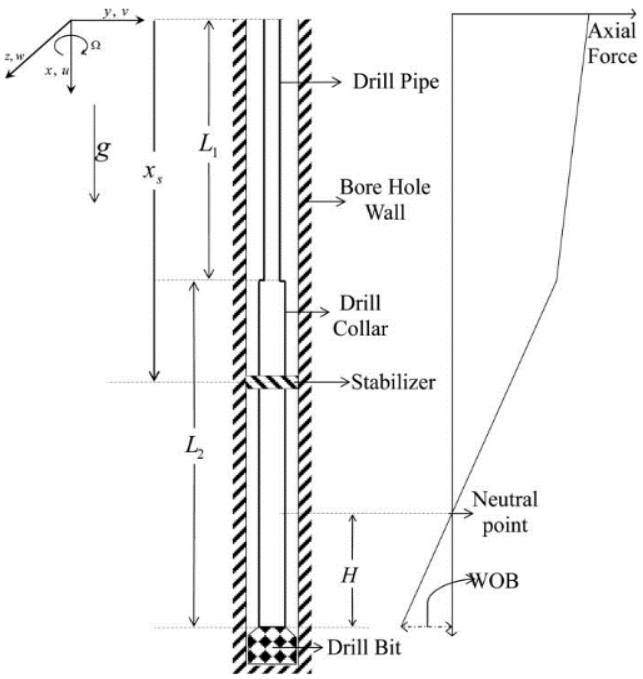

Figure 2-4 Wellbore Diagram with Tubing

the phenomenon is a little different from conventional buckling, in fact the drill string is free to deform completely, it is constrained by the walls of the well. The friction on this wall acts on the drill string while producing Torque & Drag.

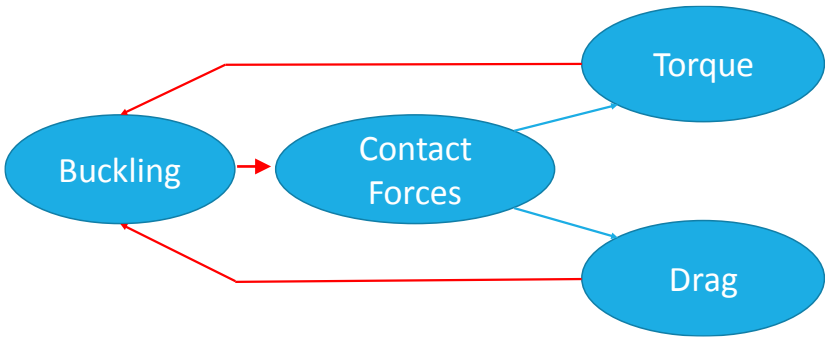

Figure 2-5 Torque-Drag-Buckling relationship

Some key parameters that guide the buckling phenomenon are the neutral point and the mudded weight or buoyancy, we define them here.

2.3 The Neutral point:

A certain point of a drill string is usually designated as the “neutral point”, in strength of materials, it is the point that is neither at tension nor compression, in the drilling industry the definition slightly differs, the weight in mud of the portion of a drilling string below the neutral point is equal to the weight on the

bit, while in reality, the hydrostatic pressure and the pump pressure fluctuate over time, causing the actual neutral point to move along the drill string, the weight in mud and weight on bit depend only upon the type of pipe or drill collar and the specific gravity of the mud. The formula for the position of the neutral point's position is

$$X_n = \frac{WOB}{w_b}$$

The distance X_n is the distance from the bit to the neutral point.

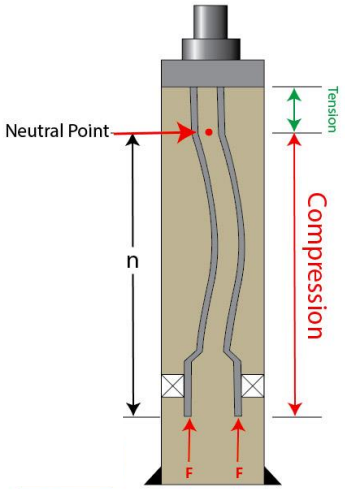

Figure 2-6Wellbore Diagram with Tubing Buckling Due to Compression Force

2.4 Weight in mud (Buoyancy)

Buoyancy is the upward force that keeps things afloat. The net upward buoyancy force equals to the amount of the weight of fluid displaced by the body volume. This force will make objects lighter when it immerses in fluid. For example, we feel ourselves lighter when we are in swimming pool because this is the effect of buoyancy.

This effect comes into consideration when modeling the loads applied on the drill string, so instead of considering the pipe's weight and the buoyancy as separate loads, we combine their effect into what is known as the weight in mud, which is determined by the weight in air of the strings, multiplied by a buoyancy factor k_b as follows:

$$w_b = w_{air} \ \ (1 - \rho_{mud}/\rho_{steel}) = w_{air} k_b \tag{2.18}$$

2.5 Buckling in vertical wells

The first work on the stability of a drill pipe was presented by Lubinski in the 1950s [10]. These studies concerned the two-dimensional buckling of drill pipes in vertical wells. The author used the polynomial series to solve the equation that governs the problem of instability. He then proposed an approximation of the critical sinusoidal buckling force of the long drill pipes induced into a vertical well:

$$F_{cs} = k \times \sqrt[3]{EIw_b^2} \quad \text{With } k = 1.94 \tag{2.19}$$

Wang (1986) [11] proposes to correct this equation, considering another value of k, which allowed him to obtain a critical force for drill pipes of almost infinite lengths. in vertical wells of the following form:

$$F_{cs} = 1.01 \sqrt[3]{EIw_b^2} \tag{2.20}$$

And recently, Wu (1993) [12] by an energy analysis has developed equations a little different from the two previous ones. These equations are intended to predict buckling in vertical wells:

$$F_{cs} = 2.55 \sqrt[3]{EIw_b^2} \tag{2.21}$$

It should be noted here that Léa (1995) [13] finds approximately the same expression of lubinski to express the force needed for a drill pipe to buckle in a vertical well:

$$F_{cs} = 1.98 \sqrt[3]{EIw_b^2} \tag{2.22}$$

These models are largely inspired by the theory of buckling vertical columns under the effect

of their own weight in which the critical force is of the form $F_{cr} = w_b L_{cr}\ with\ L_{cr} k \left(\frac{EI}{w_b}\right)^{\frac{1}{3}}$

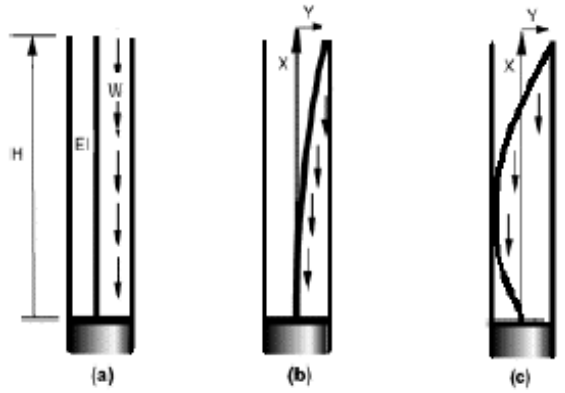

Figure 2-7 Geometry of a column subjected to its own weight

The estimated value of k from the different approximations varies according to the authors. It depends on many parameters like the type of function chosen to solve numerically the equations and especially conditions of connections. Schmidt (1998) [14] used the Rayleigh method to develop a solution to the problem: he found that the values of k ranged between 1.99 and 2.29. The value found by Lubinski is close to this interval and is confirmed, according to an experimental study, by Saliès (1994) [15]. It should be noted that the work of the latter allows to deduce:

- that k is not actually a constant
- that 1.94 is an average value
- and that the force given the Wang equation, is an asymptotic approximation because this equation uses the lower limit of the possible values of k.

These works also reveal the error made on the value of k obtained by Wu. Since the formula found depends on k, the critical force is overestimated.

Through Figure 2-8, we compare the different equations of critical force through a numerical application of the previous equations. The curves represent the variation of the critical force as a function of the weight of the drill pipes. We used standard 5.5-inch (inch) drill pipes in a 12.25 inch well.

In general, we can notice that the difference between the different curves increases as the weight increases. We observe the joint increase of the critical sinusoidal buckling force with the weight of the drill pipes. We can also see that the Wu curve is the upper envelope, the Wang curve the lower envelope and Léa and Lubinski curves average values with a very small difference between these last two curves.

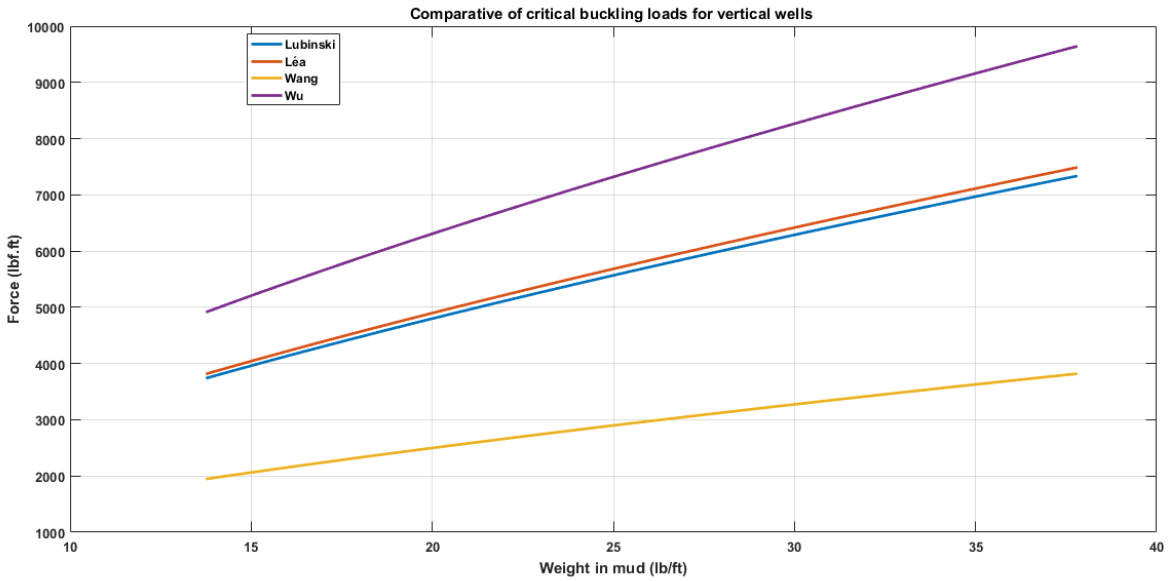

Figure 2-8 Evolution of the critical sinusoidal buckling force as a function of the weight of the drill pipes

Lubinski (1962) [16] has also been interested in helical buckling in vertical wells. He proposed a formula for analyzing buckling suitable for manual calculations. To do this, he considers the general case of a vertical column with a limit condition of embedding type imposed by the packers[8]. The drill pipe is assumed initially straight and vertical, it deforms in an elastic domain to put under a helical configuration and there is no drill pipe[9]-well friction.

[8] is a key piece of downhole equipment in many completions - a sealing device that isolates and contains produced fluids and pressures within the tubing string

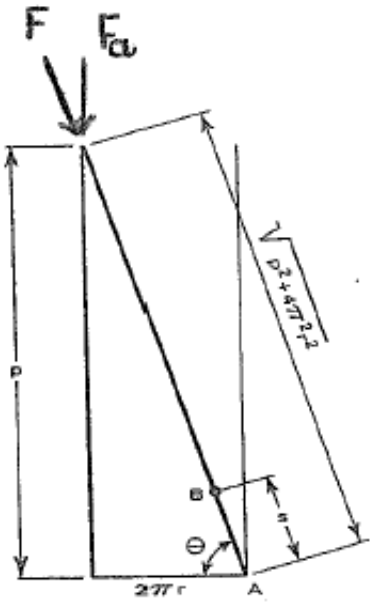

Figure 2-9Development of Helix

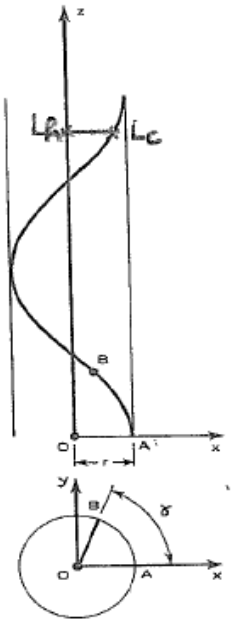

Figure 2-10 Projection of the helix

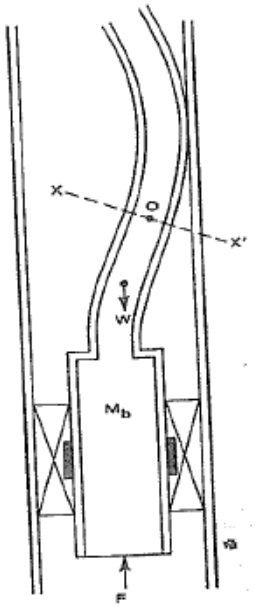

Figure 2-11 Force on tubing in absence of fluids

Based on these assumptions, it evaluates the total potential energy U of the system as follows:

$$U = U_f + U_b + U_c \tag{2.23}$$

where U_f is the potential energy of the compressive force U_c and U_b respectively the strain energy due to compression and the strain energy due to flexion.

Moreover, the decomposition of the forces F_a and F along the axis of the well and the axis of the drill string makes it possible to express the angle obtained by developing the helix by:

$$\sin(\alpha) = \frac{F_a}{F} = \frac{p}{\sqrt{p^2 + (2\pi r)^2}} \tag{2.24}$$

The ratio of the curvilinear length of the drill pipe and the projected length on the axis of the well is given by:

$$\frac{L_c}{L_h} = \frac{\sqrt{p^2 + (2\pi r)^2}}{p} \quad give\ us \quad L_h = L_c \times \frac{\sqrt{p^2 + (2\pi r)^2}}{p} \tag{2.25}$$

Now, using Hooke's law, we can express the length variation due to compression as a function of the axial stressσ_a by:

$$L_c = L\left(1 - \frac{\sigma_a}{E}\right) = L\left(1 - \frac{F\sin(\alpha)}{AE}\right) = L\left(1 - \frac{Fp}{AE\sqrt{p^2 + (2\pi r)^2}}\right) \quad (2.26)$$

The author thus deduces the expressions of each component of the total potential energy:

$$U_f = F \times L_h = \frac{FpL}{\sqrt{p^2 + (2\pi r)^2}} = \frac{(Fp)^2 \times L}{AE\sqrt{p^2 + (2\pi r)^2}} \quad (2.27)$$

$$U_c = \frac{(F_a)^2 \times L}{2AE} = \frac{(Fp)^2 \times L}{2AE(p^2 + (2\pi r)^2)} \quad (2.28)$$

$$U_b = \frac{EIL(C)^2}{2} = \frac{8 \times \pi^4 \times r^2 \times L \times EI}{(p^2 + (2\pi r)^2)^2} \quad (2.29)$$

The equilibrium condition of the system is achieved by minimizing the total potential energy of the system $\frac{du}{dp} = 0$. After simplification and resolution of the second-degree equation F obtained, Lubinski establishes the relationship between the compressive force and the pitch for a helically buckled drill pipe:

$$F = \frac{8\pi^2 EI}{P^2} \quad (2.30)$$

Cheatham (1984) [17] in furthering the analysis that led to the previous equation, proposes a framework, for a beam without taking into account the self-weight, of the relation effort-not in the form:

$$\frac{4\pi^2 EI}{P^2} < F < \frac{8\pi^2 EI}{P^2} \quad (2.31)$$

This frame allows to model both loading and unloading. The loading corresponds to the compression phase until buckling while the unloading corresponds to the decompression phase from this flamed state. To find this result, Cheatham cancels the term U_c because it is placed in a state of unloading of the drill pipe

having already buckled. This is explained by the fact that the deformation energy resulting from the compression which causes the drill pipe to flare tends towards zero during unloading. Looking more closely at this inequality, it is possible to see that the right-hand side corresponds to the relation defined by Lubinski. The left-hand member represents the effort-not relationship for the case of a beam without weight.

Cheatham (1988) [18] continued his work by an experimental analysis of helical buckling that corroborates the validity of the inequality.

2.5.1 Discussion

Lubinski's relation expresses the pitch at every point of the well for a given effort in the post-buckling phase. It is only valid at the given moment which is the one defining the passage in helical mode. The Lubinski formula does not predict the occurrence of buckling, nor how it will develop. Mitchell (1982) [19] explored the effect of the packers-imposed boundary condition imposed by the packers in the Lubinski model and the influence of the weight of the drill pipe. It highlights that packers have an important influence on the phenomenon of buckling. This can lead to additional efforts at the level of packers three times larger than those estimated by Lubinski.

Moreover, the effort-not-relation was developed by considering a vertical well, without drill pipe-wall friction, without taking into account the weight, whereas we know that in reality the well trajectories are tortuous with problems of friction. Moreover, for consider weight, Mitchell (1988) [20] proposes the following formula by considering a drill pipe that forms a z-axis helix:

$$F = \frac{8\pi^2 EI}{p(z)^2} - w_b(L - z) \tag{2.32}$$

The following table summarizes some of the formulas developed to identify critical loads for sinusoidal and helical buckling, while different approaches are key having been taken to identify critical loads for sinusoidal buckling, in the case of helical buckling, researchers agreed that they are related only by a common factor $\lambda = 2\sqrt{2} - 1$.

Table 2-1 formulas for sinusoidal and helical buckling

Critical force	Sinusoidal	Helical
Léa	$F_{cs} = 1.98\sqrt[3]{EIw_b^2}$	$F_{ch} = 3.60\sqrt[3]{EIw_b^2}$
Lubinski	$F_{cs} = 1.94\sqrt[3]{EI\ w_b^2}$	$F_{ch} = 3.53\sqrt[3]{EIw_b^2}$
Wang	$F_{cs} = 1.01\sqrt[3]{EIw_b^2}$	$F_{ch} = 1.83\sqrt[3]{EIw_b^2}$
Wu	$F_{cs} = 2.55\sqrt[3]{EIw_b^2}$	$F_{ch} = 5.55\sqrt[3]{EIw_b^2}$

In the industry, the phenomenon is deemed too dangerous and to avoid it, the weight is distributed such as the neutral point is located in the drill collars, which are stiffer than the drill pipes, chosen to handle 80% of the applied load.

2.6 Buckling in inclined and horizontal wells

With the number of horizontal oil and gas wells at its crescent, and the range of well configurations at a new zenith, new and perplexing well designs challenge the drilling industry.

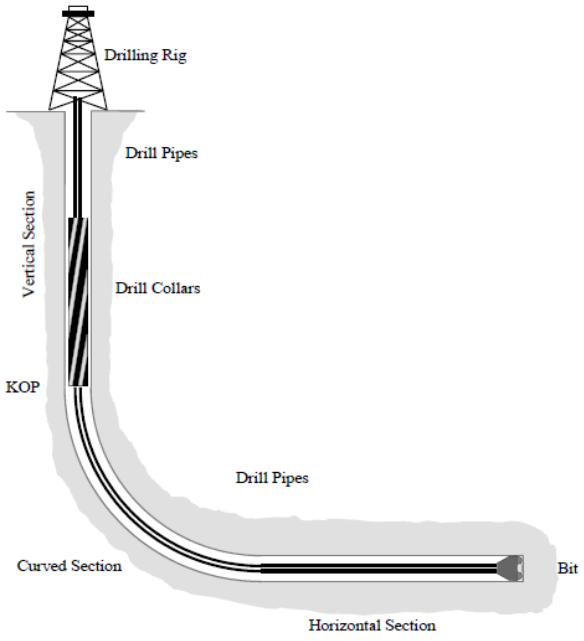

Figure 2-12 A schematic of a horizontal bore-hole drilling

There is little concern about drill collars buckling in the vertical section of the bore-hole because buckling here creates little risk to the drilling operation. The use of stabilizers in this section may further reduce any risk. [21]

2.6.1 Sinusoidal critical effort

The study of drill string stability in inclined wells was developed by Paslay (1964) [22]. He used an energy approach to achieve this stability criterion. To solve the equations obtained, the author manages to exhibit a harmonic form of angular displacement of the drill pipe. Which leads to:

$$F_{cr}(n) = \frac{(1-\nu)^2}{(1-\nu)(1-2\nu)} EIn^2 \left(\frac{\pi}{L}\right)^2 + (1-\nu)\frac{L^2 \rho_p A_s g\, sin(\theta)}{n^2 \pi^2 r_c} \qquad (2.33)$$

Where n is the number of buckling cycles that occur in a drill pipe of length L and the ratio $\frac{L}{n}$ is the pitch. This formula corresponds to the critical load that puts the drill pipe in the 1st buckling mode.

Based on Paslay's work, Dawson (1984) [23] rewrites the previous equation, which it takes as value of the Poisson's ratio 0.33:

$$F_{cr} = EI\left(n^2 + \frac{L^2 \rho_p A_s g\, sin(\theta)}{n^2 \pi^2 EI r_c}\right) \times \left(\frac{\pi}{L}\right)^2 \qquad (2.34)$$

This expression can be compared to that given by Timoshenko for a buckled beam on an elastic support. There is equivalence between the two equations if consider$l = \frac{L}{n}$ and $K = \frac{\rho_p A g \sin(\theta)}{r_c}$

The right term in Dawson's equation, due the weight of the drill pipe appears as an additional term that increases the critical load of Euler which proves that the weight opposes the appearance of buckling in the inclined wells.

It can be noted that when r tends to infinity then the classical case of Eulerian buckling is found because the problem is comparable to a compressed beam (without lateral constraint). When the inclination of the well is zero or the weight of the drill pipe is neglected, we find again Euler's formula despite taking into account the constraint of the well's wall.

The aim of the author is to then determine the smallest of these critical loads in order to obtain the mode of buckling of the structure that appears first. This mode is good sure whoever claims the minimum energy for its implementation.

The simplest way for the author was to derive the expression of $F_{cr}$with respect to n

$$\frac{\partial F_{cr}}{\partial \mathrm{n}} = 0 \ \ we\ find\ n^2 = \sqrt{\frac{L^4 \rho_p A_s g \sin(\theta)}{\pi^4 E I r_c}} \tag{2.35}$$

By replacing this value of n^2 in the Dawson Equation, we obtain the famous Dawson and Paslay formula which gives the critical effort for sinusoidal buckling in an inclined rectilinear well:

$$F_{crs} = 2\sqrt{\frac{EI\rho_p A_s g\ sin(\theta)}{r_c}} = 2\sqrt{\frac{EIw_b\ sin(\theta)}{r_c}} \tag{2.36}$$

The author deduces that the stability of a circular drill pipe in an inclined well (including horizontal wells) is defined by Dawson-Paslay equation which is independent of the length of the drill pipe. He also showed that when the inclination of the well increases, the drill pipe develops a certain buckling resistance due to the support and stress provided by the walls of the well.

This critical effort is identical to that defined by Chen and Wu. In the oil industry, this Dawson-Paslay formula is often used to analyze sinusoidal buckling. So, some choose to apply it to vertical wells as well although inclined. And for simple applications, we can use preconceived abacuses from this formula, where other authors propose to use the following criterion:

- If $\theta \leq 3°$ so we have $F_{crs} = 2\sqrt{\frac{EIw_b \sin(3)}{r_c}}$
- Else we have $F_{crs} = 2\sqrt{\frac{EIw_b \sin\theta}{r_c}}$

Discussion

The model is largely inspired by Lubinski's work. The expression of F_{cr} is established for a drill pipe that buckles under a constant external loading in a perfectly straight well. The presence of friction is neglected and neither is the possibility that the drill pipes can be rotated. It must be remembered that this formula has been established only for long drill pipes does not include the effect of connections where there is an increase in the outside diameter.

These formulas are established for cases of perfect wells (horizontal, inclined) and are subject to many assumptions. We can name:

- continuous drill pipe
- no tortuosity
- no rotation
- drill pipe-wall friction is often ignored.

The authors use different methods to determine this critical load. All express this effort as a function of w_b (mudded weight), EI, θ and r_c

$$F_{crs} = 2\sqrt{\frac{EIw_b \sin\theta}{r_c}} \tag{2.37}$$

2.6.2 Helical critical force of Chen

Chen (1990) [24] presented a new analysis of buckling in horizontal wells. Using the energy method, he has shown that the critical sinusoidal buckling force is the same as that obtained by Dawson-Paslay, the helical buckling critical force F_c which he defines as corresponding to the beginning of the process of formation of the first helix

$$F_{crh}^{chen} = 2\sqrt{2}\sqrt{\frac{EIw_b}{r_c}} = \sqrt{2} \times F_{crs} \tag{2.38}$$

His analysis reveals that the force required to put the drill pipe in helical buckling is 1.4 times greater than that required to buckle the drill pipe in sinusoidal form.

Discussion

This formulation has been developed for perfectly straight and horizontal wells. The other hypotheses of his model have not been communicated except for the fact that friction has not been taken into account.

2.6.3 Helical critical force of Wu

Wu (1993) [25] studied helical buckling in horizontal wells and presented a critical effort corresponding to the complete formation of the first helix: critical

force helical buckling of Wu (F_{crh}^{wu}). For this author, F_{crh}^{chen} is not constant during the formation of the helix, it grows during the helical buckling process, we have the formula for F_{crh}^{wu} :

$$F_{crh}^{wu} = 2\left(2-\sqrt{2}\right)\sqrt{\frac{EIw_b}{r_c}} = 2\left(2-\sqrt{2}\right) \times F_{crs} \tag{2.39}$$

According to this equation,F_{crh}^{wu} is 83% more than the critical sinusoidal buckling effort. This equation has been extended to wells with inclined trajectories by reconsidering the inclination in these formulas.

Discussion

The basic assumption of the Wu model has been justified by the experiments. On the other hand, Chen's equation comes from the study of a frictionless mechanical systemin which neither the 3D character of the wells nor the rotation of the drill pipes are taken into account. This led Wu (1993) [25] to study the influence of friction in the transmission of axial force in inclined and horizontal wells. In addition, the author in his model understands that the drill string is long enough to neglect the connection conditions. Yet many theories highlight the importance of these link-end conditions for example (Sorenson). critical force is expressed as follows:

$$F_{crh} = \lambda \times F_{crs} \tag{2.40}$$

Where $\sqrt{2} \leq \lambda \leq 2\sqrt{2}$

2.7 Comparative Study

For a drilling engineer planning a well, it is important to know the limitation of the applied loads on a drill pipe, and this for different work conditions. Different standards are taken, a conservative approach is required when working in sensitive settings, where buckling failure is to be avoided, less conservative conditions if the working conditions are safer or cut backs due to financial constraints are required. In the following works, an algorithm which takes a driller's inputs, and calculates the critical sinusoidal and helical loads based off the work of several researchers has been developed.

The algorithm requires inputs such as, the OD and ID of drill pipe, volumetric mass density $\rho_{drillpipe}$ and ρ_{mud}, the radius of open hole OD_{Hole}, Young's modulus of material E, the WOB (the weight on bit) and the planned inclination of the hole θ.

In the computations, different formulas based on the work of several researchers are used. They are summarized in the following table

Table 2-2 Summary of formulas used for critical loads computation

Researchers	Critical Sinusoidal Buckling	Critical helical Buckling
Dawson-Paslay	$F_{crs} = 2\sqrt{\frac{EIw_b \sin\theta}{r_c}}$	$F_{crh} = (2\sqrt{2}-1)\sqrt{\frac{EIw_b \sin\theta}{r_c}}$
He & al	$F_{crs} = \frac{2EI}{Rr_c}\sqrt{1+\sqrt{1+\frac{R^2 r_c w_b \sin\theta}{EI}}}$	$F_{crh} = \frac{4EI}{Rr_c}\sqrt{1+\sqrt{1+\frac{R^2 r_c w_b \sin\theta}{2EI}}}$
Wu and Juvkam-Wold	$F_{crs} = \frac{4EI}{Rr_c}\sqrt{1+\sqrt{1+\frac{R^2 r_c w_b \sin\theta}{4EI}}}$	$F_{crh} = \frac{12EI}{Rr_c}\sqrt{1+\sqrt{1+\frac{R^2 r_c w_b \sin\theta}{8EI}}}$
Qui & al	$F_{crs} = \frac{2.53EI}{Rr_c}\sqrt{1+\sqrt{1+\frac{R^2 r_c w_b \sin\theta}{3.52EI}}}$	$F_{crh} = \frac{8EI}{Rr_c}\sqrt{1+\sqrt{1+\frac{R^2 r_c w_b \sin\theta}{2EI}}}$
Liu	$F_{crs} = \frac{2EI}{Rr_c}\sqrt{1+\sqrt{1+\frac{R^2 r_c w_b \sin\theta}{EI}}}$	$F_{crh} = \frac{3.77EI}{Rr_c}\sqrt{1+\sqrt{1+\frac{0.53R^2 r_c w_b \sin\theta}{EI}}}$

These formulas require the following data

Cross section

$$A_s = \frac{(OD^2 - ID^2)\times\pi}{4} \tag{2.41}$$

Moment of Inertia

$$I = \frac{\pi\times(OD^4 - ID^4)}{64} \tag{2.42}$$

Buoyancy factor

$$K_b = BF = \frac{\rho_{tube} - \rho_{mud}}{\rho_{tube}} \tag{2.43}$$

Mudded Weight

$$w_b = K_b \times w_{air} \tag{2.44}$$

Radial clearance

$$r_c = \frac{(OD_{Hole} - OD)}{2} \tag{2.45}$$

Below, we present an example, using the same drill collars, for vertical, inclined and horizontal wellbores. A comparative study has been conducted using our algorithm to determine the optimal model for each situation.

Table 2-3 Critical loads for vertical wellbores

Input	OD(in)	ID(in)	$\rho_{tube}(sg)$	$\rho_{mud}(sg)$	OD_{Hole}(in)	$\theta(°)$	$WOB(TF)$	$E(psi)$
Values	8	3	7.85	1.5	16	3	44	30×10^6
Output	Values							
Wu juvkam	Sinusoidal critical effort (TF)		10.158					
	Helical critical force (TF)		26.379					
Dawson / Paslay	Sinusoidal critical effort (TF)		25,117					
	Helical critical force		45,925					
He&al	Sinusoidal critical effort (TF)		6.933					
	Helical critical force (TF)		11.833					
Qui al	Sinusoidal critical effort (TF)		6.610					
	Helical critical force (TF)		23.667					
Liu	Sinusoidal critical effort (TF)		6.933					
	Helical critical force (TF)		11.300					

Table 2-4Critical loads for wellbores with an inclination of θ=45°

Input	OD(in)	ID(in)	ρ_{tube} (sg)	ρ_{mud} (sg)	OD_{Hole} (in)	θ(°)	WOB(TF)	E(psi)
Values	8	3	7.85	1.5	16	45	44	30×10^6
Output	Values							
Wu-juvkam	Sinusoidal critical effort (TF)			92.571				
	Helical critical force (TF)			257.659				
Dawson / Paslay	Sinusoidal critical effort (TF)			92.325				
	Helical critical force (TF)			168.810				
He&al	Sinusoidal critical effort (TF)			57.326				
	Helical critical force (TF)			102.027				
Qui al	Sinusoidal critical effort (TF)			59.562				
	Helical critical force (TF)			204.054				
Liu	Sinusoidal critical effort (TF)			57.326				
	Helical critical force (TF)			97.041				

Table 2-5Critical loads for horizontal wells with an inclination θ=90°

Input	OD	ID(in)	$\rho_{tube}(sg)$	$\rho_{mud}(sg)$	OD_{Hole}(in)	$\theta(°)$	$WOB(TF)$	$E(psi)$
Values	8	3	7.85	1.5	16	90	44	30×10^6
Output	Values							
wu-juvkam	Sinusoidal critical effort (TF)			166.87				
	Helical critical force (TF)			479.894				
Dawson / Paslay	Sinusoidal critical effort (TF)			109.794				
	Helical critical force (TF)			200.751				
He&al	Sinusoidal critical effort (TF)			96.927				
	Helical critical force (TF)			177.820				
Qui al	Sinusoidal critical effort (TF)			106.696				
	Helical critical force (TF)			355.640				
Liu	Sinusoidal critical effort (TF)			96.927				
	Helical critical force (TF)			168.669				

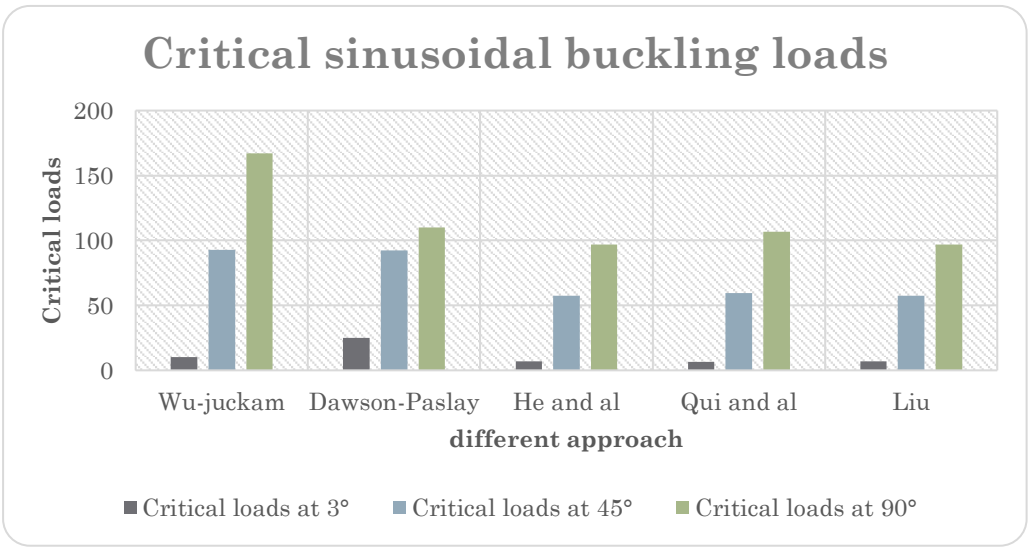

Figure 2-13 Critical sinusoidal buckling loads

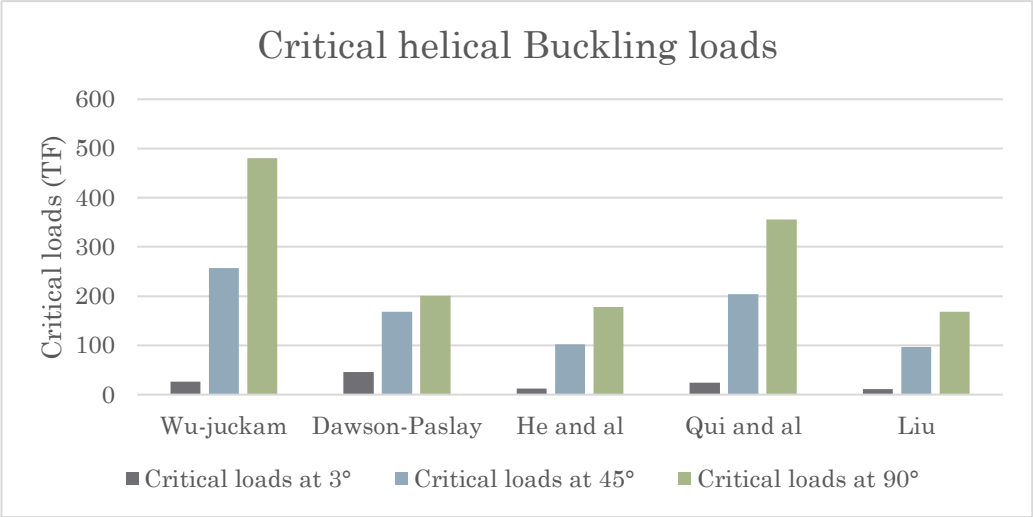

Figure 2-14 Critical helical buckling loads

Discussion

- For vertical wells, the Dawson-Paslay formula is the most conservative, by a large margin
- For inclined wellbores, with an angle of $\theta = 45°$, Wu-Juvkam and Dawson-Paslay's formulas provide close results while the He, Qui and Liu approaches provide similar results to each other.
- On the other hand, for horizontal wells, Wu-Juvkam criteria is the most conservative by a large margin. With the other 4 criteria's being providing similar results
- The Dawson-Paslay criteria provides the most balanced results regardless of inclination, this is why it is always adopted in the industry for preliminary estimations of buckling
- Across the different criteria's we can see that the critical buckling load increases as inclination increases, this is due to dissipation of the axial force through side force with the wellbore walls.
- Although the critical loads increase with inclination, there are other parameters to be taken into consideration when planning a well, such as the radius of the borehole decreasing, stick-slip vibrations, and drill string fatigue that increase with augmenting the WOB.

Chapter 3 Mathematical Model for Buckling in Vertical Wells

3.Lateral Buckling Models

Because the lateral displacement of the tubular string in wellbores is much smaller than the axial length, a linear elastic theory due to small displacements can be considered, a study is performed to determine the post-buckling behavior of a drill string between the drill bit and the first contact point, experimental data suggests that this area is the most heavily stressed during the drilling operation for straight wellbores.

This approach was first undertaken by Arthur Lubinski (1950) [10], considered the first engineering and mathematical approach to the problem of buckling in the oil and gas industry. This paper is considered a staple in the industry and a reference for all following research. However due to limited resolution capabilities at the time, only a few critical cases are considered. In the present project, we will be reviewing the resolution algorithm in order to generalize it to any drill string.

3.1 Sinusoidal and Helical buckling models

The Lubinski approach was revisited by D. Gao [26]taking into account the Torque (M_T) and the torsional loading and wellbore inclination (θ). They established the following equations:

$$\begin{cases} \dfrac{d^4u}{dz^4} + \dfrac{M_T}{EI}\dfrac{d^3v}{dz^3} + \dfrac{d}{dz}\left(\dfrac{F - w_b z\cos\theta}{EI}\dfrac{du}{dz}\right) - \dfrac{w_b \sin\theta}{EI} = 0 \\ \dfrac{d^4v}{dz^4} + \dfrac{M_T}{EI}\dfrac{d^3u}{dz^3} + \dfrac{d}{dz}\left(\dfrac{F - w_b z\cos\theta}{EI}\dfrac{dv}{dz}\right) - \dfrac{w_b \sin\theta}{EI} = 0 \end{cases} \tag{3.1}$$

u and v are the lateral displacements along x and y coordinates, respectively, z is the axial distance; F is the axial compressive force at the bottom end; M_T is the torque; EI is the bending stiffness; w_b is the weight on bit per unit length of the down-hole tubular string; α is the hole angle.

The solution to this equation is expressed as the linear combination of certain linearly independent functions, as was the case with the Lubinski study, namely:

$$w = G^T X + w_g \tag{3.2}$$

Where w is the lateral displacement; X is the vector of undetermined constants and G is the vector of linearly independent power series with respect to the variable; w_g is the lateral displacement caused by lateral tubular string weight ($q \sin\alpha$).

This model is effective for the suspended section for the down-hole tubular string with multiple connectors distributed discretely. This is due to estimating the axial force on every suspended section can be taken as a constant and the vector G in this case is given by:

$$G = \begin{bmatrix} 1 & z & \sin(\sqrt{F/EI}\,.z) & \cos(\sqrt{F/EI}\,.z) \end{bmatrix} \tag{3.3}$$

The continuity of bending moments, tangent shear force and displacements introduce the boundary conditions at the ends of the integral tubular string, the equation system is then non-linear and is solved accordingly.

This equation is converted into an algebraic equation problem, by first using a polar equation system based on two assumptions:

3.1.1 Continuous contact:

By considering the downhole tubular string being in continuous contact with the wellbore. The distributed force on the tubular string is equal to the sum of tubular string weight and contact force between the tubular string and the wellbore. Gao (2006) introducing the wellbore constraint equations [26]:

$$u = r_c \cos\alpha \tag{3.4}$$

$$v = r_c \sin\alpha \tag{3.5}$$

Obtained the following equation, based on his beam-column method

$$\frac{d^4\alpha}{dz^4} - 6\left(\frac{d\alpha}{dz}\right)^2 \frac{d^2\alpha}{dz^2} + 3\frac{M_T}{EI}\frac{d\alpha}{dz}\frac{d^2\alpha}{dz^2} + \frac{d}{dz}\left(\frac{F}{EI}\frac{d\alpha}{dz}\right) + \frac{w_b \sin\theta}{EI\, r_c}\sin\alpha = 0 \tag{3.6}$$

3.1.2 Final deformed shape is a sinusoidal wave or a helix:

This assumption is that the drill string in a post buckling equilibrium shape takes a sinusoidal wave (first buckling mode) with an equation:

$$\alpha = A\sin(\omega \cdot z) \tag{3.7}$$

Where A is the amplitude and ω is the angular velocity of the angular displacement fluctuation. The critical load is obtained by analyzing the stability of the approximate linear form of the differential equation. (Gao 1998 [27]). Relation between amplitude A and Axial force F is calculated by solving the differential equation with a perturbation method (Gao and Miska 2009 [28]).

Helical buckling is expressed as:

$$\alpha = \frac{2\pi}{p}\, z \; or \; \alpha = \frac{2\pi}{p} z + A\sin\left(\frac{2\pi}{p}\, z\right) \tag{3.8}$$

Where p is the helix pitch; A is the fluctuation amplitude caused by the tubular string weight. The analytical solution for the parameter $p = 2\pi\sqrt{2EI/F}$ is deduced from the differential equation of buckling. for a weightless tubular string without torque. The parameter A is deduced using a perturbation method.

3.2 Lubinski Model

The Model is based off the theory of elastic stability, critical conditions for which the buckling occurs are investigated. The location of points at which the buckled pipe is tangent to the wall of the hole and the force with which it contacts the wall are determined. The location of points of maximum stresses and the value of these stresses are also calculated.

3.2.1 Model considerations:

- The first consideration is that the drilling string is a continuous pipe with no tool joints, the generalization of the results to drill pipes and drill collars will be simple by the use of dimensionless units.

- The drilling string is assumed to be a beam element constituted of elastic material with Young's Modulus E.
- Each beam element section is circular, characterized by an outside diameter, OD, and an inside diameter, ID. No tool joints are taken into considerations; the generalization is made using dimensionless units during the study
- The wall of borehole is circular and rigid and remains so.
- The rotation of the beam isn't taken into account; we consider only a static mode.
- Both ends of the drill string are considered as hinged

Before detailing the modeling, some key definitions are required to clarify the development

3.2.2 Model development

The first consideration is that the drilling string is a continuous pipe with no tool joints, the generalization of the results to drill pipes and drill collars will be simple by the use of dimensionless units.

W_1: is the reaction of the elevators on the drilling string

W_2: is the vertical component of the reaction of the hole on the drilling string, also defined as the Weight on Bit (WOB)

F_2: is the horizontal component of the reaction of the bottom of the hole on the drilling string.

F_1: is the reaction of the bushings on the drilling string.

F: is the reaction of the hole on the drilling string when the pipe is buckled, known also as normal force or side force.

Also, the pipe is considered to be affected by the buoyed weight or weight in mud as defined earlier, which is applied on the center of gravity

To study the progression of the phenomenon, we will consider only the forces below a section MN, where the string is freely suspended and before the first contact occurs, these are represented in the following figure:

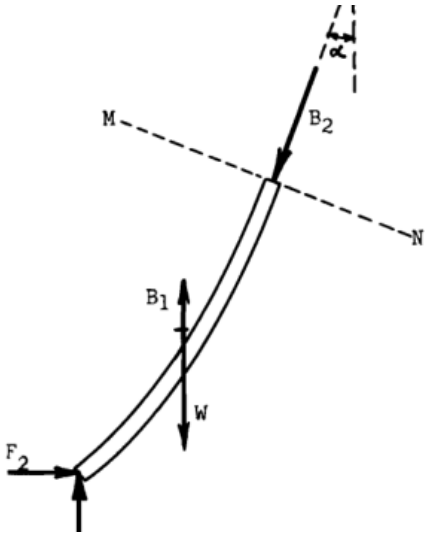

Figure 3-1 loads applied on the freely suspended section

The angle α is the deflection of the drill pipe after the buckling process initializes. For the study we chose, as axes of coordinates, X the axis of the hole, Y the axis where the displacement occurs, and the point of origin is N, as defined previously the neutral point.

The theory of small elastic displacement states, starting from the bending moment equation:

$$M = EI\frac{d^2Y}{dX^2} \tag{3.9}$$

Into the shearing force equation:

$$A = EI\frac{d^3Y}{dX^3} \tag{3.10}$$

This shearing force can also be determined by analyzing the forces applied on the drill string using newton's second law, for a static study the sum of the forces is equal to zero, projecting these forces on the MN axis provides the following equation:

$$A = (W_2 - W)\sin\alpha - F_2\cos\alpha \tag{3.11}$$

W designates the weight of the drillstring portion below the studied section

Under borehole conditions the deflection α is small; therefore, we may consider $\cos\alpha = 1$ and $\sin\alpha = \tan\alpha$, the shearing force equation becomes:

$$A = (W_2 - W)\tan\alpha - F_2 \tag{3.12}$$

Where p designates the mudded weight of the drilling string, we designate respectively X_1 and X_2 the values of X at the two ends of the drilling string. Hence:

$$X_1 = -\frac{W_1}{p} \tag{3.13}$$

$$X_2 = \frac{W_2}{p} \tag{3.14}$$

Formula (3.12) may be written as follows

$$A = [W_2 - p(X_2 - X)]\tan\alpha - F_2 \tag{3.15}$$

Substituting X_2 with its designated value, and $\tan\alpha = dY/dX$

$$A = -pX\frac{dY}{dX} - F_2 \tag{3.16}$$

Combining equations (3.12) and (3.16) we obtain the following:

$$EI\frac{d^3Y}{dY^3} + pX\frac{dY}{dX} + F_2 = 0 \tag{3.17}$$

We have thus obtained the differential equation of the buckled drilling string. By properly choosing the unit of length, the equation could be put in a simpler form, and considered dimensionless, we use the following substitutions:

$$X = m\,x \tag{3.18}$$

$$Y = m\,x$$

Wherein; m is a constant which will be chosen to make the equation dimensionless, allowing us to generalize results for all types of drilling strings

$$\frac{dY}{dX} = \frac{dy}{dx} \tag{3.19}$$

$$\frac{d^2Y}{dX^2} = \frac{1}{m}\frac{dy^2}{dx^2} \tag{3.20}$$

$$\frac{d^3Y}{dX^3} = \frac{1}{m^2}\frac{d^3y}{dx^3} \tag{3.21}$$

Substituting these equations into the differential equation and rearranging the terms we obtain the following

$$\frac{d^3y}{dx^3} + \frac{w_b}{EI}m^3\,x\frac{dy}{dx} + \frac{F_2}{EI}m^2 = 0 \tag{3.22}$$

So, the value of m should be chosen so that:

$$m^3 = \frac{EI}{w_b} \tag{3.23}$$

And we define the constant c as follows

$$c = \frac{F_2}{w_b m} \tag{3.24}$$

With these constants the differential equation takes a much simpler form:

$$\frac{d^3y}{dx^3} + x\frac{dy}{dx} + c = 0 \tag{3.25}$$

3.2.3 Solution to the differential equation

We make another substitution, introducing z where

$$z = \frac{dy}{dx} \tag{3.26}$$

Substituting the new variable into the differential equation, we obtain

$$\frac{d^2z}{dx^3} + xz + c = 0 \tag{3.27}$$

The variable z can be expressed in form of power series:

$$z = \sum_0^\infty a_n x^n \tag{3.28}$$

Substituting it in the differential equation we have

$$\sum_0^\infty n(n-1)a_n x^{n-2} + \sum_0^\infty a_n x^{n+1} + c = 0 \tag{3.29}$$

This expression is a polynomial of powers of x. This equation needs to be satisfied for any value of x; and therefore, the coefficients of x^n must all be equal to zero. And thus, the following equations are established

For $n = 0$ the coefficients are as follows $2a_2 + c = 0$

For $n = 1$ the coefficients are as follows $a_0 + 2(3a_3) = 0$

For $n = 2$ the coefficients are as follows $a_1 + 3(4a_4) = 0$

For $n = 3$ the coefficients are as follows $a_2 + 4(5a_4) = 0$

Consequently, $a_0, a_1, a_2, a_3, a_4, etc$. may all be expressed as functions of a_0, a_1 and c. Substituting these into the expression of z we have the following

$$\begin{aligned} z = a_0 \left[1 - \frac{x^3}{2\cdot 3} + \frac{x^6}{2\cdot 3\cdot 5\cdot 6} - \frac{x^9}{2\cdot 3\cdot 5\cdot 6\cdot 8\cdot 9} + \cdots\right] \\ + a_1 x \left[1 - \frac{x^3}{3\cdot 4} + \frac{x^6}{3\cdot 4\cdot 6\cdot 7} - \frac{x^9}{3\cdot 4\cdot 6\cdot 7\cdot 9\cdot 10} + \cdots\right] \\ - \frac{c}{2}x^2 \left[\frac{1}{2} - \frac{x^3}{4\cdot 5} + \frac{x^6}{4\cdot 5\cdot 6\cdot 7\cdot 8} - \frac{x^9}{4\cdot 5\cdot 6\cdot 7\cdot 9\cdot 10\cdot 11} + \cdots\right] \end{aligned} \tag{3.30}$$

Putting in Equation (3.30) $a_0 = a$ and $a_1 = b$, and expressing z by $dy/\,dx$ we obtain the following equation

$$\frac{dy}{dx} = aF(x) + bG(x) + cH(x) \tag{3.31}$$

Integrating this equation, we obtain the expression for $y(x)$

$$y = aS(x) + bT(x) + cU(x) + g \tag{3.32}$$

And differentiating equation (3.25) we obtain the expression for d^2y/dx^2

$$\frac{d^2y}{dx^2} = aP(x) + bQ(x) + cR(x) \tag{3.33}$$

The power series are defined as follows:

$$S(x) = x\left[1 - \frac{x^3}{2\cdot 3\cdot 4} + \frac{x^6}{2\cdot 3\cdot 5\cdot 6\cdot 7} - \frac{x^9}{2\cdot 3\cdot 5\cdot 6\cdot 8\cdot 9\cdot 10} + \cdots\right] \tag{3.34}$$

$$T(x) = x^2\left[\frac{1}{2} - \frac{x^3}{3\cdot 4\cdot 5} + \frac{x^6}{3\cdot 4\cdot 6\cdot 7\cdot 8} - \frac{x^9}{3\cdot 4\cdot 6\cdot 7\cdot 9\cdot 10\cdot 11} + \cdots\right] \tag{3.35}$$

$$U(x) = -\frac{x^3}{2}\left[\frac{1}{3} - \frac{x^3}{3\cdot 4\cdot 6} + \frac{x^6}{4\cdot 5\cdot 7\cdot 8\cdot 9} - \frac{x^9}{4\cdot 5\cdot 7\cdot 8\cdot 10\cdot 11\cdot 12} + \cdots\right] \quad (3.36)$$

$$H(x) = -\frac{x^2}{2}\left[1 - \frac{x^3}{4\cdot 5} + \frac{x^6}{4\cdot 5\cdot 7\cdot 8} - \frac{x^9}{4\cdot 5\cdot 7\cdot 8\cdot 10\cdot 11} + \cdots\right] \quad (3.37)$$

$$R(x) = -x\left[1 - \frac{x^3}{2\cdot 4} + \frac{x^6}{2\cdot 4\cdot 5\cdot 7} - \frac{x^9}{2\cdot 4\cdot 5\cdot 7\cdot 8\cdot 10}\right] \quad (3.38)$$

The rest of the functions, $F(x), G(x), P(x)$ and $Q(x)$ are expressed in the form of Bessel functions of fractional orders $^1/_3$, $-^1/_3$, $^2/_3$ and $-^2/_3$.

$$F(x) = \frac{1}{2}\left(3^{\frac{2}{3}}\right)\left[\Gamma\left(\frac{5}{3}\right)\right] x^{\frac{1}{2}} J_{-\frac{1}{3}}\left(\frac{2}{3}x^{\frac{3}{2}}\right) \quad (3.39)$$

$$G(x) = \left(3^{\frac{1}{3}}\right)\left[\Gamma\left(\frac{4}{3}\right)\right] x^{\frac{1}{2}} J_{+\frac{1}{3}}\left(\frac{2}{3}x^{\frac{3}{2}}\right) \quad (3.40)$$

$$P(x) = -\frac{1}{2}\left(3^{\frac{2}{3}}\right)\left[\Gamma\left(\frac{5}{3}\right)\right] x J_{+\frac{2}{3}}\left(\frac{2}{3}x^{\frac{3}{2}}\right) \quad (3.41)$$

$$Q(x) = \left(3^{\frac{1}{3}}\right)\left[\Gamma\left(\frac{4}{3}\right)\right] x J_{-\frac{2}{3}}\left(\frac{2}{3}x^{\frac{3}{2}}\right) \quad (3.42)$$

For negative values of x values, Bessel functions of the second are used.

3.2.4 Critical Buckling conditions

Let x_1 and x_2 designate the values of x for the upper and lower ends, respectively, of the drilling string. And thus, we represent $P(x)$, Q(x), $R(x)$, $S(x)$ … etc by P_1, Q_1, R_1, S_1… etc for $x = x_1$ and P_2, Q_2, R_2, S_2 for $x = x_2$.

At both ends of the drilling string, the bending moment is equal to zero (since we consider the bushings at the drill bit as hinged). Therefore, equation (3.33) gives:

$$aP_1 + bQ_1 + cR_1 = 0 \tag{3.43}$$

$$aP_2 + bQ_2 + cR_2 = 0 \tag{3.44}$$

For both ends, the displacement is also null, thus $y = 0$; and their formula (3.32) provides

$$aS_1 + bT_1 + cU_1 + g = 0 \tag{3.45}$$

$$aS_2 + bT_2 + cU_2 + g = 0 \tag{3.46}$$

With these two equations, we can eliminate the integration constant g, we obtain this system

$$\begin{cases} aP_1 + bQ_1 + cR_1 = 0 \\ aP_2 + bQ_2 + cR_2 = 0 \\ a(S_1 - S_2) + b(T_1 - T_2) + c(U_1 - U_2) = 0 \end{cases} \tag{3.47}$$

The solution of the set has physical meaning only if its determinant is equal to zero:

$$\begin{vmatrix} P_1 & Q_1 & R_1 \\ P_2 & Q_2 & R_2 \\ (S_1 - S_2) & (T_1 - T_2) & (U_1 - U_2) \end{vmatrix} = 0 \tag{3.48}$$

Under actual drilling conditions x_1, which represents the distance from the neutral point to the bushings (surface) is very large, thus it is chosen as constant $x_1 = -6$, the asymptotic limit show by extrapolation of results obtained via trial and error.

The resolution of equation (3.48) allows us to determine the critical length (x_2) representing the critical WOB for which the string buckles. The numerical value obtained is

$$x_2 = 1.94 \tag{3.50}$$

3.2.5 Contact point location for critical conditions of the first order

In the present work, we are not only interested in when a string buckles, but also on how to determine the location of the first tangency point along the drill string.

We shall determine the point of contact along the drill string, which will be designated $x_3$using the condition $dy/dx = 0$, since at that point, the curve of the buckled drillstring is tangent to the wall of the borehole.

We have from equation (3.31)

$$aF_3 + bG_3 + cH_3 = 0 \tag{3.51}$$

To complete the system, we add the boundary conditions on the displacement at both hinges, given by the previous equations (3.45) and (3.46). Those equations are recapitulated below:

$$aP_1 + bQ_1 + cR_1 = 0 \tag{3.52}$$

$$aP_2 + bQ_2 + cR_2 = 0 \tag{3.53}$$

And thus, we have the following system

$$\begin{cases} aF_3 + bG_3 + cH_3 = 0 \\ aP_1 + bQ_1 + cR_1 = 0 \\ aP_2 + bQ_2 + cR_2 = 0 \end{cases} \tag{3.54}$$

This system only has solutions if the determinant is null

$$\begin{vmatrix} F_3 & G_3 & H_3 \\ P_1 & Q_1 & R_1 \\ P_2 & Q_2 & R_3 \end{vmatrix} = 0 \tag{3.55}$$

This expression is the relation between the abscissa x_3 the point of tangency and the abscissa x_1 and x_2 the end of the string for critical conditions. As previously explained, $x_1 = -6$ and $x_2 = 1.94$.

The value of x_3 satisfying the relation (3.55) was found equal to $x_3 = 0.145$

3.2.6 Equation Coefficients for Critical Conditions of the First Order

In order to determine the shape of the buckled string axis, the distribution of bending moments, etc. we must find the values of a,b and c, but the set of equations represented earlier gives indeterminate values for these factors. And those equations do not account for the bore hole limit, for once the weight reaches the critical value, the pipe would bend more without reaching equilibrium, this explained by the fact that the equations are set for small deflections for which the curvature is equal to d^2Y/dX^2.

For large deflections for which an equilibrium would be reached, a more complicated formula should be used. However, all this is without any practical meaning, since the theoretical equilibrium of the pipe would be reached far beyond the elastic limit of the steel (large deflections), Practically, such a condition never occurs because the borehole contact stops the pipe's bending.

This is taken into account by the deflection at the point of tangency, where it is equal to the apparent radium of the hole

$$x = x_3\ , Y = r_c \tag{3.56}$$

And in dimensionless units:

$$y = \frac{r_c}{m} \tag{3.57}$$

Therefore, equation is:

$$aS_3 + bT_3 + cU_3 + g = \frac{r_c}{m} \tag{3.58}$$

At the lower end of the string, the deflection is nil as shown in equation (30) and thus eliminating g between these equations we obtain the following set of equations:

$$\begin{cases} aP_1 + bQ_1 + cR_1 = 0 \\ aP_2 + bQ_2 + cR_2 = 0 \\ a(S_3 - S_1) + b(T_3 - T_1) + c(U_3 - U_1) = 0 \end{cases} \quad (3.59)$$

In these equations $x_1 = -6$, $x_2 = 1.94$ and $x_3 = 0.145$, the solution of the sets leads to the values of $a(m/r), b(m/r), c(m/r)$. As obtained in the following table:

x_2	$a(m/r_c)$	$b(m/r_c)$	$c(m/r_c)$
1.940	+0.064	-0.406	+0.482

In dimensionless units, we find that the drill string will take the following post buckled shape:

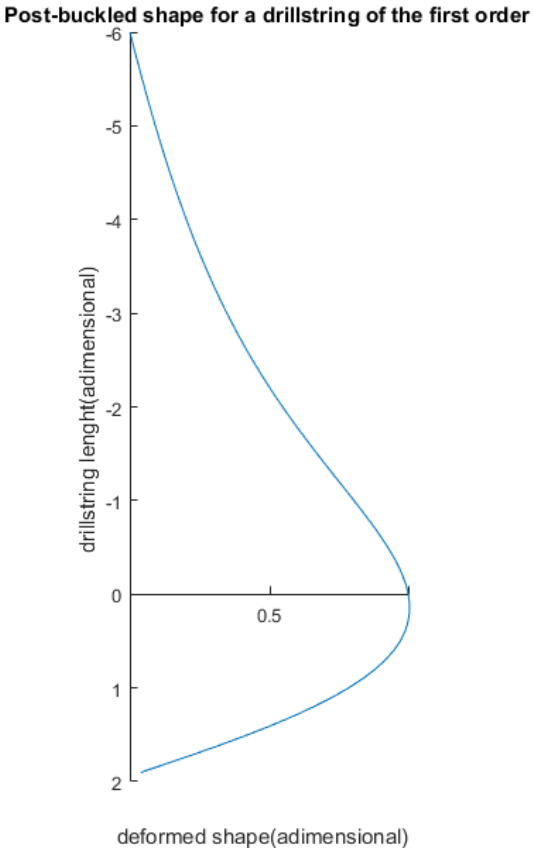

Figure 3-2 Displacement for buckling of the first order

3.2.7 Points of Tangency for Weights on the Bit Above Critical Conditions of the First Order

The previous study shows that a drill string is only stable for $x_2 = 1.94$, the case where the drillstring is freely suspended, to investigate what happens after the first order of buckling occurs, and we keep increasing the weight on bit.

It is required we adjust the original differential equation developed in (3.25), this time to account for the effect of the side force applied by the borehole at the tangency point, through an analog development, the new expression found is:

$$EI\frac{d^3Y}{dY^3} + w_b X\frac{dY}{dX} + F_2 - F = 0 \tag{3.60}$$

To simplify this equation in the same manner, we keep the same definition for m and the new constant c is

$$c_1 = \frac{F_2 - F}{w_b m} \tag{3.61}$$

The differential equation written in regards to z is:

$$\frac{d^2 z}{dx^3} + xz + c_1 = 0 \tag{3.62}$$

Integrating this differential equation gives the same kind of general solutions (3.32), (3.31) and (3.33), however all the constants become different for the lower and upper portions of the drilling string, where the contact force takes only into consideration the upper part. The upper part is governed by the following set of equations

$$y = aS_1(x) + bT_1(x) + cU_1(x) + g_1 \tag{3.63}$$

$$\frac{dy}{dx} = aF_1(x) + bG_1(x) + cH_1(x) \tag{3.64}$$

$$\frac{d^2 y}{dx^2} = aP_1(x) + bQ_1(x) + cR_1(x) \tag{3.65}$$

$$c_1 = \frac{F_1}{w_b m} \tag{3.66}$$

And for the lower part, the corresponding equations are

$$y = aS_2(x) + bT_2(x) + cU_2(x) + g_2 \tag{3.67}$$

$$\frac{dy}{dx} = aF_2(x) + bG_2(x) + cH_2(x) \tag{3.68}$$

$$\frac{d^2 y}{dx^2} = aP_2(x) + bQ_2(x) + cR_2(x) \tag{3.69}$$

$$c_2 = \frac{F_2}{w_b m} \tag{3.70}$$

Same as the last development, we consider $x_1 = -6$ the upper end of the drilling string, x_2 the lower end, and x_3 the point at which the pipe is tangent to the wall of the hole. The three boundary conditions for the upper portion of the drilling string are as follows:

- The bending moment is equal to zero at the upper end of the drilling string.
- The first derivative, $dy/\,dx$, is nil at the tangency point $x = x_3$ which leads to equation At the upper end, the deflection is also nil, $y = 0$
- At the tangency point, the deflection is equal to the borehole clearance (dimensionless units) $y = r_c/m$

These last two conditions, give two expressions from which g has been eliminated giving finally equation

The boundary conditions are the same for the lower portion of the drilling string as they were for the upper part.

One additional boundary conditions which expresses the fact that at the point of tangency $x = x_3$

The bending moments, and consequently values of d^2y/dx^2 must be equal, which leads to equation

$$\begin{cases} a_1P_1 + b_1Q_1 + c_1R_1 = 0 \\ a_1F_3 + b_1G_3 + c_1H_3 = 0 \\ a_1(S_3 - S_1) + b_1(T_3 - T_1) + c_1(U_3 - U_1) = r_c/m \\ a_2P_2 + b_2Q_2 + c_2R_2 = 0 \\ a_2F_3 + b_2G_3 + c_2H_3 = 0 \\ a_2(S_3 - S_2) + b_2(T_3 - T_2) + c_2(U_3 - U_2) = r_c/m \\ a_1P_3 + b_1Q_3 + c_1R_3 - a_2P_3 - b_2Q_3 - c_2R_3 = 0 \end{cases} \tag{3.71}$$

This set of seven equations with only six unknowns has a solution only if the following condition is met

$$\begin{vmatrix} P_1 & Q_1 & R_1 & 0 & 0 & 0 & 0 \\ F_3 & G_3 & H_3 & 0 & 0 & 0 & 0 \\ S_3 - S_1 & T_3 - T1 & U_3 - U_1 & 0 & 0 & 0 & r/m \\ 0 & 0 & 0 & P_2 & Q_2 & R_2 & 0 \\ 0 & 0 & 0 & F_3 & G_3 & H_3 & 0 \\ 0 & 0 & 0 & S_3 - S_2 & T_3 - T2 & U_3 - U_2 & r/m \\ P_3 & Q_3 & R_3 & -P_3 & -Q_3 & -R_3 & 0 \end{vmatrix} = 0 \qquad (3.72)$$

This expression, in which $x_1$is constant and equal to -6, is the relationship between x_2, distance from the neutral point to the bit, and x_3, distance from the neutral point to the tangency point. The resolution is done via a matlab algorithm of our making, for different critical lengths x_2 we obtain the following locations for contact points.

Table 3-1 Contact Point Location

x_2	x_3 (Lubinski)	Present Results	Relative error
1.940	0.145	0.145	0%
2.600	0.942	0.943	0.106 %
3.200	1.668	1.667	0.059 %
3.753	2.346	2.345	0.042 %
4.000	2.672	2.671	0.037 %
4.218	3.098	3.086	0.388 %

As seen in table 3-1, the results obtained by the developed algorithm and the original Lubinski work are close, the percentage error does not exceed 0.388% whilst offering fast run time, and the possibility to determine the contact point and post buckled shape for any drill string in a vertical well.

With the location of contact points known,x_3, one can determine the deformed shape by solving equations 3.71 and hence computing the coefficients a, b and c for both string deformations. One should notice that the obtained coefficients are multiplied by a factor m/r_c.

Table 3-2 Deformed shape coefficients

x_2	a_1	b_1	c_1	a_2	b_2	c_2
1.940 (Lubinski)	+0.064	-0.406	+0.482	+0.064	-0.406	+0.482
1.940 (present work)	+0.063	-0.406	+0.482	+0.063	-0.406	+0.482
3.753 (Lubinski)	+0.278	+0.205	-0.002	-3.175	+2.853	+1.946
3.753 (present work)	+0.278	+0.203	-0.001	-3.178	+2.852	+1.949

Knowing the coefficients for the post buckling drill string shape, we can investigate for the deformed shape. Buckling for first and second critical orders, are presented in figure below.

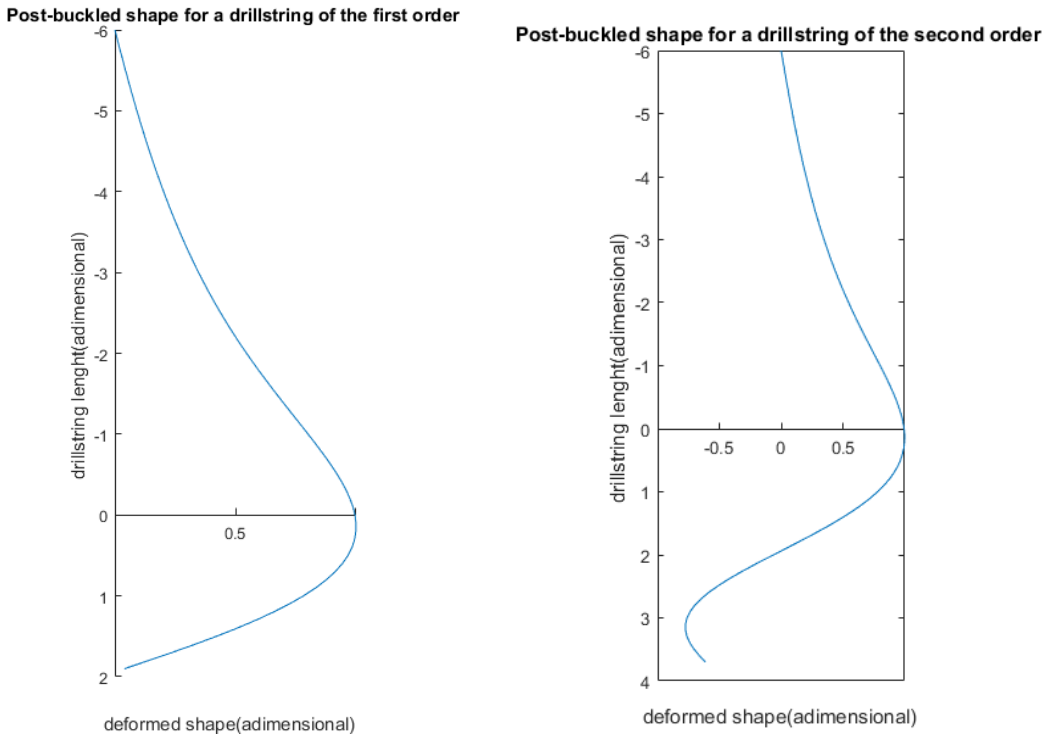

Figure 3-3 Post buckling shape for first and second critical order

3.2.8 Side force equation

One of the important parameters to study post buckling is the side force, which could cause caving and lost circulation. This can be now undertaken since the post buckled shape has been determined

As previously seen in our modeling of forces applied on the buckled drill string, the reaction F of the wall of the hole on the buckled drilling string is equal to:

$$F = F_2 - F_1 \tag{3.73}$$

The forces F_2 and F_1 are related to the constants c_2 and c_1, as previously presented in equations (3.66) and (3.70) and by substituting them into the expression for F, we obtain:

$$F = w_b\, r \left(c_2 \frac{m}{r_c} - c_1 \frac{m}{r_c} \right) \tag{3.74}$$

Let

$$f = c_2\frac{m}{r_c} - c_1\frac{m}{r_c} \tag{3.75}$$

Then F becomes

$$F = f w_b r_c \tag{3.76}$$

The value for f can be determined knowing $\left(c_2\frac{m}{r_c}\right)$ and $\left(c_1\frac{m}{r_c}\right)$, which are found by resolving boundary conditions system. For any given drill string and well, the weight per foot w_b and apparent borehole radius r_c remain constant. The side force then follows the evolution of the coefficient f. The evolution of f can be plotted for different values of x_2.

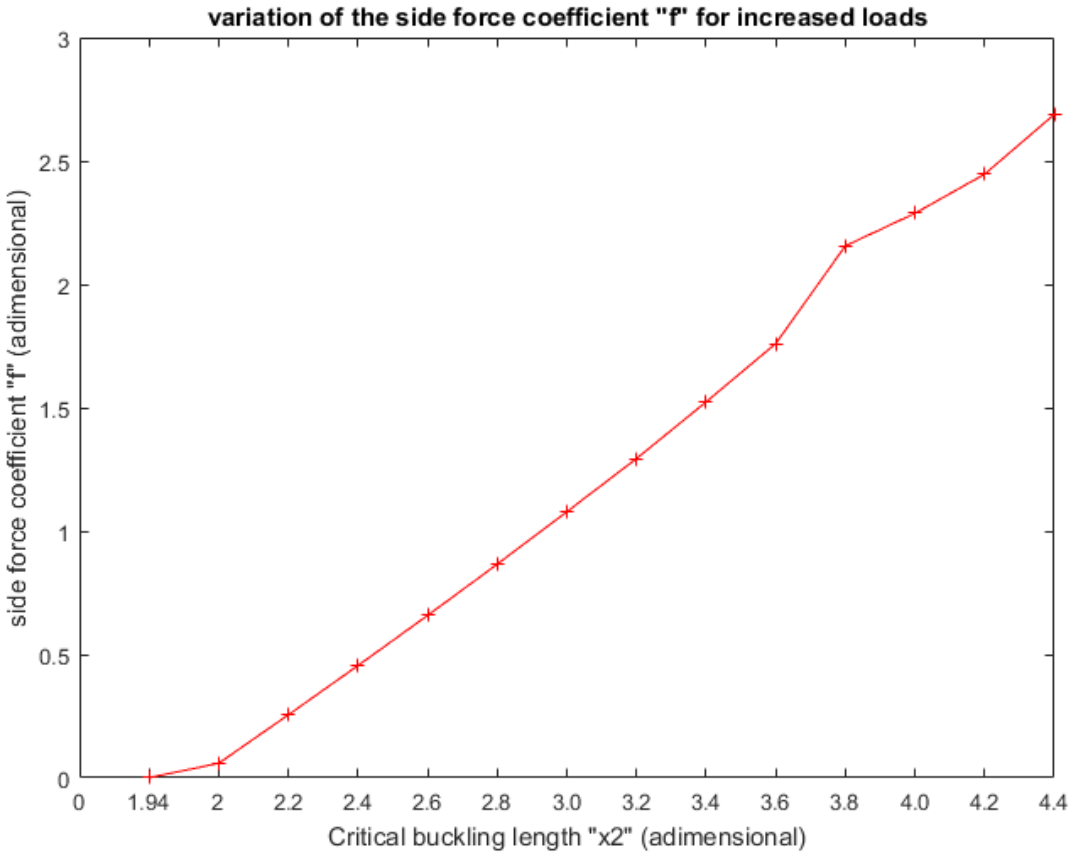

Figure 3-4 Variation of side force coefficient "f" for increased loads

From the figure, we may observe that for the weight on the bit smaller than the critical value (buckling of the first order) f is negative, that implies that the pipe needs to be pulled toward the wall in order to be bent. For the critical value ($x_2 = 1.94$) the pipe buckles, but it contacts the wall with a force equal to zero at the point of contact. Only at higher orders of buckling does the side force would have a noticeable effect.

3.2.9 Bending moment and bending stress

The other parameters to look at are the evolution of bending moment and consequently bending stress along the drill string. When the drill string buckles, its cross section becomes subjected to a bending moment generating a tension stress on one side and a compression stress on the other. As it rotates, these stresses reverse, and, consequently, they cause fatigue to the steel which could cause drill string failure or shear. This is another common issue on drilling rigs that can hinder the drilling operations greatly. The bending moment equation is given by:

$$M = EI\frac{d^2Y}{dX^2} \tag{34}$$

With the introduction of the parameter m, the expression is

$$M = w_b m^2 \frac{d^2y}{dx^2} \tag{3.78}$$

For a dimensionless study, let us introduce bending moment coefficient i by the following expression:

$$i = \frac{m}{r_c}\frac{d^2y}{dx^2} \tag{3.79}$$

With this new coefficient, the expression of bending moment is

$$M = i\, w_b m r_c \tag{3.80}$$

for any given drill pipe or drill collar, the weight per foot p and the length of one dimensionless unit m remain constant, and so does the radius of the borehole at a given section. Thus, the bending moment depends solely on the i coefficient.

The plot shown in figure 3-8highlights how this coefficient changes along the drill string, for different buckling orders (first and second)

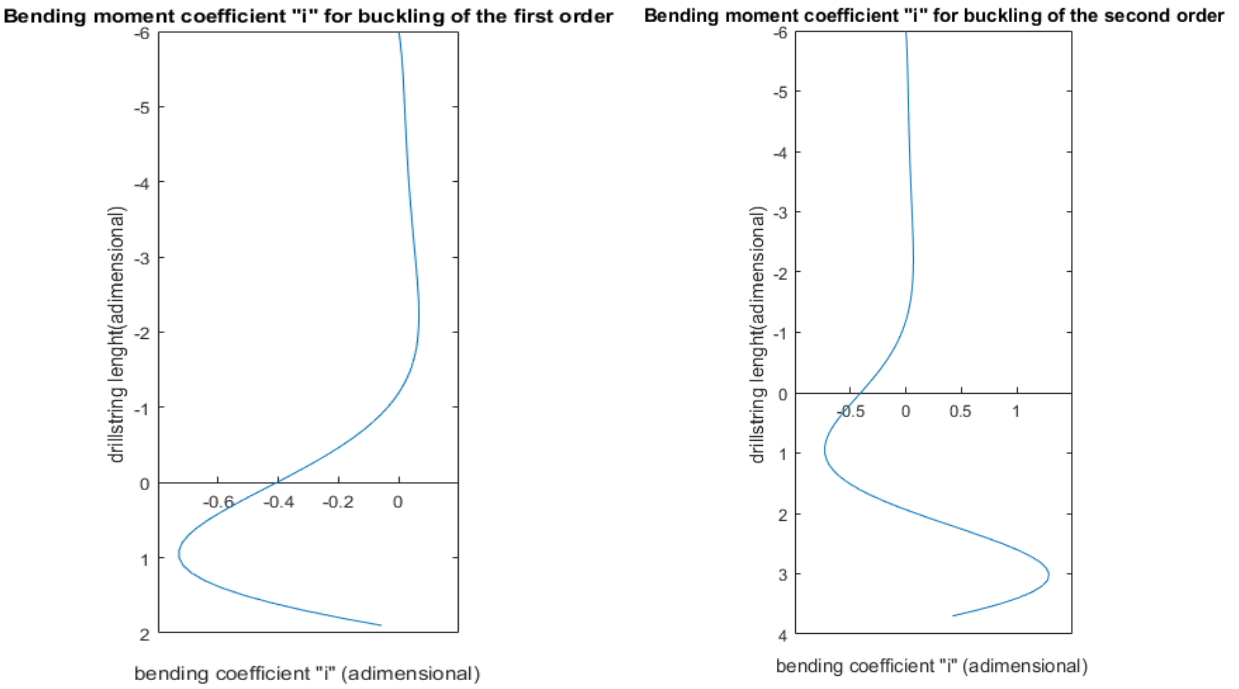

Figure 3-5 bending coefficient for buckling of the first and second order

3.3 Conclusion

- This model allows to fully define the drillstring shape, contact points and side force. The dimensionless study allows to generalize the study for all types of drill strings
- Side force is only a factor at higher orders of buckling.
- The bending moment is maximum near the bit
- The model developed provides insight into the phenomenon, providing a sense of the evolution of the post buckling behavior of the pipe, however computations show its limitations for $x_2 > 4.2$

Chapter 4 Mathematical Model for Buckling in Curved Wellbores

In the following chapter, we'll introduce another approach to determining the mechanical response of the drill string to applied loads inside an oil well, accounting all the complex effects within an oil well, to name a few:

- The three-dimensional aspect of the trajectory (Inclination and azimuth variations, curves and torsion)
- The complete degrees of freedom for the drill string within the wellbore
- The different loads interacting with the drill string

All these parameters taken into consideration, the equilibrium equations are used to determine the response of the drill string to the initial external actions, represented in the shear force T and bending moment M.

For that purpose, it is required to identify the geometry of the well, using survey points to determine wellbore curvature and torsion, adopting the Serret-Frenet coordinate system. Considering the different models for friction and torque. The equation system is solved numerically using a Runge-Kutta algorithm.

4.1 Well Trajectory

The well trajectory is assimilated to a curve, $\vec{x}(s)$, the geometry for a planned well is known, for a finished well it is reconstructed using data from a survey, using different models that are exposed as follows [6]

4.1.1 The Serret-Frenet coordinate system

From the different survey techniques, we are given a three-dimensional trajectory for the well, the given coordinate system is a fixed one (O, North, East, TVD), we add a mobile coordinate system, for each point of the main trajectory $\vec{x}(s)$,

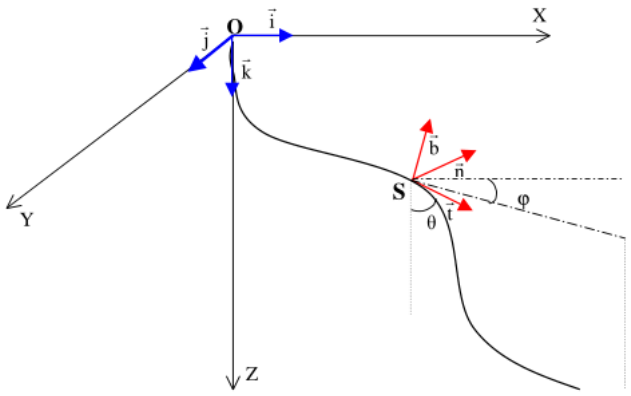

Figure 4-1 Fixed and mobile coordinate systems

we define a tangent vector $\vec{t}(s) = \frac{d\vec{x}(s)}{ds} = \vec{x}'(s)$, the derivative to the tangent vector, the normal vector $\vec{n}(s)$, is defined as follows:

$$\vec{n}(s) = \kappa(s)\frac{d\vec{t}(s)}{ds} \tag{4.1}$$

$\kappa(s)$ indicates the curvature, the third coordinate is called the binormal $\vec{b}(s)$, defined by

$$\vec{b}(s) = \vec{t}(s) \wedge \vec{n}(s) \tag{4.2}$$

The tangent vector in the mobile coordinate system $\vec{t}(s)$ is related to the fixed coordinate system via the inclination Θ and azimuth Φ angles as follows:

$$\vec{t} = \begin{pmatrix} \sin\Theta \times \cos\Phi \\ \sin\Theta \times \cos\Phi \\ \cos\Theta \end{pmatrix} \tag{4.3}$$

And thus, the normal vector $\vec{n}(s)$ is

$$\vec{n} = \frac{1}{\kappa}\begin{pmatrix} G_\Theta \cos\Theta \times \cos\Phi - G_\Phi \sin\Theta \times \sin\Phi \\ G_\Theta \cos\Theta \times \sin\Phi + G_\Phi \sin\Theta \times \cos\Phi \\ -G_\Theta \times \sin\Theta \end{pmatrix} \tag{4.4}$$

with $G_{\Theta,\Phi} = \frac{d\Theta,\Phi}{ds}$ the gradients for inclination and azimuth respectively, the binormal vector $\vec{b}(s)$ is given by:

$$\vec{b} = \frac{1}{\kappa}\begin{pmatrix} G_\Theta \cos\Theta \times \cos\Phi - G_\Phi \sin\Theta \times \sin\Phi \\ G_\Theta \cos\Theta \times \sin\Phi + G_\Phi \sin\Theta \times \cos\Phi \\ -G_\Theta \times \sin\Theta \end{pmatrix} \tag{4.5}$$

The derivatives of the unitary vectors in the Frenet coordinate system are defined by the Serret-Frenet equations, given as follows:

$$\begin{pmatrix} \frac{d\vec{t}}{ds} \\ \frac{d\vec{n}}{ds} \\ \frac{d\vec{b}}{ds} \end{pmatrix} = \begin{bmatrix} 0 & \kappa & 0 \\ -\kappa & 0 & \tau \\ 0 & -\tau & 0 \end{bmatrix} \times \begin{pmatrix} \vec{t} \\ \vec{n} \\ \vec{b} \end{pmatrix} \tag{4.6}$$

And where κ is the curvature, τ represents the torsion along the trajectory [29]

4.1.2 Survey Calculation

At each survey station, survey tools measure the inclination, azimuth, and measured depth. The measured data are transmitted to surface computers where survey calculation methods use these data as input for calculating the following

bottom location data (i.e. TVD, north/south, east/west, and dog leg severity) at each survey station.

There are several known methods of computing directional survey. The six most commonly used are: tangential, balanced tangential, average angle, curvature radius, Minimum Torsion Method (MTM), and minimum curvature (most accurate).

Minimum Torsion Method (MTM) and minimum curvature (MCM) are the most accurate and most widely used in the industry.

Average angle

In this method a straight line is assumed between survey stations 1, 2. The inclinations and azimuth are averaged. The objective is to find out the location of survey station 2 with the help of following parameters [30]

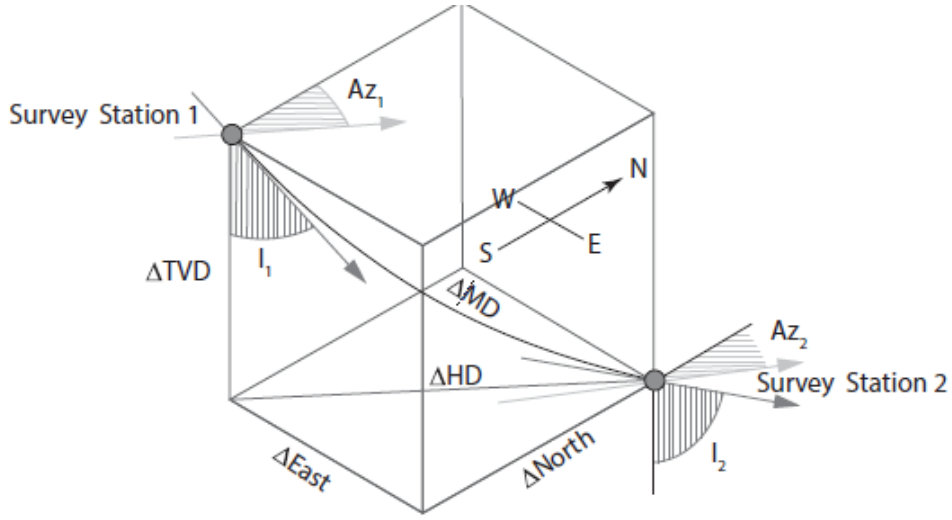

Figure 4-2 Schematic diagram for Average Angle Method

calculations:

- North coordinate
- East coordinate
- Vertical section

From Average Angle Method, following values are obtained:

$$\Delta North = \Delta MD \times \sin\left(\frac{\theta_1 + \theta_2}{2}\right) \times \cos\left(\frac{(\phi_1 + \phi_2)}{2}\right) \quad (4.7)$$

$$\Delta \text{East} = \Delta \text{MD} \times \sin\left(\frac{(\theta_1 + \theta_2)}{2}\right) \times \sin\left(\frac{(\phi_1 + \phi_2)}{2}\right) \quad (4.8)$$

$$\Delta \text{Vertical} = \Delta \text{MD} \times \cos\left(\frac{(\theta_1 + \theta_2)}{2}\right) \quad (4.9)$$

Here we have

- MD =measured depth between surveys in ft.
- θ_1 =inclination (angle) at upper survey in degrees
- θ_2 =inclination (angle) at lower in degrees
- ϕ_1 =Azimuth direction at upper survey in degrees
- ϕ_2 =Azimuth direction at lower survey in degrees

Discussion

The average angle method is easy to calculate in the field if a programmable calculator or computer is not available as provides less error and gives results within the accuracy needed in the field provided the distance between surveys is not too great.

Curvature radius

In the radius of curvature method, the wellbore is assumed to be a smooth curve between two survey stations. The radius of curvature method is currently considered to be one of the most accurate methods available. This method considers the wellbore course is a smooth curve between the upper and lower survey stations. The curvature of the arc is determined by the survey inclinations and azimuths at the upper and lower survey stations. [31]

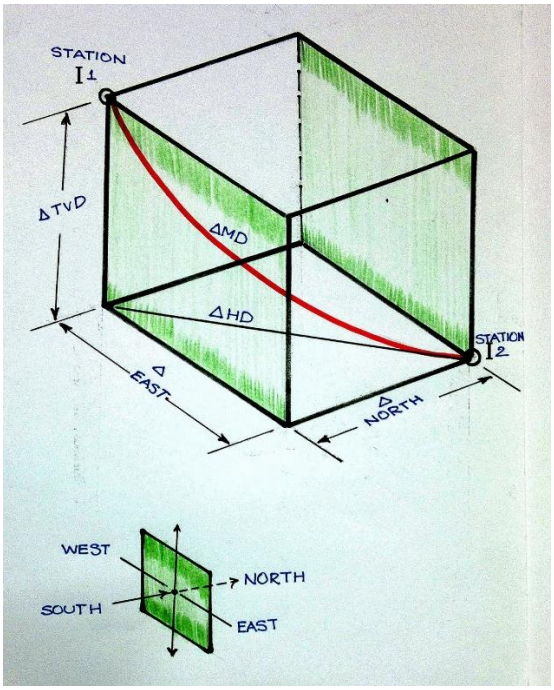

Figure 4-3 curvature radius method

$$\Delta TVD = \left(\frac{180 \times \Delta MD \times (\sin(\theta_2) - \sin(\theta_1))}{\pi(\theta_2 - \theta_1)}\right) \tag{4.10}$$

$$\Delta North = \left(\frac{180^2 \times \Delta MD \times (\cos(\theta_1) - \cos(\theta_2)) \times (\sin(\phi_2) - \sin(\theta_1))}{\pi^2(\theta_2 - \theta_1) \times (\phi_2 - \phi_1)}\right) \tag{4.11}$$

$$\Delta East = \left(\frac{180^2 \times \Delta MD \times \cos(\theta_1) - \cos(\theta_2) \times (\cos(\phi_1) - \cos(\phi_2))}{\pi^2(\theta_2 - \theta_1) \times (\phi_2 - \phi_1)}\right) \tag{4.12}$$

$$R = \frac{180}{\pi \times DLS} = \frac{180 \times C_k}{\pi \times BUR} \tag{4.13}$$

$$\Delta \mathrm{MD} = \frac{(\theta_2 - \theta_1)}{BUR} \tag{4.14}$$

Here we have

- BUR[10] = Build Rate = $\frac{\theta \times C_k}{Lenght}$
  - C_k =Is constant related to the unit of borehole curvature
- TVD = True Vertical Depth
- DLS = Dog Leg Severity
- R = Borehole Radius of Curvature

Discussion

This method is not used in field practice because the calculations are very tedious unless a programmed software is available based on this specific method.

Minimum Curvature Method (MCM)

The curvature-radius method, one of the most accurate of all listed methods, uses the inclination and hole direction measured at the upper and lower ends of the course length to generate a smooth arc representing the well path. The difference between the curvature-radius and minimum-curvature methods is that the curvature radius uses the inclination change for the course length to calculate displacement in the horizontal plane (the true vertical depth [TVD] is unaffected), whereas the minimum curvature method uses the dog-leg severity (DLS) to calculate displacements in both planes. Minimum curvature is considered to be the most accurate method, but it does not lend itself easily to normal, hand-calculation procedures. The figure below shows minimum curvature method. The minimum curvature formulas for calculating directional parameters using diagram are presented below: [1]

[10]is the positive change in inclination over a normalized length, A negative change in inclination would be the "drop rate.

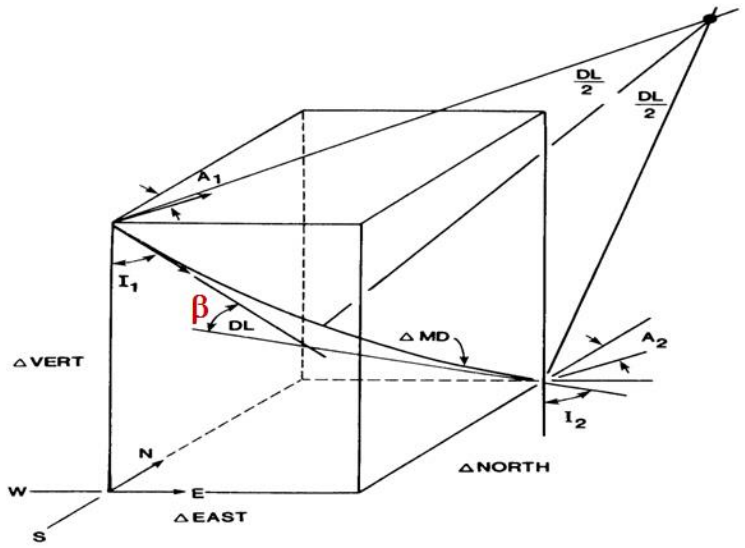

Figure 4-4 Minimum Curvature.

$$\Delta TVD = \frac{\Delta MD \times RF \times (\cos\theta_1 + \cos\theta_2)}{2} \tag{4.15}$$

$$\Delta North = \frac{\Delta MD \times RF \times (\sin\theta_1 \times \cos\phi_1 + \sin\theta_2 \times \cos\phi_2)}{2} \tag{4.16}$$

$$\Delta East = \frac{\Delta MD \times RF \times (\sin\theta_1 \times \sin\phi_{\ 1} + \sin\phi_2 \times \sin\phi_{\ 2})}{2} \tag{4.17}$$

$$DL = \cos^{-1}[\cos(\theta_2 - \theta_1) - (\sin\theta_1 \times \sin\theta_2 \times (1 - \cos(\phi_2 - \phi_1))] \tag{4.18}$$

$$RF = \frac{2}{\beta} \times \tan(\frac{\beta}{2}) \tag{4.19}$$

Where:

- MD Measured Depth between surveys in ft
- θ_1 Inclination (angle) of upper survey in degrees
- θ_2 Inclination (angle) of lower in degrees
- ϕ_1 Azimuth direction of upper survey
- ϕ_2 Azimuth direction of lower survey
- RF Ratio Factor

- When the dogleg is equal to 0, the formula for ratio factor (R.F.) is undefined. In this case, simply assign the ratio factor the value of 1.0.

- DL The dog leg angle or overall angle change must be in radians

Discussion

This the most accurate, it further adds a Ratio Factor to smoothen the spherical arc formed by using radius of curvature method.

Minimum Torsion Method (MTM)

This method based on the main theorem of left curves and the geometric properties of the constant pitch helix. The main advantage of the proposed technique is to be able to describe the left portions of the trajectory by helical arcs whose curvature and geometric torsion may be non-zero. The problem of the reconstruction of the three-dimensional geometry of a wellbore (and thus of the initial undistorted geometry of the drill string) has been solved grace to the implementation of this new method. [32]

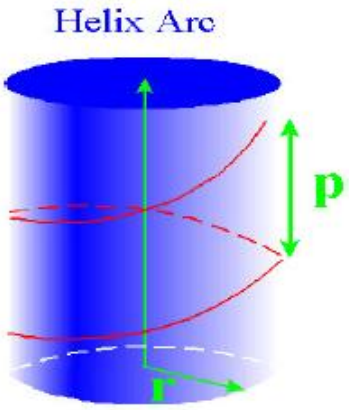

Figure 4-5 helix arc with constant pitch

Reasons for Taking Surveys

- To allow accurate determination of well coordinates at a series of measured depths and determine the current location.
- To plot the well path over the measured depth.

- To measure the inclination and azimuth at the bottom of the hole and hence determine where the well is heading.
- To determine the orientation of tool, face of deflection tools or steerable systems.
- To locate dog legs and allow calculation of dogleg severity values. [6]

Wellbore Torsion

It's an important parameter to be considered for the well path design is wellbore torsion. Let $r = r(s)$ be the equation of a well path where r is the radius vector of a point A, on the trajectory and s is the arc length. The binormal vector b, the product of the unit tangent and the unit normal is given as:

$$b = t \times n \tag{4.20}$$

Where

$$t = \frac{dr}{ds} \ and \ n = \frac{d^2r}{ds^2} \tag{4.21}$$

The Frenet-Serret formula provides a set of three orthonormal unit vectors at any given survey point on the wellbore path. The vector n is orthogonal to τ and lies in the osculating plane at the point A.

This geometric torsion is often neglected when designing the well path; it is interchangeably used and confused with wellbore tortuosity[11]. Borehole torsion provides the extent of departure of a well trajectory from a plane curve. It is the rate of rotation of the binormal vector of the well trajectory with respect to curved length and depicts the extent of torsion of a wellbore trajectory (Fitchard and Fitchard 1983 [33]; Xiushan 2005 [34]; and Xiushan 2006 [35]). The expression defining borehole torsion is as follows:

[11]In fluid mechanics, tortuosity is the ratio between the length of path to the straight-line distance between those two points. It is termed as a property of a curve with 'many turns'. Not only in oil and gas, but it is also be applied in different fields:

$$\tau = \begin{cases} +|\dot{b}|, if\ \dot{b}\ and\ n\ are\ in\ the\ opposite\ direction \\ -|\dot{b}|, \quad if\ \dot{b}\ and\ n\ are\ in\ the\ same\ direction \end{cases} \tag{4.22}$$

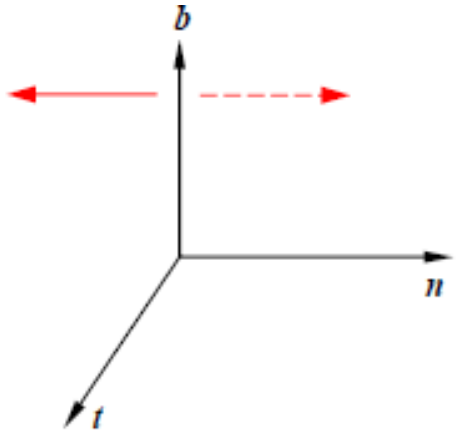

Figure 4-6 Borehole torsion sign.

The positive and negative signs for borehole torsion have the following meanings:

if a point moves along a wellbore trajectory in the onward direction and if the derivative of the unit binormal vector with respect to the measured depth $\dot{b}$ is in the direction opposite to the unit principal normal vector n, then the sign of borehole torsion τ, is positive. Otherwise, the sign of τ is negative.

From the definitions of moving frame and borehole torsion, we can derive $\dot{b}\ //n$ and obtain the following equation:

$$\dot{b} = -\tau \times n \tag{4.23}$$

Multiplying by n from the right yields:

$$\tau = -\dot{b}.n = b.\dot{n} \tag{4.24}$$

Proceeding through some transformations using differential geometry, the basic formula for calculating borehole torsion is (Fitchard 1983 [33]; Xiushan 2005 [34] and Xiushan 2006 [35]):

$$\tau = \frac{(\dot{r}, \ddot{r}, \dddot{r})}{k^2} = \frac{1}{k^2}\begin{vmatrix} \dot{N} & \dot{E} & \dot{H} \\ \ddot{N} & \ddot{E} & \ddot{H} \\ \dddot{N} & \dddot{E} & \dddot{H} \end{vmatrix} \tag{4.25}$$

Using a differential model of the wellbore trajectory, the relations between coordinate increments and curved-section length, inclination angle, and azimuth angle for a small interval are given by:

$$\begin{cases} \dfrac{\mathrm{dN}}{\mathrm{dL}} = \sin(\theta) \times \cos(\phi) \\ \dfrac{\mathrm{dE}}{\mathrm{dL}} = \sin(\theta) \times \sin(\phi) \\ \dfrac{\mathrm{dH}}{\mathrm{dL}} = \cos(\theta) \\ \dfrac{\mathrm{dS}}{\mathrm{dL}} = \sin(\theta) \end{cases} \tag{4.26}$$

The successive derivatives of the equation above with respect to curved length are:

$$\begin{cases} \dot{N} = \sin(\theta) \times \cos(\phi) \\ \dot{E} = \sin(\theta) \times \sin(\phi) \\ \dot{H} = \cos(\theta) \end{cases} \tag{4.26}$$

$$\begin{cases} \ddot{N} = k_\alpha \cos(\theta)\cos(\phi) - k_\phi \sin(\theta)\sin(\phi) \\ \ddot{E} = k_\alpha \cos(\theta)\cos(\phi) + k_\phi \sin(\theta)\cos(\phi) \\ \ddot{H} = -k_\alpha \sin(\theta) \end{cases} \tag{4.27}$$

$$\begin{cases} \dddot{N} = \dot{k}_\alpha \cos(\theta)\cos(\phi) - \dot{k}_\phi \sin(\theta)\sin(\phi) - 2k_\alpha k_\phi \cos(\theta)\, cos(\phi) - \left(k_\alpha^2 + k_\phi^2\right)\sin(\theta)\cos(\phi) \\ \dddot{E} = \dot{k}_\alpha \cos(\theta)\sin(\phi) + \dot{k}_\phi \sin(\theta)\cos(\phi) + 2k_\alpha k_\phi \cos(\theta)\, cos(\phi) - \left(k_\alpha^2 + k_\phi^2\right)\sin(\theta)\sin(\phi) \\ \dddot{H} = -\dot{k}_\alpha \sin(\theta) - k_\alpha^2 \cos(\theta) \end{cases} \tag{4.28}$$

Substituting these equations in our initial formula yields the following expression, a formula to calculate the borehole torsion at any point (Shan et al. 1993 [36]; Xiushan and Zaihong 2001 [37]; and Xiushan 2006 [35]):

$$\tau = \frac{k_\alpha \dot{k}_\phi - k_\phi \dot{k}_\alpha}{k^2} \sin(\theta) + k_\phi \left(1 + \frac{k_\alpha^2}{k^2}\right) \cos(\theta) \tag{4.29}$$

While designing the well path, care should be taken to use the borehole torsion because the value of the borehole curvature is always positive, but the borehole torsion value can be positive or negative. A zero-borehole curvature, $\kappa = 0$, will depict a straight section and a zero-borehole torsion, $\tau = 0$, will depict a plane curve, and vice versa.

- θ *I*nclination angle, (°)
- ϕ Azimuth angle, (°)
- k_α Rate of inclination change (dropping off is a negative value)
- k_ϕ Rate of azimuth change (decreasing azimuth is a negative value),
- k Curvature of wellbore trajectory
- $\dot{k_\alpha}$ First derivative of inclination change rate,
- $\dot{k}_\phi$ First derivative of azimuth change rate
- τ Torsion of wellbore trajectory
- b Unit binormal vector of wellbore trajectory
- E East coordinate (west is negative), m or ft
- H Total vertical depth, m
- N North coordinate (south is negative), m or ft
- n Unit principal normal vector of wellbore trajectory
- t Unit tangent vector of wellbore trajectory
- $\dot{}$ First derivative
- r Radius vector

Borehole curvature

The industry defines the included angle between two tangent vectors of wellbore trajectory at different two points as dogleg angle. Generally, these two tangent vectors are not in the same plane, so that dogleg angle displays as a space angle. Dogleg angle is also named as overall angle, which means that it includes both inclination change and azimuth change. In mathematics and drilling engineering, this is called the bending angle.

$$\mathrm{DL_{AB}} = \cos^{-1}[(\cos(\theta_A) \times \cos(\theta_B)) \ + (\cos(\Phi_B - \phi_A) \times \sin(\theta_A) \times \sin(\theta_B))] \tag{4.30}$$

$$DLS_{AB} = \frac{\cos^{-1}[(\cos(\theta_A) \times \cos(\theta_B)) + (\cos(\phi_B - \phi_A) \times \sin(\theta_A) \times \sin(\theta_B))]}{MD_2 - MD_1} \quad (4.31)$$

$$DLS = \frac{DL}{MD_B - MD_A} \times 100 \text{ [deg/100ft]} \quad (4.32)$$

Chosen approach: A Hybrid Method

In the industry, the choice for a survey reconstruction method is based off computation time constraints and sensitivity of the drilling operation. It is often opted for a MCM approach. In this work, due to the requirement to identify both wellbore curvature and torsion, we propose to hybrid between the two approaches: The MCM approach and wellbore torsion approach. The choice that leads us to this proposal is that the wellbore torsion, which is often neglected in the industry, can have noticeable effects in sections where DLS is high, or where high variation of the azimuth angle occur.

4.2 Model hypothesis

The structure is assimilated to a beam, with the following mechanical properties

- The beam is made of a material with a Young modulus E, shear modulus G, and a Poisson coefficient ν.
- In the absence of external loads, the beam remains straight, the center of the cross section is by an abscise s.
- The cross section is identified by and outer and inner diameter, these remain constant for a given drill pipe or collar.
- The wellbore is assimilated to a cylinder with rigid walls, whether the well is open or cased
- We consider that the structure is under the effect of the following loads:
    - External loads at the surface ($s = 0$) and at the bit ($s = L$)
    - Its own weight, offset with buoyancy effect

- Normal contact forces with the wellbore, assumed to be continuous, similar to a soft string model
- Although the beam is considered static, the torque due to rotation is taken into account via a friction torque.
- The friction forces (due to axial displacement and rotation) are Coulomb forces, related to the contact force via axial and rotational friction coefficients (resp. μ_a and μ_r)

4.3 Applied loads

4.3.1 The buoyed weight

The primary load applied on the drill string is its own weight, the force is applied at the center of gravity downwards, this weight is offset by the buoyancy effect (Archimedes upward thrust). the force is given by the following expression

$$\overrightarrow{w_b} = \rho_a A_s \vec{g} - \rho_b A_s \vec{g} = \rho_a A_s \left(1 - \frac{\rho_b}{\rho_a}\right) g\, \vec{k} = w_b \vec{k} \tag{4.33}$$

A_s the cross-section area of the beam element,
ρ_a the density of steel,
ρ_b the density of the mud,
g the specific gravity

For the present development, the buoyed weight is expressed in the mobile coordinate system with the following form:

$$\overrightarrow{w_b} = w_{bt}\vec{t} + w_{bn}\vec{n} + w_{bb}\vec{b} \tag{4.34}$$

4.3.2 Contact force and friction forces

Let us note $\overrightarrow{f_c}$ the side load applied by the rigid walls on the beam element cross section, this force is considered normal to the contact area. Within our equations, this force remains unknown and needs to be determined.

The axial displacement of the drill string (up or down) creates an axial friction force, proportionate to the side load (as defined in our initial hypothesizes), given by $\mu_a|\overrightarrow{f_c}|\vec{t}$, where the axial friction force is positive when Pulling out of the hole (POOH) and negative when drilling down.

In addition to the axial displacement of the beam structure, we take into consideration the rotation. This movement creates a friction moment. In the coulomb model, the load applied is tangent to the cross section, and is equal to $-\mu_r\vec{t} \wedge \overrightarrow{f_c}$, this force also applies a torque which is given by $\mu_r r_e|\overrightarrow{f_c}|\vec{t}$

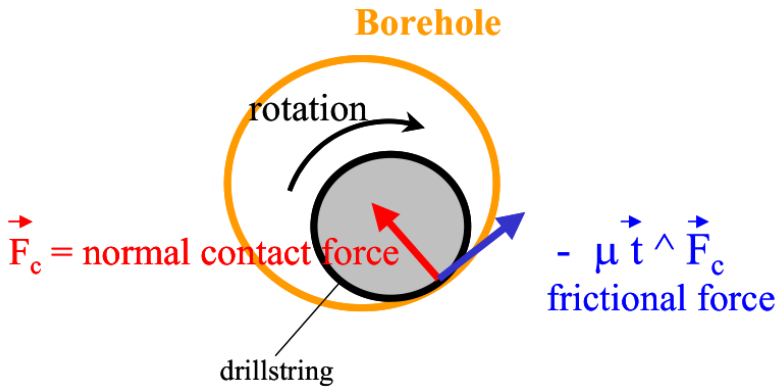

Figure 4-7 Friction force applied to the drill string

As with the weight of the drill string, these forces are represented in the mobile coordinate system. Since they are in the $(\vec{n}, \vec{b})$ plane, there is no tangent component. And thus, the side force is:

$$\overrightarrow{f_c} = f_{cn}\vec{n} + f_{cb}\,\vec{b} \tag{4.35}$$

4.4 Equilibrium equations

For a given cross section of the drill string, and following the previous hypotheses and taking into consideration the applied loads, the equilibrium equations for a static drill string, at the initial state are:

$$\begin{cases} \dfrac{d\vec{T}}{ds} + \vec{f} = \vec{0} \\ \dfrac{d\vec{M}}{ds} + \vec{t}\Lambda\vec{T} + \vec{m} = \vec{0} \end{cases} \tag{4.36}$$

$\vec{T}$ represents the tension
$\vec{M}$ represents the moment
$\vec{f}$ represents the loads applied on the drillstring
$\vec{m}$ represents the moments applied on the drill string

The external loads $\vec{f}$, are the sum of the buoyed weight and the friction forces due to axial displacement and rotation.

$$\vec{f} = (w_{bt} + \mu_a f_c)\vec{t} + (w_{bn} + f_{cn} + \mu_r f_{cb})\vec{n} + (w_{bn} + f_{cb} - \mu_r f_{cn})\vec{b} \tag{4.37}$$

And the moments applied on the drill string is:

$$\vec{m} = \mu_r r_e f_c \vec{t} \tag{4.38}$$

The tension and moment represented in the $(\vec{t}, \vec{n}, \vec{b})$ coordinate system are:

$$\vec{T} = T_t\vec{t} + T_n\vec{n} + T_b\vec{b} \tag{4.39}$$

$$\vec{M} = M_t\vec{t} + M_n\vec{n} + M_b\vec{b} \tag{4.40}$$

This vector equation system provides us with six differential equations. The variables that need to be determined are numbered eight, those are the three components for tension (T_t, T_n, T_b), the three components for moment (M_t, M_n, M_b) and the contact force components (f_{cn}, f_{cb})

In the TNB coordinate system, the normal and binormal moments are proportional to curvature, and stiffness, they are given as:

$$M_n = 0 \tag{4.41}$$

$$M_b = EI\,\kappa \tag{4.42}$$

And thus, the normal and binormal components can also be expressed as functions of the moments:

$$T_n = -\frac{dM_b}{ds} = -EI\frac{d\kappa}{ds} \tag{4.43}$$

$$T_b = \kappa M_t - \tau M_b = \kappa M_t - EI\kappa\tau \tag{4.44}$$

And thus, by replacing these expressions for T_n and T_b in the differential equations system, we now have 4 equations with 4 unknowns, as follows:

$$\begin{cases} \dfrac{dMt}{ds} + \mu_r r_e f_c = 0 \\ \dfrac{dTt}{ds} + EI\kappa\dfrac{d\kappa}{ds} + w_{bt} + \mu_a f_c = 0 \\ \kappa(T_t - \tau M_t) + EI\left(\kappa\tau^2 - \dfrac{d\kappa''}{ds}\right) + w_{bn} + \mu_r f_{cb} + f_{cn} = 0 \\ \kappa\dfrac{dMt}{ds} + Mt\dfrac{d\kappa}{ds} - EI\left(2\tau\dfrac{d\kappa}{ds} + \kappa\dfrac{d\tau}{ds}\right) + w_{bb} - \mu_r f_{cn} + f_{cb} = 0 \end{cases} \tag{4.45}$$

The system can further be simplified into a 2-equations system as follows

$$\begin{cases} \dfrac{dTt}{ds} = -w_{bt} - \mu_a f_c - EI\kappa\dfrac{d\kappa}{ds} \\ \dfrac{dMt}{ds} = -\mu_r r_e f_c \end{cases} \tag{4.46}$$

And expressing $f_c$by:

$$f_c = \frac{-\mu_r r_e Q2\kappa + \sqrt{Q1(Q2^2 + Q3^2) + (\mu_r r_e Q2\kappa)^2}}{Q1} \tag{4.47}$$

The parameters Q_i are given by

$$\begin{cases} Q1 = 1 + \mu_r{}^2\,(1 - \kappa^2 r_e{}^2) \\ Q2 = Mt\dfrac{d\kappa}{ds} - EI\left(2\tau\dfrac{d\kappa}{ds} + \kappa\dfrac{d\tau}{ds}\right) + w_{bb} \\ Q3 = \kappa(T_t\ - \tau M_t) + EI\left(\kappa\tau^2 - \dfrac{d\kappa''}{ds}\right) + w_{bn} \end{cases} \tag{4.48}$$

The normal and binormal components of the side force f_{cn} et f_{cb}can be obtained via the following expressions

$$\begin{cases} f_{cn} = -\dfrac{\mu_r(\kappa\,\mu_r r_e f_c - Q2) + Q3}{1 + \mu_r{}^2} \\ f_{cb} = \dfrac{\kappa\,\mu_r r_e f_c - Q2 - \mu_r Q3}{1 + \mu_r{}^2} \end{cases} \tag{4.49}$$

The boundary conditions to the differential equations system are known on the bit for $s = L$, considering

$$M_t(L) = Torque\ On\ Bit \tag{4.50}$$

$$T_t(L) = Weight\ On\ Bit \tag{4.51}$$

4.5 Resolution

The differential equations are of first order, with 2 variables and known boundary conditions on the bit. For the solution, the choice of the 4th order Runge-Kutta methods due to its simplicity, fairly accuracy and little computational time requirements.

For a general problem:

$$dT_t/ds = f(s, T_t, M_t), \quad T_t(L) = WOB \tag{4.52}$$

$$dM_t/ds = g(s, T_t, M_t), \quad M_t(L) = TOB \tag{45.53}$$

The approximate solution (T_{ti}, M_{ti}) at a given cross section s_i

$$T_{ti+1} = T_{ti} + (h/6)\,(k_{n1} + 2k_{n2} + 2k_{n3} + k_{n4}) \tag{4.54}$$

$$M_{ti+1} = M_{ti} + (h/6)\,(l_{n1} + 2l_{n2} + 2l_{n3} + l_{n4}) \tag{4.55}$$

And where the formulas for each of the k's and l's are:

$$k_{n1} = f(s_i, T_i, M_i) \tag{4.56}$$

$$l_{n1} = g(s_i, T_i, M_i) \tag{4.57}$$

$$k_{n2} = f(s_i + h/2, T_i + 0.5hkn_1, M_i + 0.5hl_{n1}) \tag{4.58}$$

$$l_{n2} = g(s_i + h/2, T_i + 0.5hkn_1, M_i + 0.5hl_{n1}) \tag{4.59}$$

$$k_{n3} = f(s_i + h/2, T_i + 0.5hkn_2, M_i + 0.5hl_{n2}) \tag{4.60}$$

$$l_{n3} = g(s_i + h/2, T_i + 0.5hkn_2, M_i + 0.5hl_{n2}) \tag{4.61}$$

$$k_{n4} = f(s_i + h, T_i + hkn_3, M_i + hl_{n3}) \tag{4.62}$$

$$l_{n4} = g(s_i + h, T_i + hkn_3, M_i + hl_{n3}) \tag{4.63}$$

4.6 Results and discussion

To validate our algorithm, we used a drill string given by the survey provided by SONATRACH. This one includes Inclination and Azimuth at different MD points with a step of 9.14m.

With these inputs, the algorithm determines the Northing, Easting and TVD, thus reconstructing the well geometry, as can be seen in the following figure

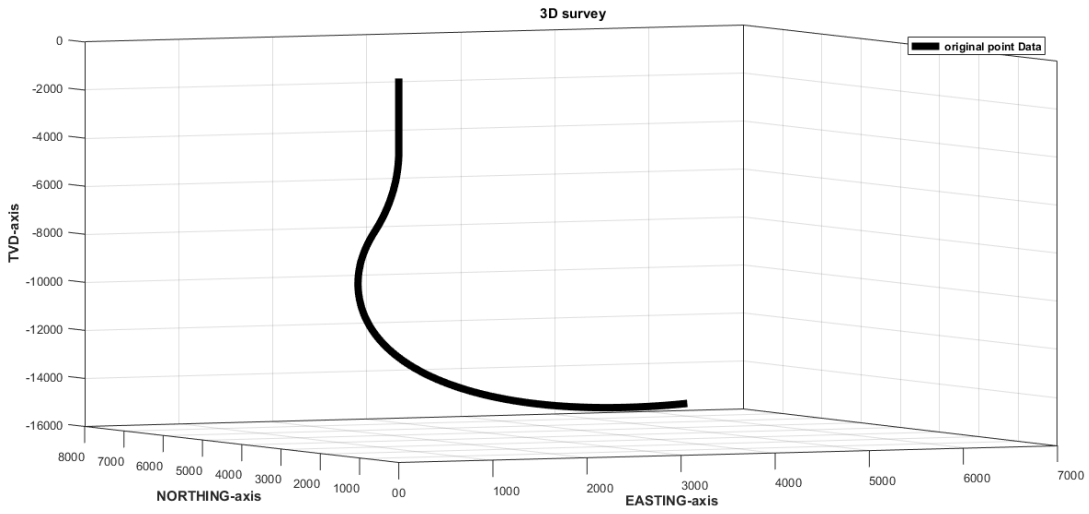

Figure 4-8 3D Well Survey

The obtained results are validated using the survey tool of the commercial code WellScan. In the following table compares some values for TVD, Easting and Northing that were obtained using WellScan and our algorithm.

Tableau 4-1 Comparative table for TVD, Easting and Northing

MD (ft)	Inc θ (°)	Azi ϕ (°)	TVD (ft) WellScan	Easting (ft) Wellscan	Northing (ft) Wellscan	TVD (ft) actual results	Easting(ft) actual results	Northing (ft) actual results
5007.81	11.26	0	4994.91	0	196.78	5001.64	0	190.09
6837,01	19.81	2.38	6748.85	1.90	708.37	6762.47	1.90	709.78
15233.33	53.45	44.71	13851.21	2320.54	4071.52	14266.73	2390.16	4193.57

Table 4-1 Relative error for survey

MD (ft)	Error TVD (%)	Error Easting (%)	Error Northing (%)
5007.81	1.8	1.8	1.8
6837.01	0.2	0.2	0.2
15233.33	3	3	3

It is noticed that the results are relatively close, with an error not exceeding 3%,

Afterwards, the calculations for the curvature (DLS) and torsion at each point are performed through our algorithm. Defining the components in the Serret-Frenet

coordinate system. The figures below represent the graphs outputted by our algorithm and the commercial code WellScan respectively.

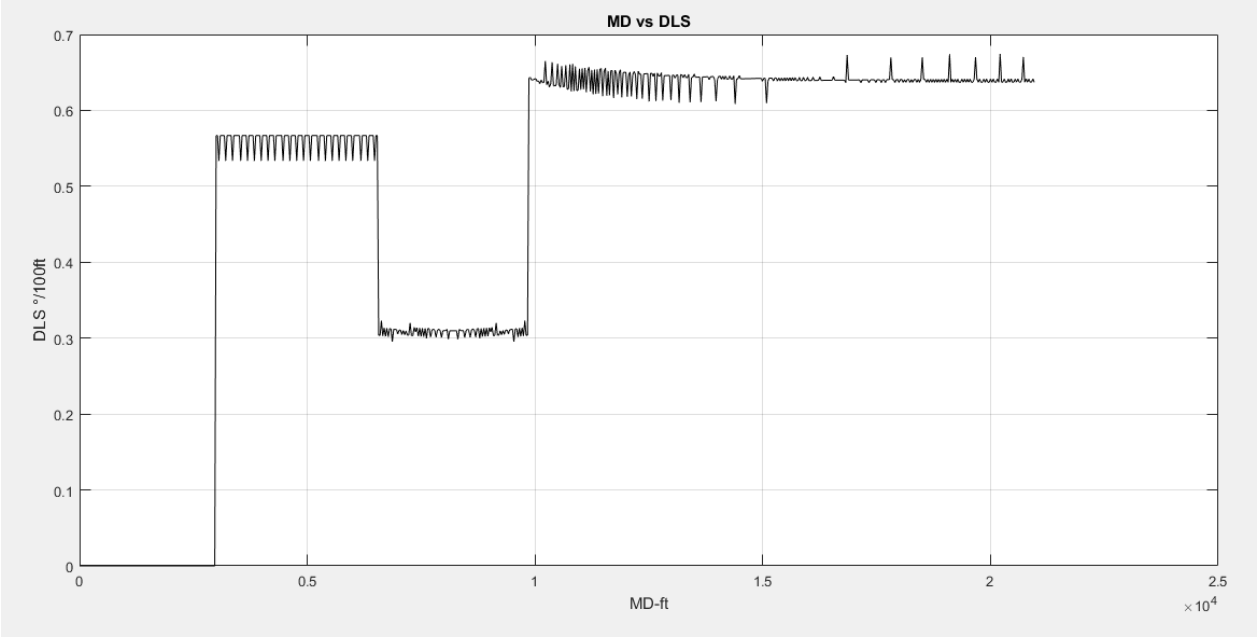

Figure 4-9 Curvature (DLS) provided by our algorithm

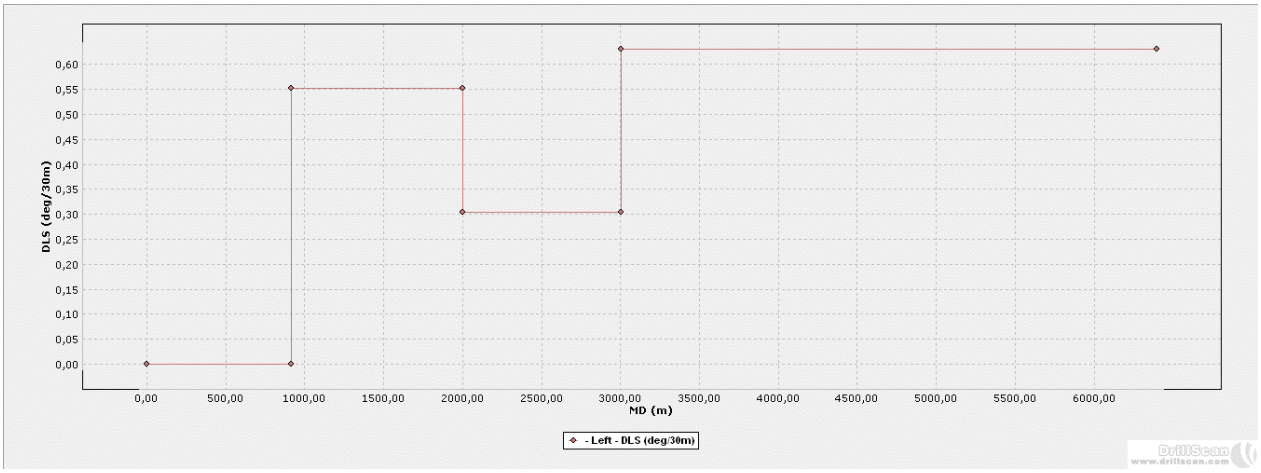

Figure 4-10 Curvature (DLS) provided by WellScan software

We notice that the commercial code WellScan, doesn't provide data for wellbore torsion. Thus, to validate the developed algorithm, we use a reference work given by Samuel Robello 2009 [38]. The following table summarizes the actual results compared to reference [38] for torsion and WellScan for DLS.

Table 4-2 Comparative of DLS calculations

MD(ft)	$\theta(°)$	$\phi(°)$	DLS (WellScan) $(°/100ft)$	DLS (actual work) $(°/100ft)$
6567.12	20	0		
6657.08	19.93	0.79	0.32	0.3097
6896.98	19.78	2.91	0.30	0.3065
7046.91	19.69	4.26	0.31	0.3091

Table 4-3 Comparative of torsion calculations

MD(ft)	$\theta(°)$	$\phi(°)$	τ (Samuel [38]) (°/100ft)	τ (actual work) (°/100ft)
5000	20	120		
5100	22	115	-9.85	-9.8097
5300	24	120	4.57	4.6564
5400	26	125	8.81	8.7952

The error between the two is in the following tables

Table 4-4 Error calculations between actual work and Robello calculation

Relative error	
DLS (%)	τ(%)
3.32	0.4
2.12	2
0.3	0.2

One can observe that the present results are well in concordance with those given by Samuel Robello [38] and the commercial code WellScan. In fact, the relative error does not exceed 3.5% and 2% for DLS and torsion, respectively.

At this stage, the geometry is now fully defined. the data of the well-defined geometry are processed by the algorithm from which we determine the bending moment along the drill string for the initial configuration. The results are plotted in the following figure:

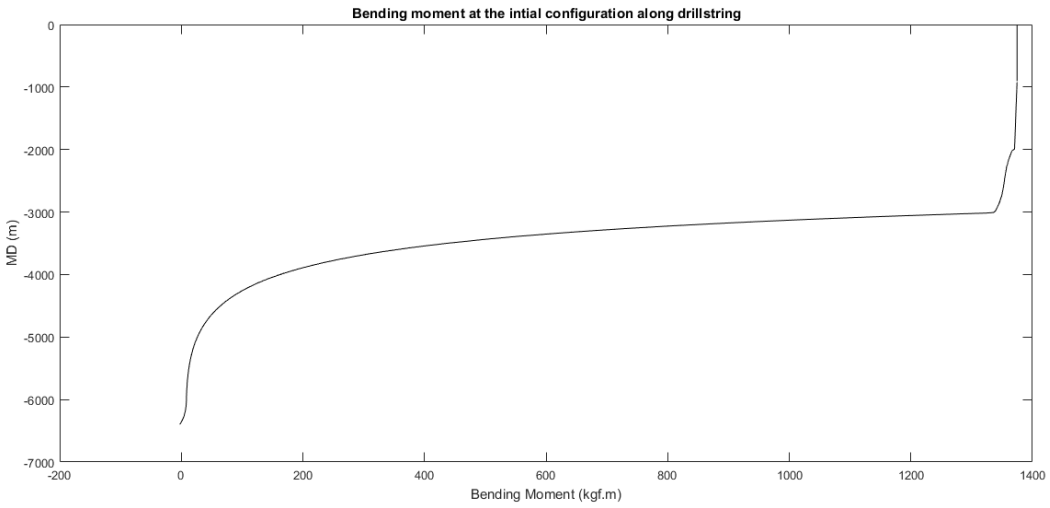

Figure 4-11 Bending Moment along the drill string at the initial configuration

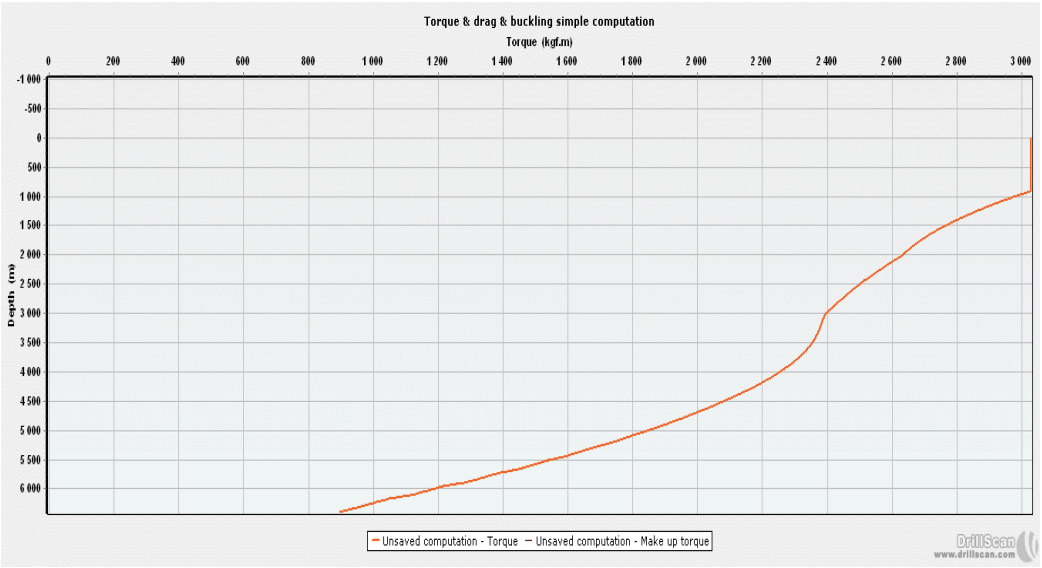

Figure 4-12 Torque along the drill string at the Final Configuration (WellScan)

In comparison to the bending moment at the final configuration, provided by the WellScan software, we notice a similar shape between the two graphs, with changes at the KOP for the curved section with inclination change only (1000m-3000 m), and the curved section with both azimuth and inclination change (3000m-7000m). The model responds well to changes in wellbore geometry.

Chapter 5 Study of the impact of curvature and tortuosity on torque, drag and buckling

This chapter is to emphasize more on such phenomenon problem of buckling, torque and drag. For this purpose, we intend to conduct this through hypothetical and real wells. throughout the study we are going to see how curvature and tortuosity key parameters for buckling affect torque and drag, as it can be seen through the analysis, the importance of conducting planned studies in gaining time, money and reducing risk.

5.1 Effects of wellbore curvature on torque, drag & buckling.

One of the problematic a drilling engineer often faces in the planning of horizontal wells is setting Kick Off Points, these points establish the curvature and geometry of the well.

We will investigate the effects of this parameter by setting up 3 hypothetical wells, each with identical drill strings (Drill collars only, OD 8-inch, ID 3 inch) and varying geometries, these are represented below to highlight the effects of curvature.

The first well is set according to the following survey points:

Table 5-1 Survey points for well 1

Well 1		
MD (m)	Inc (deg)	Azi (deg)
0	0	0
1000	0	0
2000	20	0
3000	20	30
5000	90	50

this set up generates a maximum DLS of 1.05 °/30m for the final segment, and a DLS of 0.6 °/30m, as represented in the figure below:

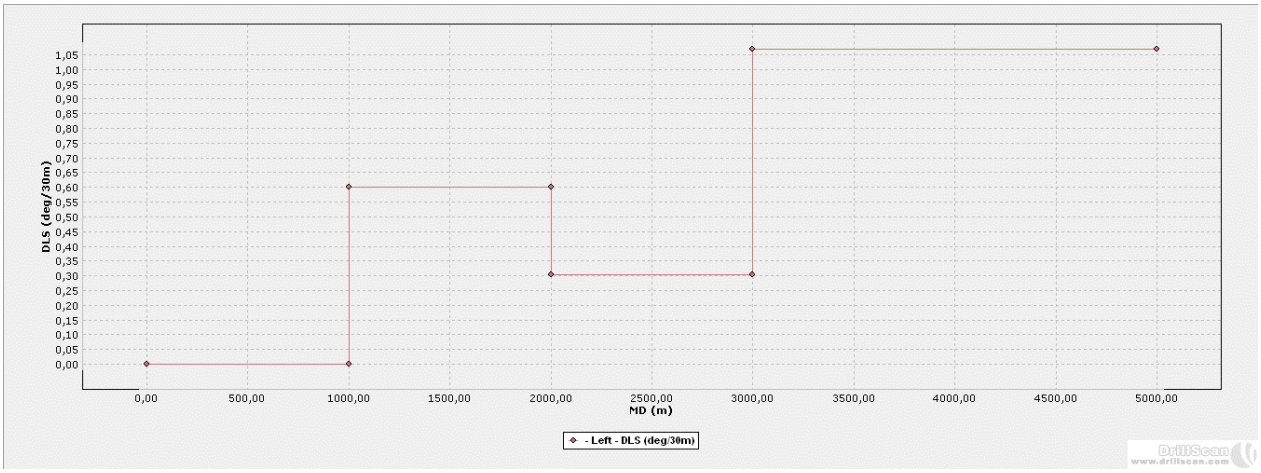

Figure 5-1 DLS for well 1

For the second well, we decrease the radius of curvature by shorting the buildup section by 500m for both buildup segments. The other points remain identical. The new survey points are represented in the table below:

Table 5-2 Survey points for well 2

Well 2		
MD (m)	Inc (deg)	Azi (deg)
0	0	0
1000	0	0
1500	20	0
3500	20	30
5000	90	50

This leads to an increase of DLS in the first segment to 1.2 °/30m and 1.41 °/30m in the final buildup, as represented in the following figure:

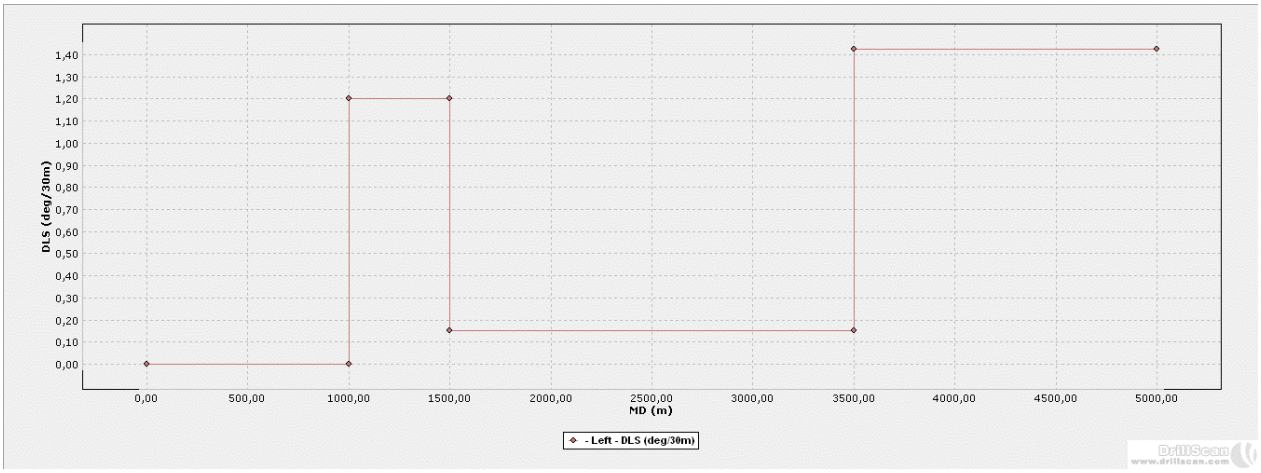

Figure 5-2 DLS for well 2

For the final set up, we increase inclination and azimuth further for the buildup segments to 50° and 70° respectively, the new survey points are:

Table 5-3 Survey points for well 3

Well 3		
MD (m)	Inc (deg)	Azi (deg)
0	0	0
1000	0	0
1500	50	0
3500	50	50
5000	90	70

This leads to a further noticeable increase in DLS for the first segment to 3 °/30m. For the final segment the increase in azimuth leads to a decrease in DLS to 0.82 °/30m

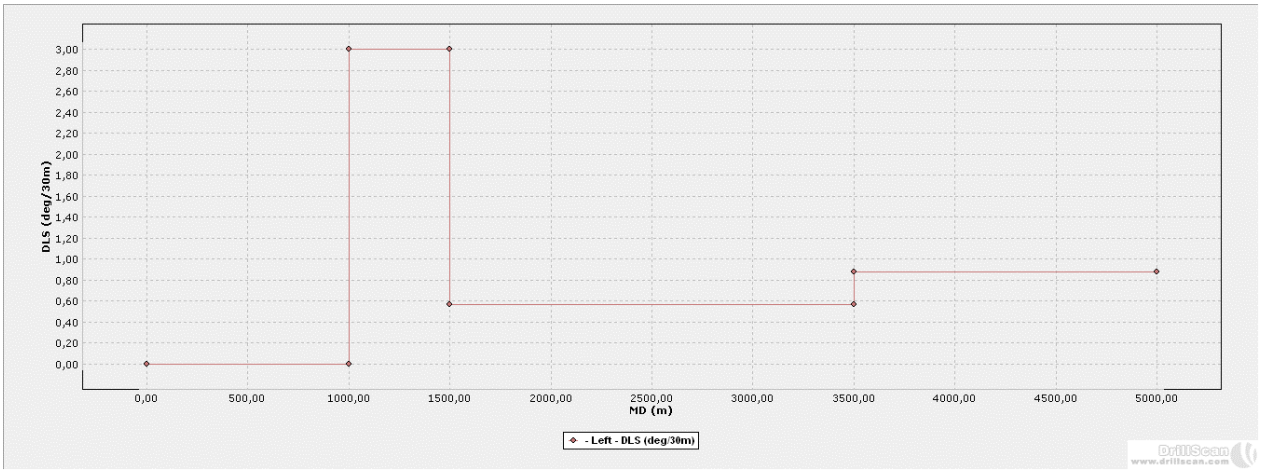

Figure 5-3 DLS for well 3

The drilling parameters used are represented in the table below

Table 5-4 Drilling parameters used in the simulation

Parameter	*Unit*	**Value**
String depth	*(m)*	5000.00
RPM	*(rpm)*	60.00
Rate of penetration	*(m/h)*	10.00
Weight on bit	*(tf)*	20.00
Torque on bit	*(kgf.m)*	900.00
Mud weight	*(SG)*	1.50000
Casing friction	*(nu)*	0.30
Open hole friction	*(nu)*	0.30

the resulting graphs for bending moment and side force are presented below for the three set ups

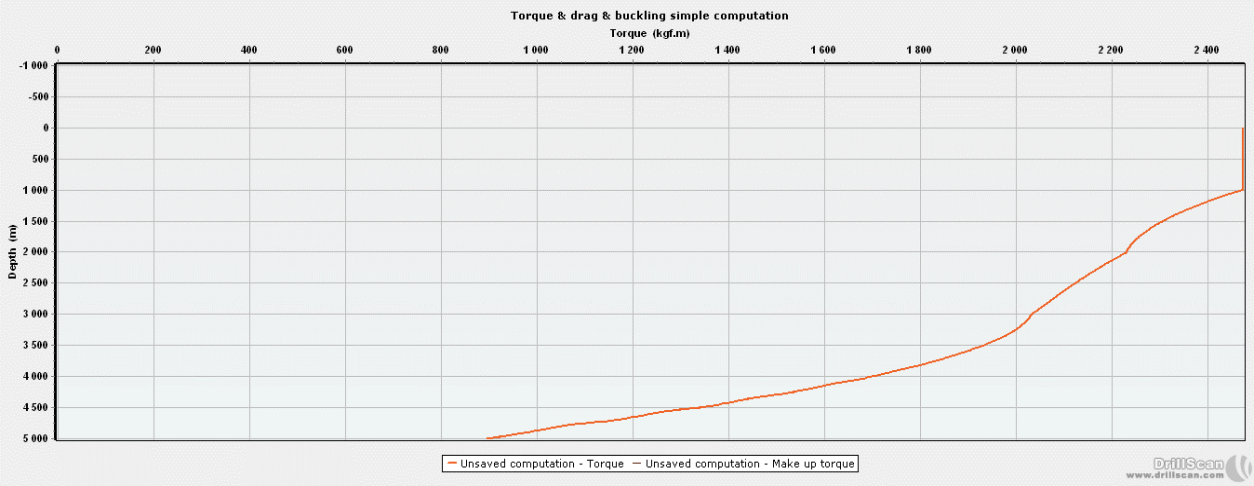

Figure 5-4 Torque for well 1

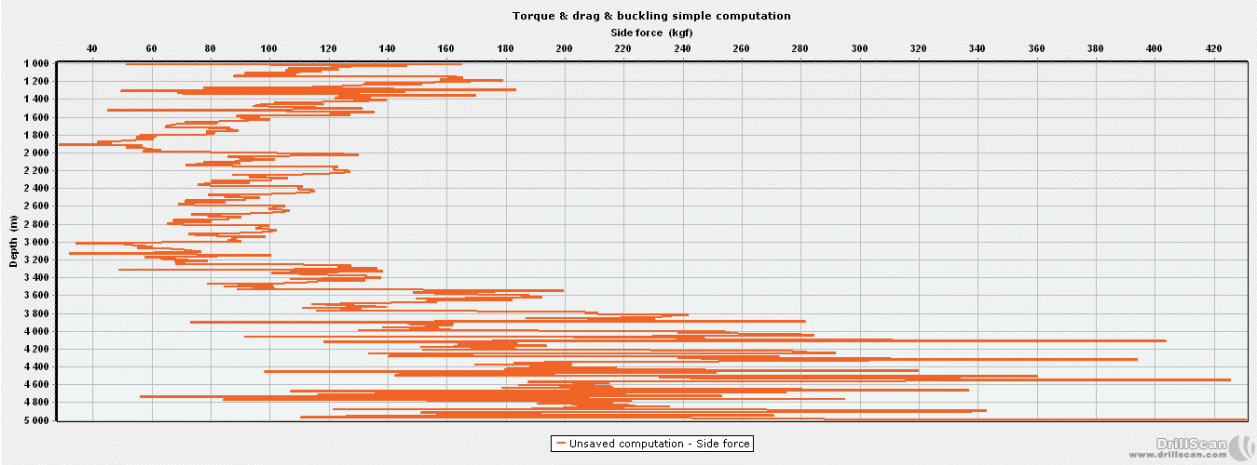

Figure 5-5 Side force for well 2

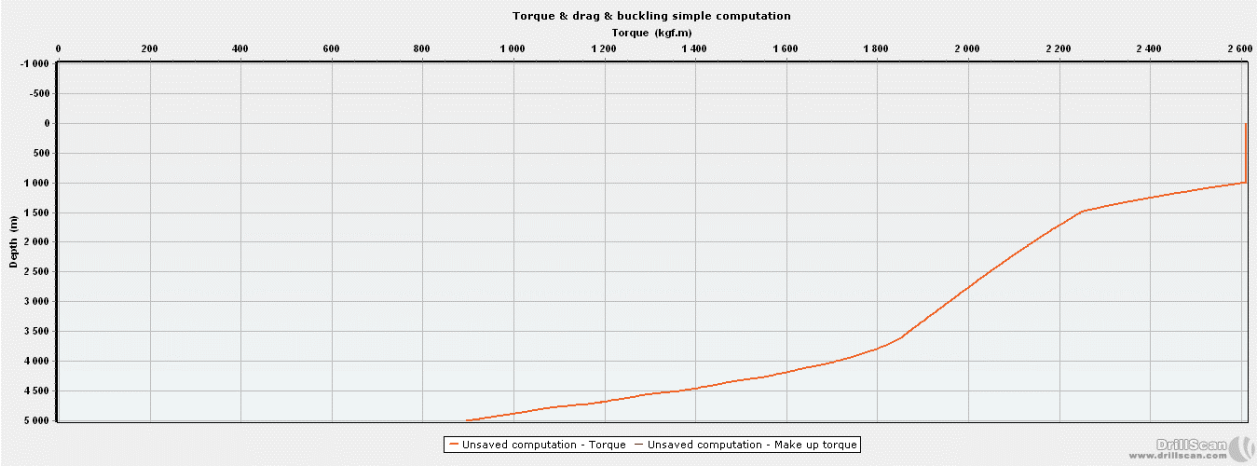

Figure 5-6 Torque for well 2

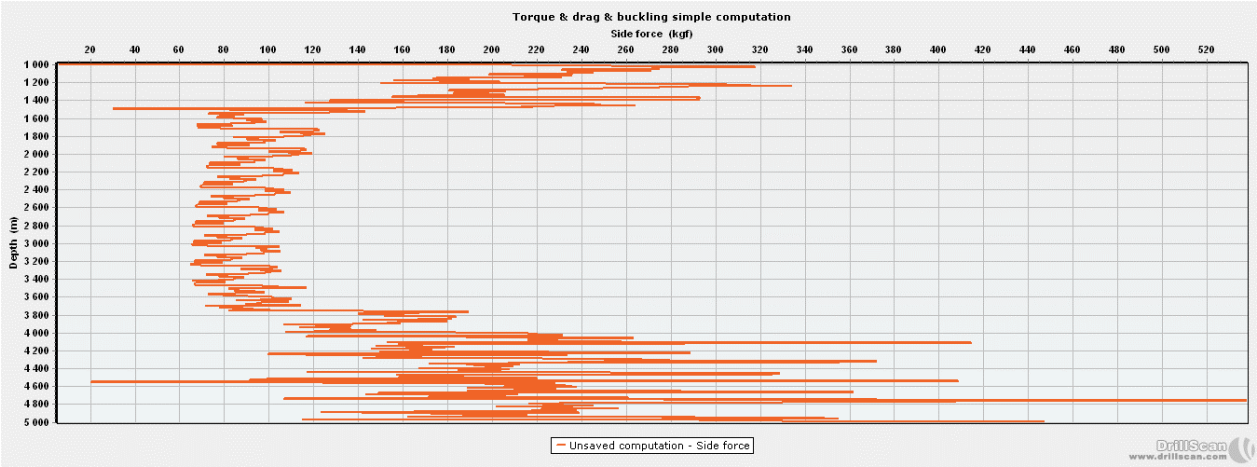

Figure 5-7 Side force for well 2

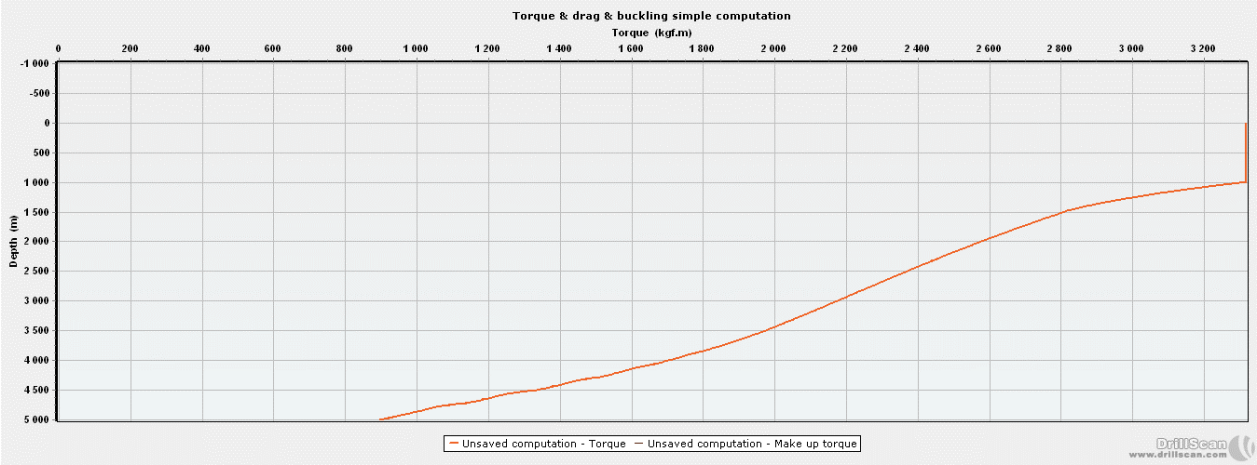

Figure 5-8 Torque for well 3

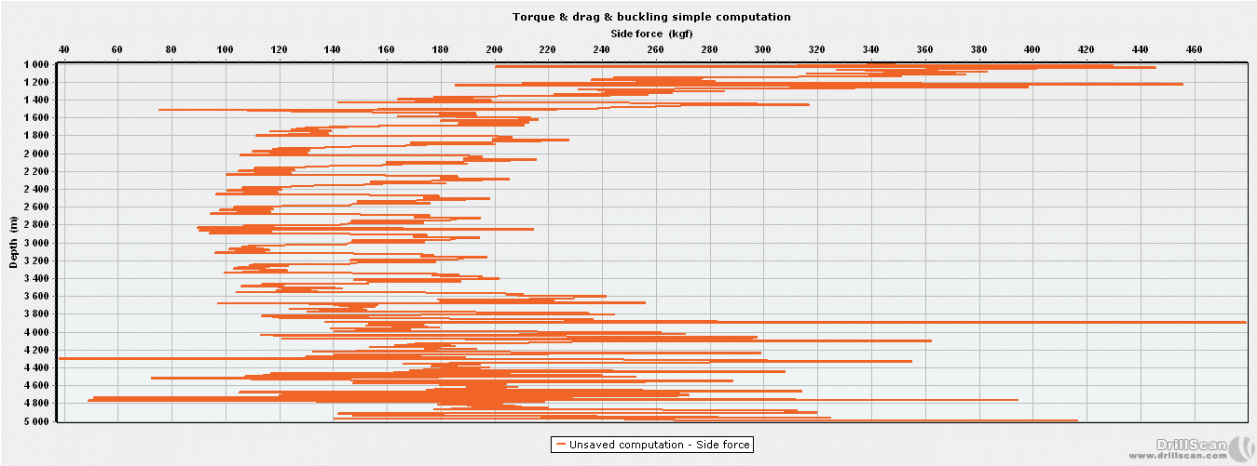

Figure 5-9 Side force for well 3

Observation and Discussion

Using this set up, the torque is at a maximum on the surface, reaching a value of $M_{max} = 24.50\ kN.m$, with lower values at the second build up segments, to dissipation as friction moment with the well walls. This is seen in the side force graph, where side force peaks in the horizontal section at $F_{cmax} = 43.084\ kN$ generating a bending stress of $\sigma_{max} = 135\ MPa$ and a mean value of $F_{cmoy} = 3.80\ kN$.

Decreasing the radius of curvature increases the torque, it is noticed that the maximum value of torque on surface is $M_{max} = 2615\ kgf.m$ and increasing the curvature by increasing inclination is as done in the third well, creates an increase in torque up to $M_{max} = 3328\ kgf.m$

At the KOP of 3500m we can notice the presence of an inflection in the first two wells causing a quick increase in torque. This is due to the large discrepancy between the azimuth and inclinations between the two segments. As it also noticed that the inflection doesn't appear in the last well.

However, side force responds differently in the three wells, although the decrease in radius of curvature (increase in DLS) causes an increase in side force between the first and the second set ups it is in fact, decreased in the third set up, going from a max value of $537\ kgf$ to $479\ kgf$.

The bending stress along the drill string, which is one of the key parameters that need to be monitored in order to avoid fatigue, decreases with the increase of curvature (or DLS). Numerical values of bending stress showing a decrease from $\sigma_{max} = 135\ MPa$ to $\sigma_{max} = 127\ MPa$. However, in the final set up, an increase in bending stress is noticed with the increase of inclination and azimuth with a value of $\sigma_{max} = 153\ MPa$

From these conclusions we understand that the drilling engineer, when planning the trajectory of a well, has different tools to ensure the safest and optimized design, for example decreasing curvature to minimize bending stress and avoid drill string failure, or increasing inclination and azimuth to reduce side force on the wellbore walls to avoid excessive friction that can cause drillstring failure.

5.2 Effect of tortuosity on buckling

Wellbore tortuosity can be defined as the occurrence of borehole spiraling or oscillation of wellbore path, while a planned wellbore is considered is often considered smooth, an actual well trajectory is often "rough" and creates variation of the inclination and azimuth angles presented by surveys and predicted trajectories. The industry has no standard for quantifying tortuosity, often expressed in deg/100 ft (or deg/30m) similar to expression of dogleg severity (DLS) however generally it is expressed as the ratio of the summation of the total curvature, including build and walk rates, to the survey stations length. These can be applied using different models. To investigate the effect of tortuosity we will consider the sinewave method [38].

Sinewave method

This method modifies the inclination and azimuth of the survey point based on the concept of a sine wave shaped ripple running along the wellbore using a specified magnitude and wave length. And thus, the angle change is modified using the following relationship

$$\Delta\alpha = \alpha_T \sin\left(\frac{D}{P}2\pi\right) \tag{5.1}$$

These parameters are determined based on evaluation from historical data from offset or similar wells. The final inclination and azimuth are given as follows:

$$\theta = \theta_{survey} + \Delta\theta \tag{5.2}$$
$$\phi = \phi_{survey} + \Delta\phi \tag{5.3}$$

To highlight the effect of tortuosity, we will be using the data from well one of the previous experience, and we will apply a tortuosity with a sinewave model, using a magnitude of 1° and a period of 300m, these are characteristic of highly tortuous well, small perturbation to highlight the effect of tortuosity.

This tortuosity is applied in the first build up segment of the well, located between MD's 1000 and 2000, where the set inclination is 20° and the azimuth angle is 0°.

The graph for DLS is shown below:

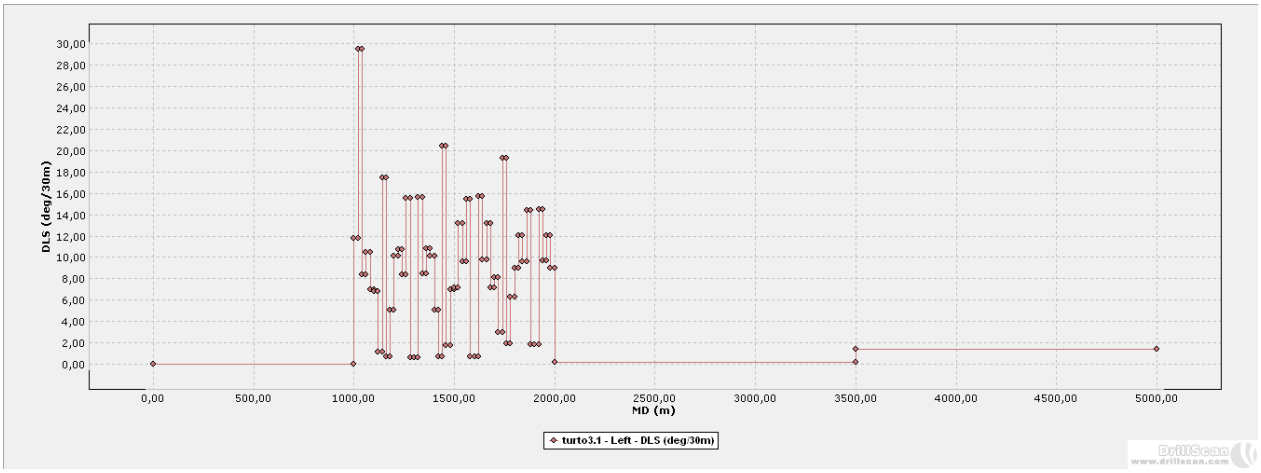

Figure 5-10 DLS for a tortuous well M=1° period 300m

One can notice that even a small roughness has caused a significant increase in DLS throughout the segment with a maximum DLS of 29°/30m and a mean value of 13°/30m

Below we represent the values of torque and tension, for the non-tortuous and tortuous wells

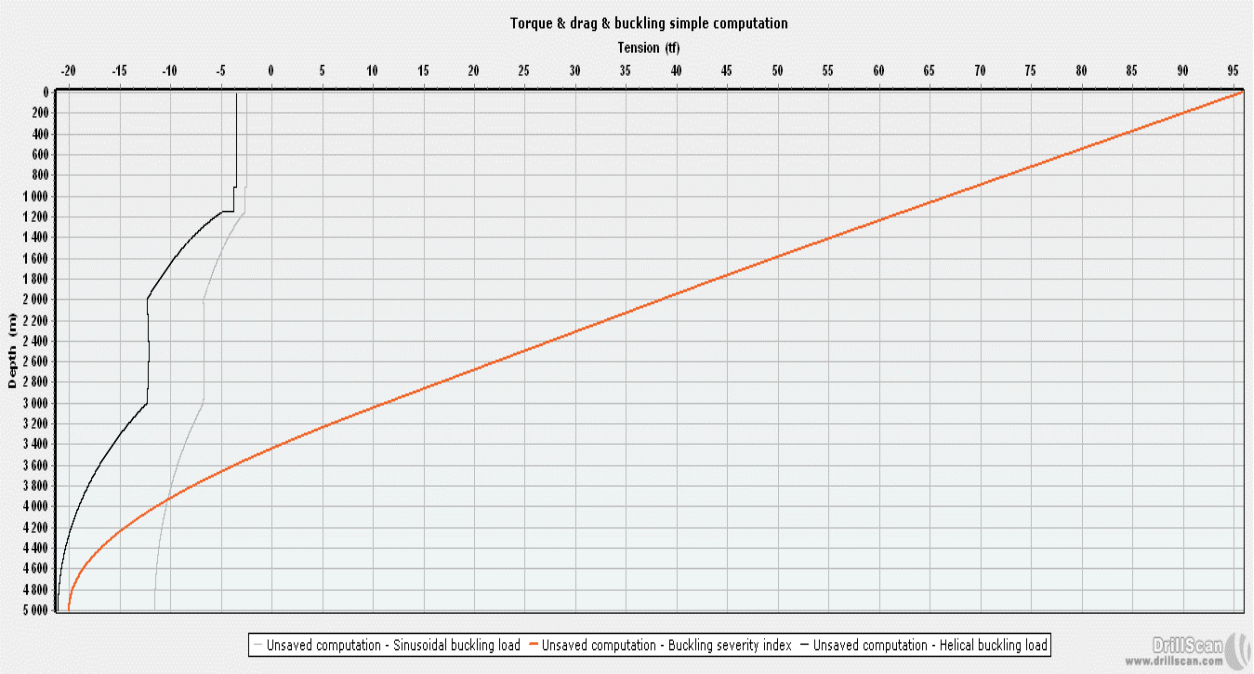

Figure 5-11 Tension for non-tortuous well

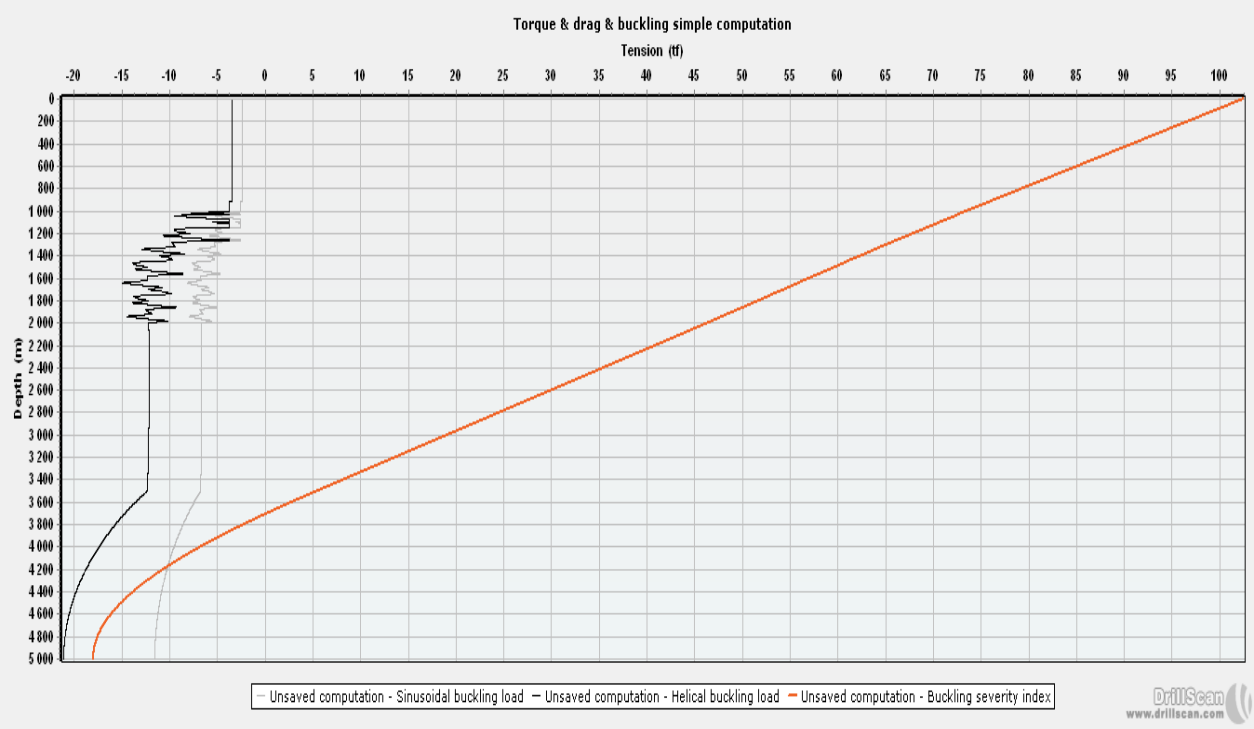

Figure 5-12 Tension for the tortuous well

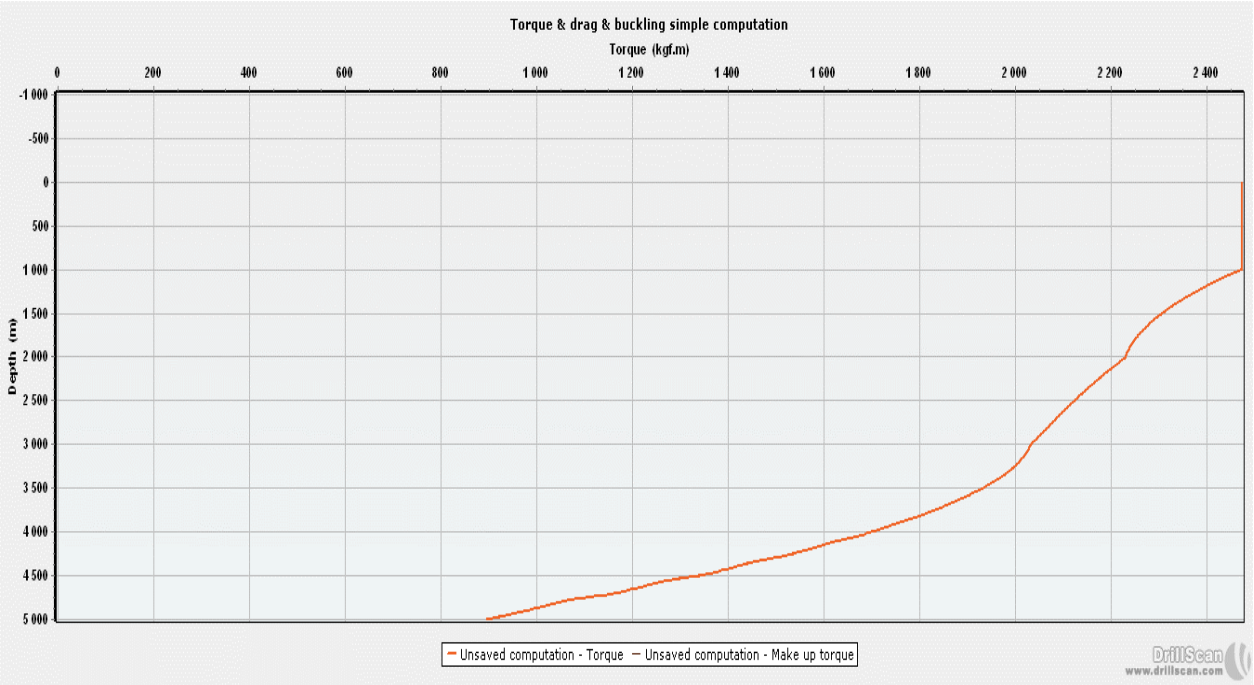

Figure 5-13 Torque for the non-tortuous well

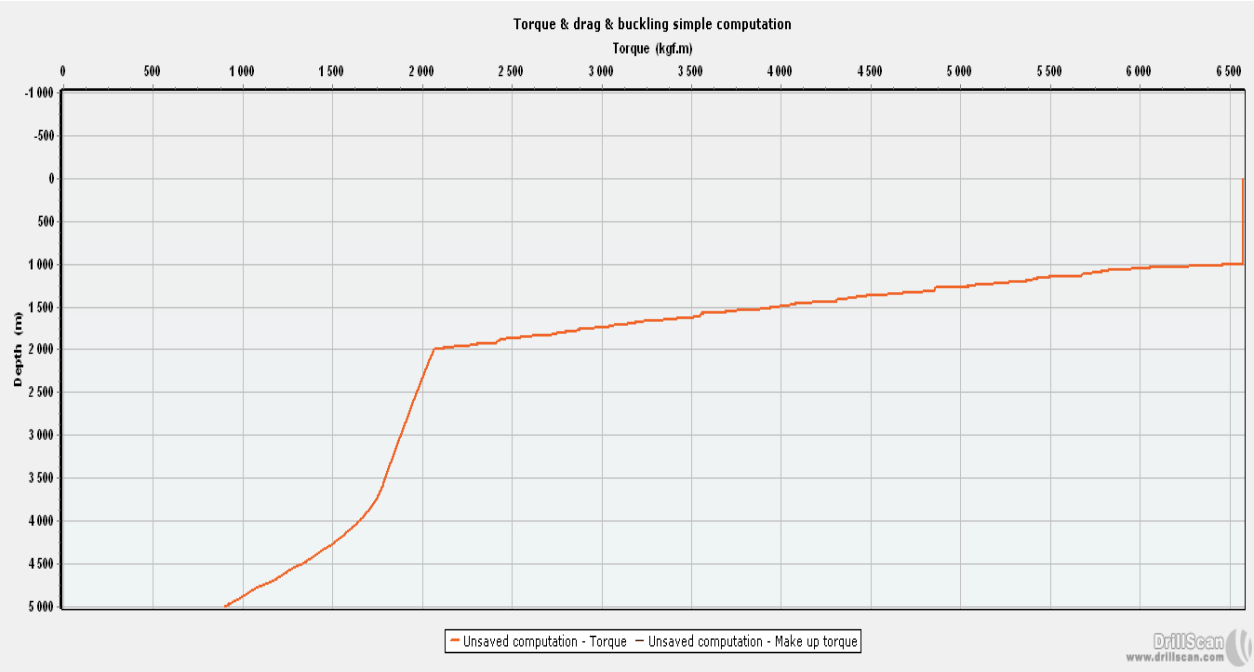

Figure 5-14 Torque for the tortuous well

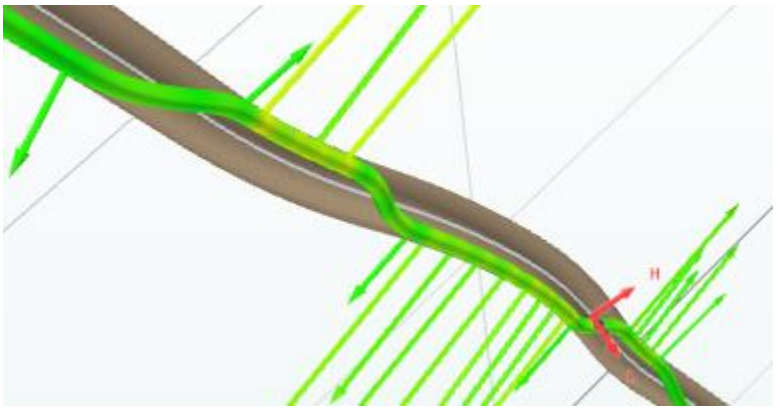

Figure 5-15 post buckled shape with tortuosity

Discussion

From the figures representing tension, it is noticeable that tortuosity does not affect axial force transfer (WOB) by a large effect, causing only a slight increase from 96 TF in the non-tortuous well to 103 TF in the tortuous well.

When considering torque at the tortuous segment, for a non-tortuous well, torque increases from 2240 kgf.m to the max value of 2400 kgf.m. In the tortuous well, the torque is up to a value 6650 kgf.m. That is caused by the buckled shape of the drill

string which is heavily influenced by wellbore roughness (figure 5-15). This is especially true when considering drill pipes which are a lot less stiff than drill collars. The additional contact points generate a significant increase in friction and thus in the makeup torque.

Tortuosity when coupled with pipe stiffness can lead to a noticeable effect on buckling, torque and drag. Tortuosity is as well difficult to theoretically model as it is expensive to experimentally determine in the field (through the use of gyros). Thus, depending on the sensitivity of the operation, it is the duty of the field engineer to identify the critical parameters and invest in modeling them.

5.3 Comparative of torque and drag using planned and actual data survey

The planning of a well involves interpolating inclination and azimuth from the key KOPs and using this planned trajectory. Estimation for the torque and tension required on the surface are performed, and maximum bending stress and side force are estimated to take precaution against drill string fatigue and cavitation.

However, in practice, with actual survey data, these parameters need to be revaluated, on one hand, to save the final well data and on the other to serve as a starting point for future preliminary analysis on similar or nearby wells.

Using the commercial code WellScan, and using well data for the ONIZ-502, provided by SONATRACH. Computation for torque and drag are performed using the planned data for the well, and another computation using actual survey points collected after well completion.

The drillstring composition and drilling parameters are presented in the tables below:

Table 5-5 Drill string for ONIZ-502

Item	Joints	OD (in)	ID (in)	Weight (lb/ft)	Length (m)
5"Impreg Bit	1	6			0.25
Motor	1	4.75	3	48	9.5
NM Pony DC	1	4.5	2.5	45	4.5
MWD	1	4.75	3	40	10
DC	1	4.75	2.5	45	4.5
Circulating Sub	1	4.75	2.5	45	0.6
3.5" DP	75	3.5	2.7	13.5	686
3.5" HWDP	27	3.5	2 1/16	25.3	252
4.75" Hydraulic Jar	1	4.75	2.25	37	9.1
3.5" HWDP	8	3.5	2 1/16	25.3	75
3.5" DP	85	3.5	2.7	13.3	768

The computations are run with the following parameters

Table 5-6 Drilling parameters for the ONIZ-502 computation

Rotation speed (rpm)	40
ROP (m/h)	10
WOB (TF)	10
TOB (kgf.m)	0

For the planned computation, the following KOP's are introduced

Table 5-7 ONIZ-502 Planned KOP's

ONIZ-502 planned		
MD (m)	Inc (deg)	Azi (deg)
0	0	0
3120	0	0
3353.492	23.5	320
3478.052	54	320
3558.722	89.295	89.295
4208.903	89.295	89.295

the completed well survey is performed by Halliburton, providing 95 survey points, for an MD ranging from MD=0 m to $MD = TD = 4034.37\,m$. We represent the key KOP's in the following table

Table 5-8 Actual survey points for ONIZ-502

ONIZ-502 actual survey		
MD (m)	Inc (deg)	Azi (deg)
0	0	0
3150	0	0
3350	31.175	330
3480	72.765	330
3560	86.00	330
4034.67	86.00	330

The results obtained from the numerical simulation are presented in the graphs below, expressing torque, tension and side force, respectively. Figures highlighting the maximum bending stresses along the drill string are also presented.

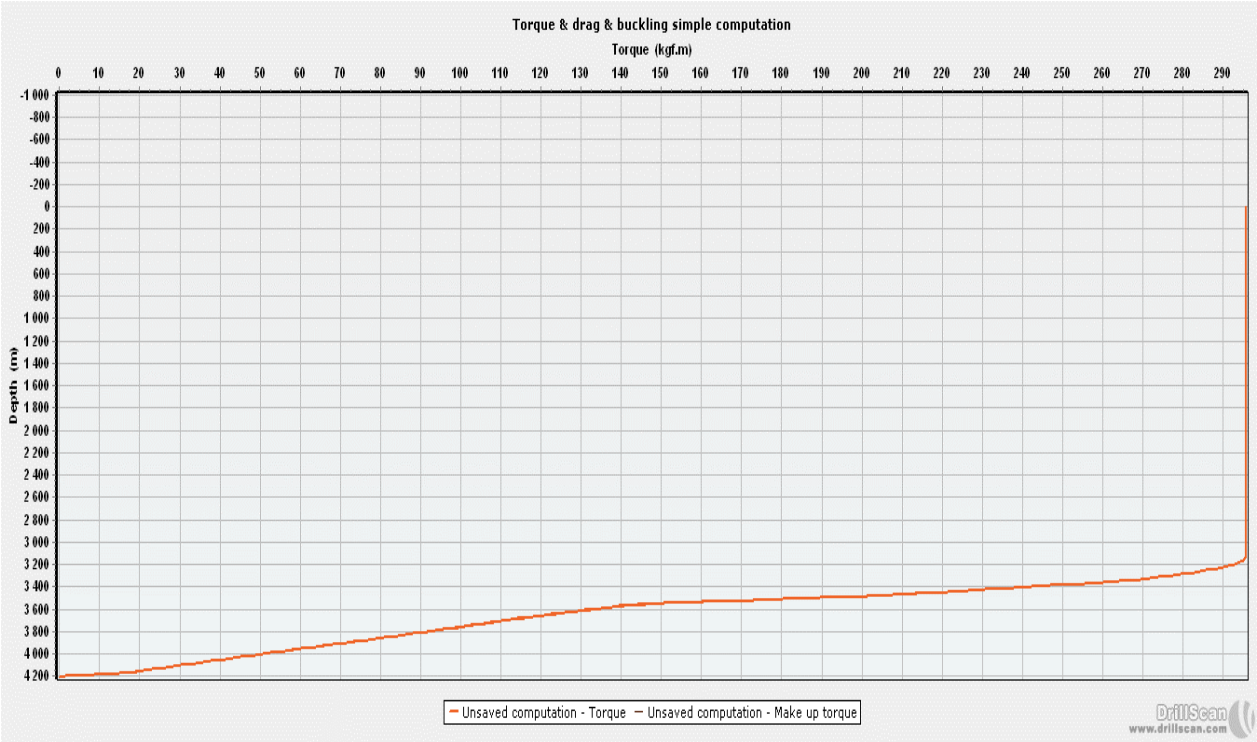

Figure 5-16 Torque for the planned ONIZ-502

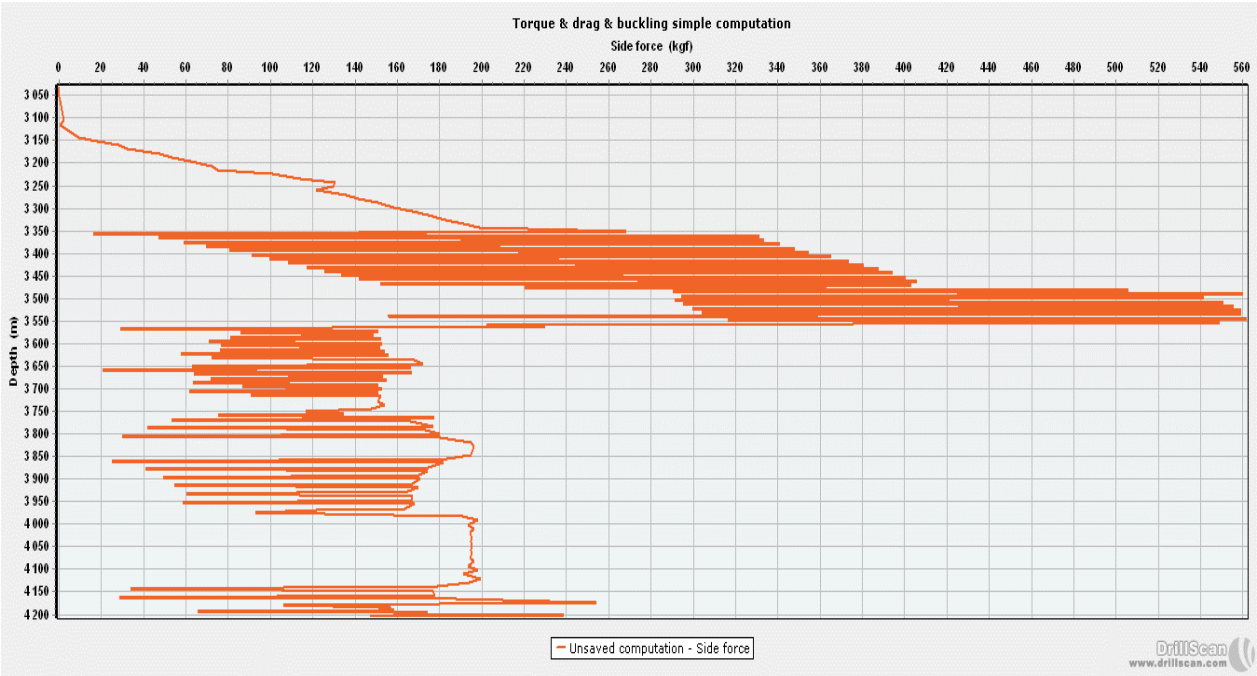

Figure 5-17 Side force for planned ONIZ-502

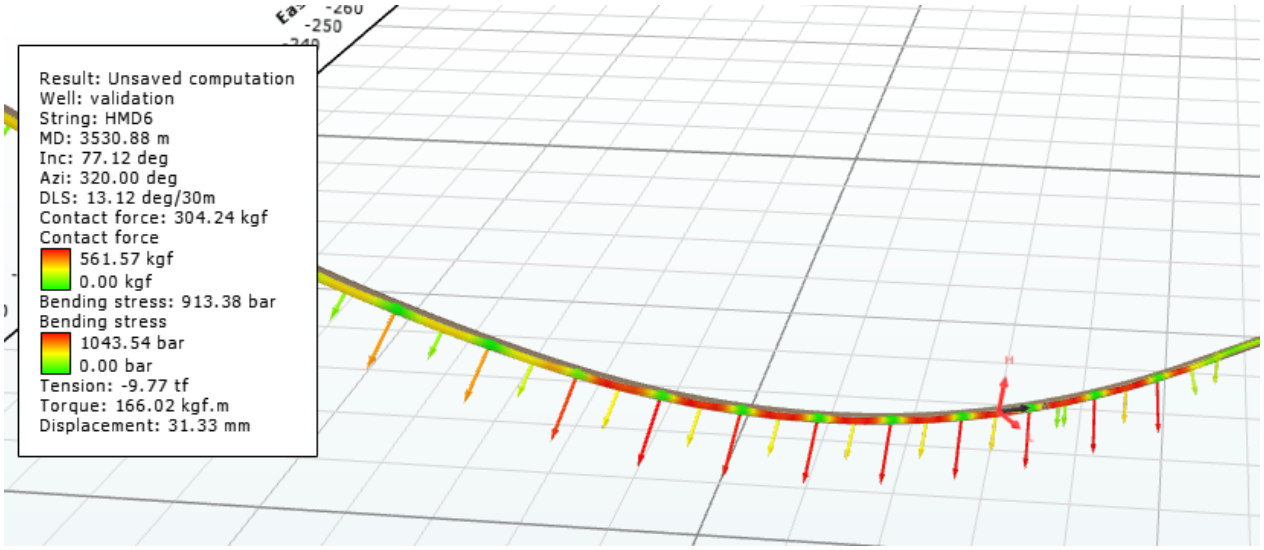

Figure 5-18 Maximum bending stress along the drill string

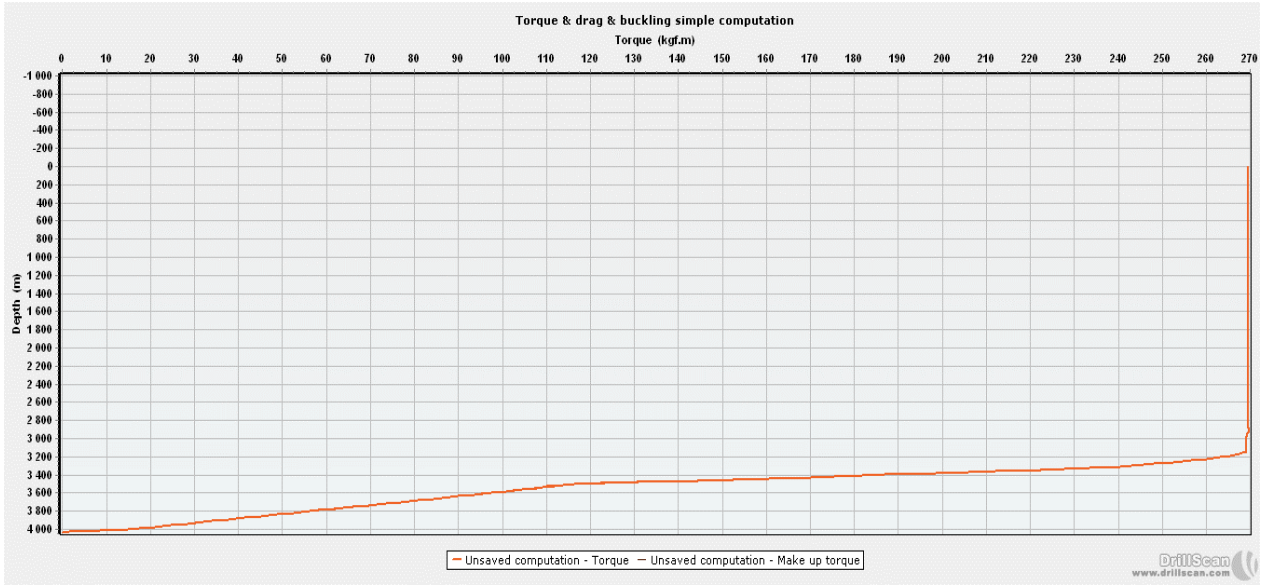

Figure 5-19 Torque in the surveyed ONIZ-502

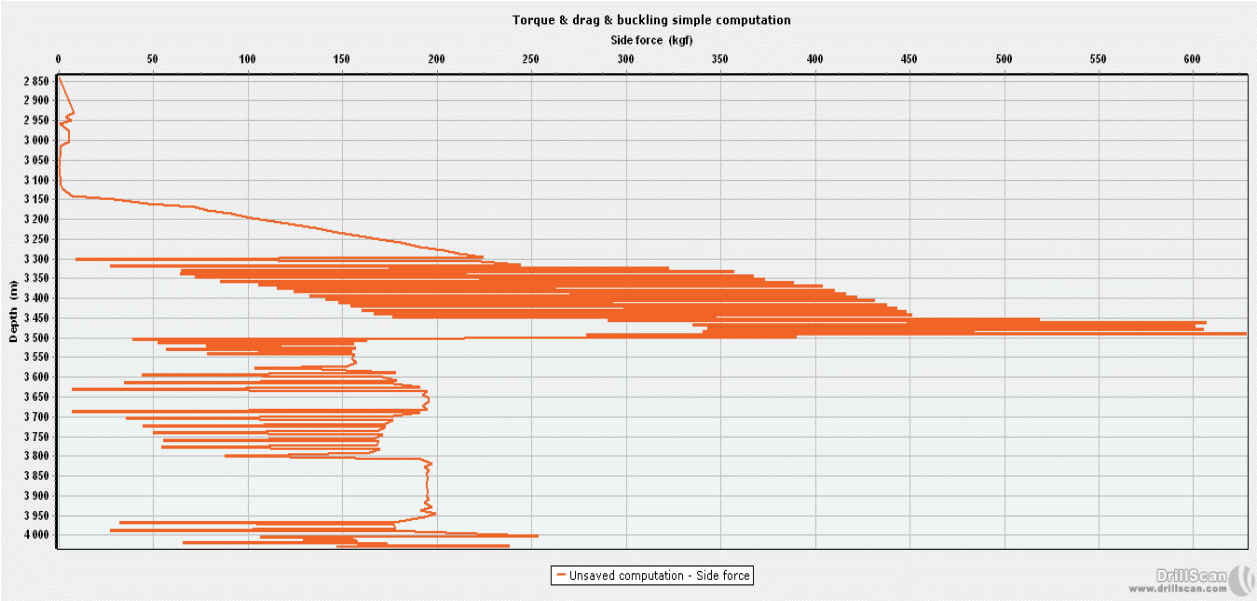

Figure 5-20 Side force in the surveyed ONIZ-502

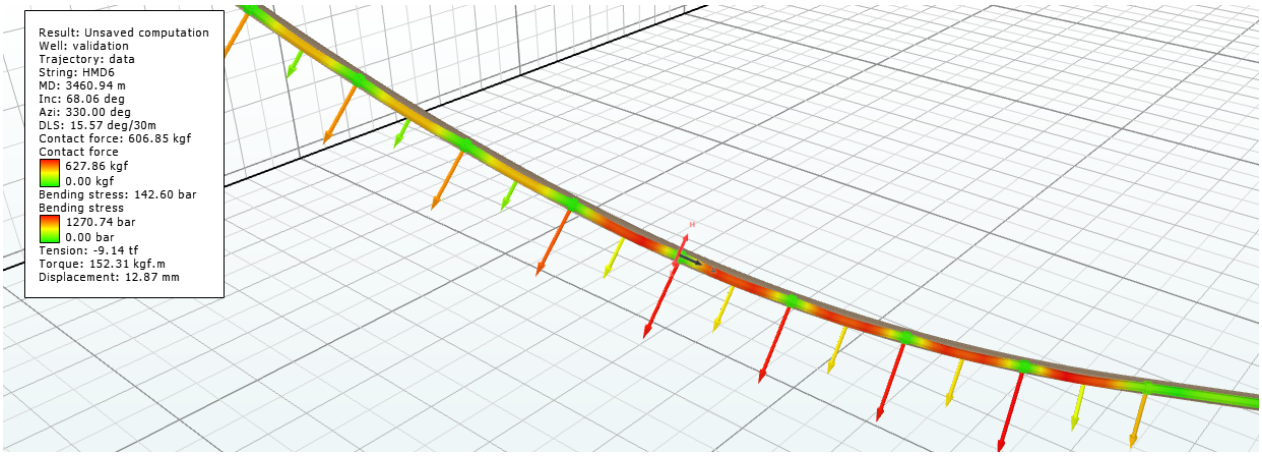

Figure 5-21 Maximum bending stress along the surveyed ONIZ-502

Observations and discussion

Comparing data from planned and actual surveys of the ONIZ-502 for values of torque on surface, maximum side force and maximum bending stress, one can notice the following:

- Torque on surface using the planned survey is estimated at 269.751 $kgf.m$ whereas it remains almost constant at 270 $kgf.m$ for the actual surveyed well.

- An increase in maximum side force along the drill string of 10.5% is registered, with numerical values going from 561.57 $kgf\ to$ 627.86 kgf.
- An increase of 16% in the maximum bending stress along the drill string is registered, with numerical values going from 104.3 MPa to 120.7 MPa.

The values are generally underestimated between planned and actual survey computations. This can be explained by a number of factors including but not limited to: the imperfection in geology, oscillation from the motor and different events during the drilling operations. However, the planned computation remains a valuable tool, as it allows a close estimate of the important factors during the drilling operations, insuring that they are within commonly accepted values in the industry.

Conclusion

Buckling is influenced by several parameters, some related to

- Well geometry: inclination, azimuth, curvature, tortuosity.
- Drillstring properties: type of string, dimension, material.
- Geology: friction factor
- Drilling operation: ROP, rotational speed, torque on bit, weight on bit, mud weight…etc.

A detailed study of the effect of the parameters on the drilling operations, mainly torque, drag and bending stresses along the drill string to identify buckling severity needs to be conducted. With knowledge of how these parameters interact with each other and thus affect buckling phenomenon. Proper hypothesis can be established for the development of a mathematical model predicting buckling and estimating torque and drag in drilling operations.

Conclusion

The main objective of our project is to investigate the buckling phenomenon of drillstrings within wellbores of different geometries: Vertical, inclined and horizontal. A problematic proposed by the research center and development of SONATRACH in order to develop its own software for torque & drag.

As mechanical engineers possessing little experience within the drilling industry, and thus to successfully complete this work, we delved into the subject, conducting an extensive research, learning through case studies, attending conferences and seminars, contacting industry experts and acquiring firsthand experience in drilling rigs through an internship.

Through a comparative study, the most practical model "Lubinski" for buckling in vertical wells was established. An algorithm capable of treating all drill strings present in the industry was developed. This algorithm was used to analyze post buckling shape and bending moment, as well as side force.

In the case of inclined wellbores, the Dawson-Paslay formula was established. It is known to be the most practical and recommended to the industry for estimating buckling in inclined wellbores.

For curved wellbores a hybrid survey method was adopted based on MCM and wellbore torsion formulas to determine curvature and torsion within a wellbore, as well as reconstructing the geometry (TVD, East, North). Based on this data, a computation for bending moment along the drill string at initial configuration was established.

Finally, an analysis of the impact of well geometry on drilling parameters (Torque & drag) was conducted highlighting how such a tool can be used to assist a drilling engineer in optimizing planned operations.

This work can be used as a basis for a more detailed analysis of buckling, a project that holds a great interest for the mechanical engineering and development laboratory as well as for the research center and development of SONATRACH.

It would be valuable to investigate the problem using a finite element analysis which is a common approach in the industry and has been validated experimentally. Other algorithms with focus on decreasing computational time can be developed.

Extensions should be done on the present model to account for curved wellbores, thus estimating the displacements for the initial configuration and using an iterative process for contact point management and studying the non-continuous contact.

A scaled down experimental set up can be designed to approximate actual downhole conditions from which registered displacements can be used to validate the presented models.

Bibliography

[1] M. E. Hossain and b. A. Al-Majed, "**Fundamentals of Sustainable Drilling**". Scrivener Publishing LLC, 2015.

[2] S. Z.Miska and Robert F.Mitchell, **"Fundamentals of Drilling Engineering"**. Society of petroleum Engineers, 2011.

[3] William C. Lyons and G. J. Plisga, **"BS-Standard Handbook of Petroleum and Natural Gas Engineering"** third Edition, United States of America: Elsevier Ltd , 2010.

[4] William C. Lyons and G. J. Plisga , **"BS-Standard Handbook of Petroleum and Natural Gas Engineering"** second Edition, United States of America: Elsevier Ltd, 2004.

[5] J. J.Azar and R. G. Samuel, **"Drilling engineering Formulas"** PennWell Corp, 2007. USA

[6] Baker Hughes "**Directional Surveying Drilling & Evaluation Technologies**", Company Manual, USA, 1998.

[7] J. H. B. S. Junior, "**A Mathematical model for buckling in curved wells**". PhD Thesis School of Mines, Colorado, 1996.

[8] B. K. ÇAĞLAYAN, "**Torque and Drag application for deviated and curved wellbores**" PhD Thesis, Middle East Technical School, 2014.

[9] S. Timoshenko and J. Goodier, Theory of Elasticy, Mc-Graw-Hill Book

Company, 1951.

[10] Lubinski.A, "**A study of the buckling of rotary drilling strings**," American Petroleum Institute journal *vol 57* pp. 117-143 USA, 1950.

[11] W. C. Yu. "**A Critical review of the heavy elastica**" International Journal of Mechanical Science vol 106, pp 106-132 1986.

[12] W. J and J.-W. H. C "**Helical buckling of pipes in extended reach and horizontal wells**" Transaction of the Amercian Association of Mechanical Engineers, vol 36, pp. 42-71, 1993.

[13] L. J, P. P. D and S. W. R, "**Interpreation of calculated forces on sucker rods**" Society of Petroleum Enginers Production & Facilites journal, 1995.

[14] J. B. Shmid, "**Modifying Rayleigh's own Method for Estimating Buckling Loads and other Eignevalues**" Technical Report, 1998.

[15] J. B. Saliès, "**Experimental and Mathematical Modeling of Helical Buckling of Tubulars in Directional Wellbores**" in *Eastern Regional Conference and Exhibition*, Charleston, 1994.

[16] A. Lubinski, S. A. W and L. L. 1. J, "**Helical buckling of tubing sealed in packers**" Journals of Petroleum Technology, vol 30, pp. 33-56, 1962.

[17] P. Cheatham, "**Helical postbuckling configuration of a weightless column under the action of an axial load**" Society of Petroleum Engeers Journal, vol 59, pp. 21-36 1984.

[18] J. Cheatham and Y. C. Chen, "**New design considerations for tubing and casing buckling in inclined wells**," in *Offshore Technology Conference*, Houston, 1988.

[19] R. F. Mitchell, "**Buckling behavior of well tubing: The Packer Effect**" American Institute of Mechanical Engineers journal vol 103, pp. 54-68, 1982.

[20] R. F. Mitchell, "**New Concepts for Helical Buckling**" American Institute of Mechanical Engineers journal vol 109, pp. 136-190, 1988.

[21] J. H. B. S. Junior, "**A Mathematical Model for Mechanical Buckling of Drillstring Within Curved Boreholes**" Techincal report, university of south Dacota, 1996.

[22] P. R. Paslay and B. B. D, "**The stability of a circualr rod laterally constrained to be in contanct with an inclined circular cylinder**" Journal of Applied Mechanics vol 25, pp. 253-266, 1964.

[23] R. Dawson and Paslay, R. R, "**Drill Pipe Buckling in Inclined Holes**" Journal of Petroleum Technology vol 103, pp. 56-84, 1984.

[24] Y. C. Chen and J. B. Cheatham, "**Wall Contact Forces on Helically Buckled Tubulars in Inclined wells**" American Society of Petroleum Engineers Journal vol 66, pp. 231-256 , 1990.

[25] J. Wu and H. C. Juvkam-Wold, "**Study of helical buckling of pipes in horizontal wells**" Technical report, university of Oklahoma City, 1993.

[26] D.-L. Gao and Wen-Jun Huang, "**A review of down-hole tubular string buckling in well engineering**" Society of Petroleum Engineers, Technical report, 2015.

[27] D. Gao, F. Liu and B. Xu, "An analysis of helical buckling of long tubulars in horizontal wells," in *Sixth International Oil and Gas Conference and Exhibition in China*, 1998.

[28] S. Z. Miska and Guohua Gao, "Effects of Boundary Conditions and Friction on Static Buckling of Pipe in a Horizontal Well," Society of Petroleum Engineers, USA, 2009.

[29] J. AKOWANOU, "**Modélisation tridimensionnelle du flambage des tiges dans les puits de forage à trajectoire complexe**" Thèse de Doctorat, Ecole Nationale Superieur des Mines de Paris, Paris, 2009.

[30] G. R. Samuel, **"Formulas and Calculations for Drilling Operations, United States of America".** Technical Report, Scrivener, 2010.

[31] B. S.Aadnoy, L.Cooper, S. Z.Miska and R. F.Mitchell, "**Advanced Drilling and Well Technology**". Technical Report, Society of petroleum Engineers, 2009.

[32] A. Belaid, "**Modélisation tridimensionnelle du comportement mécanique de la garniture de forage dans les puits à trajectoires complexes : application à la prédiction des frottements garniture-puits**" Thèse de Doctorat, Ecole Nationale Supérieur des Mines de Paris, paris, 2005.

[33] E. Fitchard and S. A. Fitchard, **"The Effect of Torsion on Borehole Curvature**", *Oil & Gas Journal vol 102,* pp. 121-124, 1983.

[34] L. Xiushan, "**Average Borehole Cruvature Calcculation of Hole Trajectory**" *Oil & Gas Journal vol 124* pp. 11-15, 2005.

[35] L. Xishuan, "**New Technique Calculates Borehole Curvature, Trosion**" *Oil & Gas Journal vol 125,* pp. 41-49, 2006.

[36] W. Shan, L. Xiushan and Z. Daqian, "**The Shape of the Space Curve of Borehole Trajectory,**" *Journal of Drilling Petroleum Institute vol 69,* pp. 32-36, 1993.

[37] L. Xishuan and S. Zaihong, "**Numerical Approxiation Improves Well Survey Calculation,**" *Oil & Gas Journal vol 71,* pp. 50-54, 2001.

[38] R. Samuel and Xiushan Liu, "**Wellbore Tortuosity, Torsion, Drilling Indices and Energy: What do They have to do with Well Path Design,**" Society of Petroleum Engineers journal, vol 156, pp. 127-167, USA, 2009.

Appendix

5.4 Matlab algorithm for vertical wells

```
%=========================% LUBENSKI METHODS %=============================%
function sol= lubenski4(x3, od, id, rhot, rhom, thetha, e, l, odh, wob, x1)
%UNTITLED Summary of this function goes here
% Detailed explanation goes here
%=========================% INPUTs %=============================%
od=input('od=');                    %outer diameter
id=input('id=');                    %inner diameter
rhot=input('rho tube=');            %volumetric mass density of drill string
rhom=input('rho mud=');             %volumetric mass density of mud
thetha=input('thetha=');            %inclination
e=input('E=');                      %young's modulus
odh=input('odh=');                  %diameter of well
wob=input('wob=');                  %weight on bit
L=input('LENGTH=');                 %length of drill string
syms x3;

%==================================% Calculations %==================%
disp('the cross section');
 s=(pi()/4)*(od^2-id^2);
disp(' moment of inertia of plane area');
 i=(pi()/64)*(od^4-id^4);
disp('buoyancy factor ');
 kb=(rhot-rhom)/rhot;
 disp('buoyed pipe weight en lb/in');
 w=(kb*rhot*s*1000*0.0254^2)/1.4882/12
 disp('radial clearance en lb/in ');
 rc=(odh-od)/2
 disp('length in inch');
 length=L/0.0254;
 disp('build rate ');
 bur=(100*thetha)/(L/0.3048)
 disp('radius of curvature in inch');
 R=68765/bur
 disp('radius of curvature in feet');
 Rft=R/12
 m=((e*i)/w)^(1/3)
 x2=wob/w*m

  %=========================% OUTPUTS %=============================%

 %=========================% les forces critique %====================%
  if(thetha~=0)
disp('critical loads using Dawson / Paslay ');
fc=((2*sqrt((e*w*i*sin(thetha*pi()/180))/rc))/2204.632) %Sinusoidal critical loads
fchil=(2*sqrt(2)-1)*fc                                  % Helical critical loads
  end
    if(thetha==0)
disp('critical loads using lubenski vertical wells ');
fclubenski=(1.94*((e*i*w^2)^(1/3)))/2204.632            %  Sinusoidal  critical
loads
disp('critical loads using the energy method vertical wells');
fcenergie=(2.55*((e*i*w^2)^(1/3)))/2204.632         % Sinusoidal critical loads
fchelical=(5.55*((e*i*w^2)^(1/3)))/2204.632         % Helical critical loads
```

```
 end
%=========================% LUBENSKI methods %======================%
n=25;
S=sym(zeros(1,n));F=sym(zeros(1,n));G=sym(zeros(1,n));H=sym(zeros(1,n));
P=sym(zeros(1,n));Q=sym(zeros(1,n));R=sym(zeros(1,n));T=sym(zeros(1,n));
U=sym(zeros(1,n));
for i=1:n
    syms x
    Ps=4:3:3*i-2;
    S(i)=((-1)^i)*x^(3*i)*prod(Ps)*(1/factorial(3*i+1));
    F(i)=((-1)^i)*x^(3*i)*prod(Ps)*(1/factorial(3*i));
    Pg=2:3:3*i-1;
    G(i)=((-1)^i)*x^(3*i)*prod(Pg)*(1/factorial(3*i+1));
    Ph=3:3:3*i;
    H(i)=((-1)^i)*x^(3*i)*prod(Ph)*(1/factorial(3*i+2));
    Pp=4:3:3*i+1;
    P(i)=((-1)^i)*x^(3*i)*prod(Pp)*(1/factorial(3*i+2));
    Q(i)=((-1)^i)*x^(3*i)*prod(Pg)*(1/factorial(3*i));
    R(i)=((-1)^i)*x^(3*i)*prod(Ph)*(1/factorial(3*i+1));
    T(i)=((-1)^i)*x^(3*i)*prod(Pg)*(1/factorial(3*i+2));
    U(i)=((-1)^i)*x^(3*i)*prod(Ph)*(1/factorial(3*(i+1)));
end
S(x)=x*(1+sum(S));
F(x)=1+sum(F);
G(x)=x*(1+sum(G));
H(x)=-1*x^2*(0.5+sum(H));
P(x)=-1*x^2*(0.5+sum(P));
Q(x)=1+sum(Q);
R(x)=-1*x*(1+sum(R));
T(x)=x^2*(0.5+sum(T));
U(x)=-1*x^3*((1/6)+sum(U));

cte=1;
matrice=[P(x1) Q(x1) R(x1) 0 0 0 0; F(x3) G(x3) H(x3) 0 0 0 0; S(x3)-S(x1)
T(x3)-T(x1) U(x3)-U(x1) 0 0 0 1;0 0 0 P(x2) Q(x2) R(x2) 0;0 0 0 F(x3) G(x3)
H(x3) 0;0 0 0 S(x3)-S(x2) T(x3)-T(x2) U(x3)-U(x2) 1;P(x3) Q(x3) R(x3) -P(x3) -
Q(x3) -R(x3) 0];
o=det(matrice);
o=sym2poly(o);
x3=roots(o);
x3= double(x3(imag(x3)==0 & x3>0 & x3<x2));
disp('the points of contact is at ')
disp(x3);

sol=inv([P(x1) Q(x1) R(x1) 0 0 0; F(x3) G(x3) H(x3) 0 0 0; S(x3)-S(x1) T(x3)-
T(x1) U(x3)-U(x1) 0 0 0;0 0 0 P(x2) Q(x2) R(x2);0 0 0 F(x3) G(x3) H(x3);0 0 0
S(x3)-S(x2) T(x3)-T(x2) U(x3)-U(x2)])*[0; 0 ;1; 0 ;0; 1];
sol=vpa(sol)

end
```

5.5 Matlab code for curved wellbores

```
clear
clc
%depth
MD1=xlsread('Input.xlsx','Input','A2:A701');
MD2=xlsread('Input.xlsx','Input','A3:A702');

% en deg
thetaA=xlsread('Input','Input','B2:B701');
thetaB=xlsread('Input.xlsx','Input','B3:B702');
phiA=xlsread('Input.xlsx','Input','C2:C701');
phiB=xlsread('Input.xlsx','Input','C3:C702');

%FC=xlsread('Input.xlsx','Input','D2:D702');
% en rad
ThetaA=deg2rad(thetaA);
ThetaB=deg2rad(thetaB);
PhiA=deg2rad(phiA);
PhiB=deg2rad(phiB);
%================================================================================
=%
DL=rad2deg(acos(cos(ThetaA).*cos(ThetaB)+cos(PhiB-
PhiA).*sin(ThetaA).*sin(ThetaB)));
SAB=MD2-MD1;

DLS=DL./SAB/0.3048;
%==================================
imax=length(DLS);
s=xlsread('Input.xlsx','Input','A2:A702');%ft
s=s.*0.3048;%ft to m
Inc=xlsread('Input','Input','B2:B702');
Azi=xlsread('Input','Input','C2:C702');
Inc=Inc.*(pi/180);
Azi=Azi.*(pi/180);
%Ginc
Ginc=zeros(1,imax);
Ginc(imax)=(Inc(imax)-Inc(imax-1))/(s(imax)-s(imax-1));
Gazi=zeros(1,imax);
Gazi(imax)=(Azi(imax)-Azi(imax-1))/(s(imax)-s(imax-1));
for i=1:imax-1
    Ginc(i)=(Inc(i+1)-Inc(i))/(s(i+1)-s(i));
```

```
    Gazi(i)=(Azi(i+1)-Azi(i))/(s(i+1)-s(i));
end
Azi=xlsread('Input','Input','C2:C702');
Beta=DLS;
dBeta=zeros(1,length(Beta));
%dBeta(1)=0;
dBeta(imax)=(Beta(imax)-Beta(imax-1))/(s(imax)-s(imax-1));
for i=1:length(Beta)-1
dBeta(i)=(Beta(i+1)-Beta(i))/(s(i+1)-s(i));
end
d2Beta=zeros(1,length(Beta));
d2Beta(1)=(dBeta(2)-dBeta(1))/(s(2)-s(1));
d2Beta(imax)=(dBeta(imax)-dBeta(imax-1))/(s(imax)-s(imax-1));
for i=2:length(Beta)-1
d2Beta(i)=(1/((s(i+1)-s(i))^2))*(Beta(i+1)-2*Beta(i)+Beta(i-1));
end
%Tau
Ka=(thetaB-thetaA)./SAB.*100;
Kphi=(phiB-phiA)./SAB.*100;
alph_bar=(thetaA+thetaB)./2;
Kv=Ka;
Kh=Kphi./sin(deg2rad(alph_bar));
K=sqrt(Kv.^2+Kh.^2.*sin(deg2rad(alph_bar)).^4);
Tau=Kh.*(1+2.*Kv.^2./K.^2).*sin(deg2rad(alph_bar)).*cos(deg2rad(alph_bar));
TauN=isnan(Tau(i));
for i=1:length(Tau)
    TauN(i)=isnan(Tau(i));
if TauN(i)
    Tau(i)=0;
end

end
    %=====================================================
dTau=zeros(1,length(Tau));
dTau(imax)=Tau(imax)-Tau(imax-1)/(s(imax)-s(imax-1));
for i=1:length(Tau)-1
dTau(i)=(Tau(i+1)-Tau(i))/(s(i+1)-s(i));
end
%===============

%inputs
Cim=0.0254;%convert from inch to m
od=9*Cim; %m
id=3*Cim;%m
```

```
ODH=16*Cim;%m
SteelW=7850;%kg/m^3
MudW=1500;%SG
WOB=0;%tf to N
TOB=-900*9;%kgf.m t N.mE=210*10^9;%Pa
nu=0.33;%Poisson cefficient
E=210*10^9;%PA
G=E/(2*(1+nu));%Shear Modulus
mua=0.3;%axial friction coefficient
mur=0.6;%radial friction coefficient

%Properties
As=(pi/4)*(od^2-id^2);%surface area, m^2
bf=(SteelW-MudW)/SteelW;% buoyancy factor adim
I=(pi()/64)*(od^4-id^4);%quadratic moment
wb=SteelW*As*bf*9.81;%weight in mud N/m
rc=(ODH-od)/2;%radial clearance m
%weight in frenet
wbt=zeros(1,imax);
wbn=zeros(1,imax);
wbb=zeros(1,imax);
mt=zeros(1,imax);
tt=zeros(1,imax);
mn=zeros(1,imax);
mn(imax)=Beta(imax)*E*I;
mt(imax)=TOB;
tt(imax)=WOB;

tn=zeros(1,imax);
tb=zeros(1,imax);
tn(imax)=-E*I*dBeta(imax);
tb(imax)=-E*I*Beta(imax)*Tau(imax)+(Beta(imax)*mt(imax));

for i=imax:-1:4
    h=s(i)-s(i-1);
    if Beta(i) ~=0
Beta_i=Beta(i);
dBeta_i=dBeta(i);
d2Beta_i=d2Beta(i);
Inc_i=Inc(i);
Azi_i=Azi(i);
Ginc_i=Ginc(i);
Gazi_i=Gazi(i);
```

```
Tau_i=Tau(i);
dTau_i=dTau(i);
tt_i=tt(i);
mt_i=mt(i);
%{
wbt(i)=wb*cos(Inc(i));%projection on tangent
wbn(i)=wb*(1/Beta(i))*-Ginc(i)*sin(Inc(i));%projection on normal
wbb(i)=wb*(1/Beta(i))*-Gazi(i)*sin(Azi(i));%projection on binormal
Q1(i)=1+mur^2*(1-Beta(i)^2*rc^2);
Q2(i)=mt(i)*dBeta(i)-E*I*(2*Tau(i)*dBeta(i)+Beta(i)*dTau(i))+wbb(i);
Q3(i)=Beta(i)*(tt(i)-Tau(i)*mt(i))+(E*I)*(Beta(i)*Tau(i)^2-d2Beta(i))+wbn(i);
fc(i)=(((Q1(i)*(Q2(i)^2+Q3(i)^2)+(mur*Beta(i)*rc*Q2(i))^2)^0.5)-
mur*Beta(i)*rc*Q2(i))/Q1(i);
%}
wbt_i=wb*cos(Inc_i);                    %projection on tangent
wbn_i=wb*(1/Beta_i)*-Ginc_i*sin(Inc_i); %projection on normal
wbb_i=wb*(1/Beta_i)*-Gazi_i*sin(Azi_i); %projection on binormal
Q1_i=(1+mur^2*(1-Beta_i^2*rc^2));
Q2_i=mt_i*dBeta_i-E*I*(2*Tau_i*dBeta_i+Beta_i*dTau_i)+wbb_i;
Q3_i=Beta_i*(tt_i-Tau_i*mt_i)+(E*I)*(Beta_i*Tau_i^2-d2Beta_i)+wbn_i;
fc_i=(((Q1_i*(Q2_i^2+Q3_i^2)+(mur*Beta_i*rc*Q2_i)^2)^0.5)-
mur*Beta_i*rc*Q2_i)/Q1_i;
fc(i)=fc_i;
%dTt=-E*I*Beta_f*dBeta_f-wbt-mua*fc;
%dMt=-mur*rc*fc;
k1=-E*I*Beta_i*dBeta_i-wbt_i-mua*fc_i;
l1=-mur*rc*fc_i;
%==================K2==============================%

Beta_i=Beta(i-1)+((Beta(i)-Beta(i-1))/h)*(h/2);
dBeta_i=dBeta(i-1)+((dBeta(i)-dBeta(i-1))/h)*(h/2);
d2Beta_i=d2Beta(i-1)+((d2Beta(i)-d2Beta(i-1))/h)*(h/2);
Inc_i=Inc(i-1)+((Inc(i)-Inc(i-1))/(h))*(h/2);
Azi_i=Azi(i-1)+((Azi(i)-Azi(i-1))/(h))*(h/2);
Ginc_i=Ginc(i-1)+((Ginc(i)-Ginc(i-1))/(h))*(h/2);
Gazi_i=Gazi(i-1)+((Gazi(i)-Gazi(i-1))/(h))*(h/2);
Tau_i=Tau(i-1)+((Tau(i)-Tau(i-1))/(h))*(h/2);
dTau_i=dTau(i-1)+((dTau(i)-dTau(i-1))/(h))*(h/2);
tt_i=tt(i)-0.5*h*k1;
mt_i=mt(i)-0.5*h*l1;
wbt_i=wb*cos(Inc_i);
wbn_i=wb*(1/Beta_i)*-Ginc_i*sin(Inc_i);
wbb_i=wb*(1/Beta_i)*-Gazi_i*sin(Azi_i);
Q1_i=(1+mur^2*(1-Beta_i^2*rc^2));
```

```
Q2_i=mt_i*dBeta_i-E*I*(2*Tau_i*dBeta_i+Beta_i*dTau_i)+wbb_i;
Q3_i=Beta_i*(tt_i-Tau_i*mt_i)+(E*I)*(Beta_i*Tau_i^2-d2Beta_i)+wbn_i;
fc_i=(((Q1_i*(Q2_i^2+Q3_i^2)+(mur*Beta_i*rc*Q2_i)^2)^0.5)-
mur*Beta_i*rc*Q2_i)/Q1_i;

k2=-E*I*Beta_i*dBeta_i-wbt_i-mua*fc_i;
l2=-mur*rc*fc_i;

%=========================K3=================================%
tt_i=tt(i)-0.5*h*k2;
mt_i=mt(i)-0.5*h*l2;
Q1_i=1+mur^2*(1-Beta_i^2*rc^2);
Q2_i=mt_i*dBeta_i-E*I*(2*Tau_i*dBeta_i+Beta_i*dTau_i)+wbb_i;
Q3_i=Beta_i*(tt_i-Tau_i*mt_i)+(E*I)*(Beta_i*Tau_i^2-d2Beta_i)+wbn_i;
fc_i=(((Q1_i*(Q2_i^2+Q3_i^2)+(mur*Beta_i*rc*Q2_i)^2)^0.5)-
mur*Beta_i*rc*Q2_i)/Q1_i;

k3=-E*I*Beta_i*dBeta_i-wbt_i-mua*fc_i;
l3=-mur*rc*fc_i;
%=========================K4=================================%
Beta_i=Beta(i-1);
dBeta_i=dBeta(i-1);
d2Beta_i=d2Beta(i-1);
Inc_i=Inc(i-1);
Azi_i=Azi(i-1);
Ginc_i=Ginc(i-1);
Gazi_i=Gazi(i-1);
Tau_i=Tau(i-1);
dTau_i=dTau(i-1);
tt_i=tt(i)-h*k3;
mt_i=mt(i)-h*l3;
Q1_i=1+mur^2*(1-Beta_i^2*rc^2);
Q2_i=mt_i*dBeta_i-E*I*(2*Tau_i*dBeta_i+Beta_i*dTau_i)+wbb_i;
Q3_i=Beta_i*(tt_i-Tau_i*mt_i)+(E*I)*(Beta_i*Tau_i^2-d2Beta_i)+wbn_i;
fc_i=(((Q1_i*(Q2_i^2+Q3_i^2)+(mur*Beta_i*rc*Q2_i)^2)^0.5)-
mur*Beta_i*rc*Q2_i)/Q1_i;

k4=-E*I*Beta_i*dBeta_i-wbt_i-mua*fc_i;
l4=-mur*rc*fc_i;
%=========================Solution============================%
tt(i-1)=tt(i)-(h/6)*(k1+2*k2+2*k3+k4);
mt(i-1)=mt(i)-(h/6)*(l1+2*l2+2*l3+l4);
    end
```

```
end
for i=1:length(mt) %vertical section correction
if mt(i)==0
    mt(i)=max(mt);
end
end
```